PREETHI RAVIKUMAR

POLYMERIC NANOFIBROUS AEROSOL SAMPLING FILTERS: DESIGN, VALIDATION AND APPLICATIONS

DOCTORAL DISSERTATION

Kaunas
2024

KAUNAS UNIVERSITY OF TECHNOLOGY

PREETHI RAVIKUMAR

POLYMERIC NANOFIBROUS AEROSOL SAMPLING FILTERS: DESIGN, VALIDATION AND APPLICATIONS

Doctoral dissertation
Technological Sciences, Environmental Engineering (T 004)

2024, Kaunas

This doctoral dissertation was prepared at Kaunas University of Technology, Faculty of Chemical Technology, Department of Environmental Technology during the period of 2019–2023.

The doctoral right has been granted to Kaunas University of Technology together with Lithuanian Energy Institute and Vytautas Magnus University.

Research supervisor:
Prof. Dr. Dainius MARTUZEVIČIUS (Kaunas University of Technology, Technological Sciences, Environmental Engineering, T 004).

Edited by: English language editor Brigita Brasienė (Publishing House *Technologija*), Lithuanian language editor Rita Malikėnienė (Publishing House *Technologija*).

Dissertation Defence Board of Environmental Engineering Science Field:
Prof. Dr. Linas KLIUČININKAS (Kaunas University of Technology, Technological Sciences, Environmental Engineering, T 004) **– chairperson;**
Prof. Dr. Gintaras DENAFAS (Kaunas University of Technology, Technological Sciences, Environmental Engineering, T 004);
Prof. Dr. Violeta MAKAREVIČIENĖ (Vytautas Magnus University, Technological Sciences, Environmental Engineering, T 004);
Prof. Dr. Jurgita OVADNEVAITĖ (University of Galway, Ireland, Natural Sciences, Physics, N 002);
Chief Researcher Dr. Simas RAČKAUSKAS (Kaunas University of Technology, Technological Sciences, Materials Engineering, T 008).

The dissertation defence will be held on 21 October 2024, at 2 p.m. in a public meeting of the Dissertation Defence Board of the Environmental Engineering science field in the Rectorate Hall at Kaunas University of Technology.

Address: K. Donelaičio 73-402, LT-44249 Kaunas, Lithuania.
Phone: (+370) 608 28 527; e-mail doktorantura@ktu.lt

The dissertation was sent out on 20 September, 2024.
The doctoral dissertation is available on http://ktu.edu and at the libraries of Kaunas University of Technology (Gedimino 50, LT-44239 Kaunas, Lithuania), Lithuanian Energy Institute (Breslaujos 3, LT-44403 Kaunas, Lithuania) and Vytautas Magnus University (K. Donelaičio 52, LT-44244 Kaunas, Lithuania).

KAUNO TECHNOLOGIJOS UNIVERSITETAS

PREETHI RAVIKUMAR

POLIMERINIAI NANOPLUOŠTINIAI AEROZOLIO ĖMINIŲ ĖMIMO FILTRAI: KŪRIMAS, APIBŪDINIMAS IR TAIKYMAS

Daktaro disertacija
Technologijos mokslai, aplinkos inžinerija (T 004)

2024, Kaunas

Disertacija rengta 2019–2023 metais Kauno technologijos universiteto Cheminės technologijos fakultete, Aplinkosaugos technologijos katedroje.

Doktorantūros teisė Kauno technologijos universitetui suteikta kartu su Lietuvos energetikos institutu ir Vytauto Didžiojo universitetu.

Mokslinis vadovas:
prof. dr. Dainius MARTUZEVIČIUS (Kauno technologijos universitetas, technologijos mokslai, aplinkos inžinerija, T004).

Redagavo: anglų kalbos redaktorė Brigita Brasienė (leidykla „Technologija“), lietuvių kalbos redaktorė Rita Malikėnienė (leidykla „Technologija“).

Aplinkos inžinerijos mokslo krypties disertacijos gynimo taryba:
prof. dr. Linas KLIUČININKAS (Kauno technologijos universitetas, technologijos mokslai, aplinkos inžinerija, T 004) **– pirmininkas**;
prof. dr. Gintaras DENAFAS (Kauno technologijos universitetas, technologijos mokslai, aplinkos inžinerija, T 004);
prof. dr. Violeta MAKAREVIČIENĖ (Vytauto Didžiojo universitetas, technologijos mokslai, aplinkos inžinerija, T 004);
prof. dr. Jurgita OVADNEVAITĖ (Golvėjaus Nacionalinis Airijos universitetas, Airija, gamtos mokslai, fizika, N 002);
vyr. m. d. dr. Simas RAČKAUSKAS (Kauno technologijos universitetas, technologijos mokslai, medžiagų inžinerija, T 008).

Disertacija bus ginama viešame Aplinkos inžinerijos mokslo krypties disertacijos gynimo tarybos posėdyje 2024 m. spalio 21 d. 14 val. Kauno technologijos universiteto Rektorato salėje.

Adresas: K. Donelaičio g. 73-402, LT-44249 Kaunas, Lietuva.
Tel. (+370) 608 28 527; el. paštas doktorantura@ktu.lt

Disertacija išsiųsta 2024 m. rugsėjo 20 d.
Su disertacija galima susipažinti interneto svetainėje http://ktu.edu, Kauno technologijos universiteto bibliotekoje (Gedimino g. 50, LT-44239 Kaunas, Lietuva), Lietuvos energetikos instituto skaitykloje (Breslaugos g. 3, LT-44403 Kaunas, Lietuva) ir Vytauto Didžiojo universiteto bibliotekoje (K. Donelaičio g. 52, LT-44244 Kaunas, Lithuania).

CONTENT

LIST OF FIGURES

LIST OF TABLES

LIST OF ABBREVIATIONS

2D – 2 dimensional;
3D – 3 dimensional;
AgNP – silver nanoparticle;
ATP – adenosine triphosphate;
BEAS-2B – an immortalized human bronchial epithelium cell line;
CA – cellulose acetate;
CTAB – hexadecyl trimethyl ammonium bromide;
CuNP – copper nanoparticle;
DEHS – bis(2-ethylhexyl) sebacate;
DMF – N,N-dimethylformamide;
DOE – design of experiments;
DSC – differential scanning calorimetry;
FBS – fetal bovine serum;
FTIR – Fourier transform-infrared;
GONP – graphene oxide nanoparticle;
LDH – lactate dehydrogenase;
MTT – (3- (4,5-dimethylthiazol-2-yl)-2,5-diphenyltetrazolium bromide;
MWCNTs – multi walled carbon nanotubes;
NaCl – sodium chloride;
NPs – nanoparticles;
PA6 – polyamide 6;
PAN –poly(1-acrylonitrile);
PBS – phosphate buffered saline;
PC – polycarbonate;
PCL – poly(ε)caprolactone;
PGA – poly(glycolic acid);
PLA – poly(lactic acid);
PLGA – poly(lactic-co-glycolicacid);
PM – particulate matter;
SDS – sodium dodecyl sulphate;
SEM – scanning electron microscopy;
SWCNTs – single walled carbon nanotubes;
WCA – water contact angle;
XRD – X-ray diffraction analysis.

INTRODUCTION

According to the Global Burden of Disease, compared to other health risk factors, ambient air pollution is associated with a greater probability of mortality, and the difficulty with public health is still present. Asthma, bronchitis and pulmonary disease, lung cancer, hypertension, high blood pressure, neurodegenerative diseases are associated with one of the most complex and harmful air contaminants, i.e., fine particulate matter [1, 2].

In order to comprehend its environmental levels in both indoor and outdoor air, its sources and environmental transformations, fine particulate matter has been the subject of thousands of research projects as well as the mechanisms underlying its detrimental impacts on the human health. According to [3], there are numerous techniques for determining the concentration of particulate matter in ambient air, including inertial, gravitational, centrifugal, thermal, real-time optical measurement, aerodynamic size measurement, electrical mobility method, electrical detection mass spectrometry and combinations of the aforementioned.

One of the earliest, most well-known and most used techniques for sampling aerosols is the collection of aerosol particles on a filtering substrate. The fibrous matrixes, membranes and foams make up the majority of the filtering substrates. Membrane filters (porous membranes, capillary membranes) have great stability and capture efficiency, but at the cost of a considerable pressure drop within the thickness of the filtering membrane layer. They are made of polymers (such as polytetrafluoroethylene, cellulose esters). Foam filters are made of either an inorganic substance (such as stainless steel) or a polymer (such as polypropylene) and function as a volume mesh of big pores to capture coarse particles. The building blocks of fibrous matrices are dense meshes of fibres with erratic orientations. Typically, cellulose or natural materials, such as glass or quartz, are used to create fibrous matrixes. Despite being one of the most often used substrates for aerosol sampling, fibrous filters have a number of drawbacks: because of their large surface area, higher volatility substances (e.g., some PAHs or organometallic compounds) found in the sampled particles a) evaporate from the filter during prolonged storage, b) affect the results of a chemical analysis (such as metals in aerosol particles) and c) some formulations of pure mineral fibres (such as quartz) are mechanically unstable and disintegrate during handling.

In recent decades, there has been a significant expansion in the study of aerosol cytotoxicity, notably in the setting of nanoparticles. This increase in attention is partly attributable to the growing concerns about the possible health effects of aerosolized nanoparticles, which are already commonplace in many industrial and environmental atmospheres. Due to the variety of these particle properties and their complicated interactions with biological systems, conducting thorough assessments of aerosol nanoparticles continues to be a challenging task, despite the rising corpus of the research. These studies are further complicated by the absence of established techniques for determining nanoparticle toxicity. The demand for trustworthy and affordable methods to evaluate nanoparticle cytotoxicity in vitro is constantly

increasing due to the broad variety of nanoparticulate materials and their potential cytotoxicity.

Numerous research have looked at the cytotoxicity of nanoparticles in vitro and in vivo. In order to successfully construct studies that assess the cytotoxicity of nanoparticles, aerosolized nanoparticles provide a substantial barrier. Standardized methodologies for the assessment of aerosolized nanoparticle toxicity must be developed for the precise characterisation of this particular environmental contaminant.

Traditional aerosol sampling techniques have undergone continuous improvement and have been shown to be moderately successful in capturing airborne nanoparticles. Polytetrafluoroethylene, quartz fibre and glass fibre have all been used in studies. The choice of material was determined by the material's chemical inertness, physical characteristics, including pore size, and particle retention effectiveness. However, evaluating cytotoxicity in vitro often necessitates different procedures and assays, which makes the overall evaluation process more complex and inconsistent. The effectiveness and variety of aerosol sampling techniques have increased with the introduction of new multipurpose sample filters. The variety of aerosols that can be effectively collected is increased by these novel materials, such as nanofibre and bio-inspired filters, which have vast surface areas and customizable pore sizes.

The ability to analyse the toxicity of nanoparticles has expanded thanks to the developments in in vitro cytotoxicity study. Flow cytometry, confocal microscopy and high throughput 'omics' approaches are now frequently used in nanotoxicology studies in addition to more conventional cytotoxicity assays, e.g., MTT assay for cell viability, LDH assay for membrane integrity and Annexin V staining for apoptosis. In order to simulate nanoparticle toxicity scenarios in vitro, many cell culture models have been used. It is crucial to remember that these cell culture models might not accurately capture the intricacy of interactions and reactions that take place in a living organism.

Therefore, a wide range of factors, including the physicochemical characteristics of nanoparticles, the choice of cytotoxic assay, aerosol sampling techniques and cell culture models, must be considered in order to accurately assess the cytotoxicity of nanoparticles and their potential impact on human health. The shortcomings and difficulties of in vitro techniques for determining nanoparticle toxicity must be considered as well.

However, there is still a gap between the cytotoxicity testing and aerosol sampling in available scientific literature. The realism and accuracy of later cytotoxicity assessments may be compromised as a result of the changes in particle properties and probable losses during handling, storage and transportation caused by this gap. Recent studies have promoted an integrated strategy that combines in situ aerosol sampling with later in vitro toxicity investigation to overcome this problem.

The unique design of an aerosol sampling filter (composite three-layer fibrous matrix) has overcome this challenge that features a top nanofibrous layer, which serves as an efficient filter for aerosol particle collection as well as a 2D-fibrous cell

cultivation scaffold. The aerosol sampling filter is constructed as a composite filter disc comprising at least three non-woven fibrous layers. The three-layer-structure forms a fibrous matrix that features high mechanical stability during aerosol sampling and subsequent handling and in vitro cell cultivation. This extends the use of aerosol sampling filters by specifically designing these to be used in the toxicological analysis of the collected particles.

A wide variety of aerosol types can be captured by a nanofibrous matrix acting as a sample filter. Additionally, it can be used with the following cytotoxicity tests by decreasing the unpredictability caused by the extraction and filtration of particles; this method not only speeds the procedure but enables instantaneous cytotoxicity analysis as well. The platform's goal was to deliver a multi-parameter toxicity profile that took into account genotoxicity, oxidative stress, inflammation and cell viability. This thorough investigation, which goes beyond the usual cytotoxicity assessments, will provide insightful information about the potential health hazards related to the aerosol exposure.

This study verifies the "cells on particles" technology by testing it against nanoparticles that simulate probable aerosol exposure in work situations. It overcomes the limitations of separate techniques by merging aerosol sampling and in vitro cytotoxicity analysis on a single platform, guaranteeing that the evaluated particles closely mirror those in the original aerosol and boosting the relevance of the toxicological data acquired.

Aim of the doctoral thesis

The aim of the thesis is to develop and validate nanofibrous aerosol particle sampling filters.

Objectives:

1. To design, fabricate and characterize nanofibrous filter substrate suitable for the collection of aerosol particles.
2. To validate the developed nanofibrous sampling filters as platforms for the subsequent cytotoxicity analysis of collected particles in vitro.
3. To research the properties of nanofibrous sampling filters in various air flow regimes towards collecting the variety of particles.

Statements presented for the defense

1. The manufacturing of fibrous filters from polymers by electrohydrodynamic processing allows to attain suitable properties regarding precise control over the fibre composition and size.
2. The aerosol sampling platforms based on nanofibrous layers are suitable for testing the cytotoxicity of collected aerosol particles in terms of biocompatibility and quantitative response of cells to the nanoparticles.
3. The utilization of similar polymeric materials for manufacturing of both nanofibre and microfibre layers ensures mechanical stability and high overall collection efficiency, suitable to be applied to the aerosol sampling.

Scientific novelty

1. The thesis presents a production method of a novel nanofibrous sampling filter for collecting aerosol particles. Specifically, the sampling filter comprises a layered composite arrangement of nano- to sub-micro-metre-sized polymeric fibres, which provides a superior particle retention efficiency, mechanical stability and variety of opportunities for post-processing by a plurality of physico-chemical or toxicological analysis techniques. The design and manufacturing methods for these sampling filters have been disclosed in the European patent application EP22170405.9, submitted to the European Patent Office on 28 April 2022.
2. On a basis of the nanofibrous aerosol sampling filter, a novel method of in vitro aerosol particle cytotoxicity assessment was suggested, based on the application of a single platform for aerosol particle collection and subsequent cytotoxicity investigation.
3. The integration of Modde 7 software for precise control of electrospinning parameters optimized PC and CTAB layers for air filtration. This approach achieved a 99.9% filtration efficiency using PC nanofiber media on a 3D substrate.

Structure and outline of the dissertation

This doctoral thesis includes an introduction, a literature review, materials and methods, results and discussion, conclusions, a reference list, and a list of publications related to the dissertation topic. The thesis is comprised of 134 pages, including 30 figures and 8 tables.

Publication of the research results

The findings of this study have been published in two peer-reviewed articles in journals listed in the CA Web of Science database. The outcomes of the experiments were presented at four international conferences.

Practical significance

The presented aerosol sampling and particle cytotoxicity assessment method is primarily designed to be used for the assessment of air pollution in indoor, occupational and ambient environments. These filters play an important role in governmental air monitoring campaigns, where they are heavily utilized. However, their significance extends beyond mere sampling; the ability to control particle collection surface morphology and precursor polymer opens avenues for scientific exploration, particularly in the development of new aerosol particle analysis techniques.

Author's contribution

The author of the dissertation has conducted the analysis that is given and discussed in this thesis. The veracity of the experimental data is fully accepted by the author.

The author conducted the research and data collection process, actively contributing to the manuscript preparation for the publication of the results. The laboratory inquiries, data analysis, interpretation and manuscript composition are all presented in the chapter titled "Design, Fabrication, and Characterization of Nanofibrous Aerosol Sampling Filter Substrate".

The author performed the analysis on the experimental data and prepared the manuscript accordingly. The laboratory experiments, data analysis, interpretation and manuscript composition were all supported by the content outlined in the chapter titled "Composite Nanofibrous on 3D Printed Support Polycarbonate Filter for Aerosol Particle Filtration and Sampling".

The laboratory experiments, data processing, interpretation and manuscript creation were conducted in partnership with State Research Institute Centre for Innovative Medicine (IMC). This collaborative effort is presented in the experimentation chapter titled "Evaluation of A Single Platform for Both Aerosol Particle Collection and Cytotoxicity Evaluation In Vitro".

1. LITERATURE REVIEW

1.1. Understanding the significance of aerosol sampling and electrospun substrates

Aerosol particles, which are tiny particles suspended in the surrounding air, are known to have a negative impact on the human health. They enter human airways and settle in the upper respiratory tract (known as the inhalable aerosol fraction), middle respiratory tract (referred to as the thoracic fraction) and lower respiratory tract (referred to as the respirable fraction), depending on their size. Due to its small size, the latter portion of aerosol particles is particularly significant, since it can reach the lungs, penetrate the alveoli and then enter the circulation. These particles can originate from several different places, such as natural sources, e.g., dust and sea spray, as well as human-caused sources, such as transportation, industrial activity and agricultural practices. According to their size, the particles can be categorized as PM 10 or PM 2.5: PM 10 denotes particles having a diameter of at least 10 micrometres, whereas PM 2.5 denotes particles with a diameter of at least 2.5 micrometres. PM 2.5 particles are particularly concerning because they are small enough to be inhaled and can penetrate deep into the lungs, leading to a variety of health problems. Air pollution caused by particulate matter has been linked to a variety of health problems, such as lung cancer, heart disease and respiratory infections [4, 5]. Chronic health issues as asthma and chronic obstructive pulmonary disease (COPD) [6] can develop as a result of prolonged exposure to PM. The risk of stroke and other cardiovascular disorders has been linked to exposure to PM2.5 in particular [7]. The programs for monitoring air quality are used to gauge airborne particulate matter concentrations and provide data for air quality-related policy choices. The strategies to reduce particulate matter pollution include reducing emissions from transportation and industrial sources, promoting clean energy and encouraging sustainable land-use practices. Everyone is impacted by the air pollution; however, particular demographics, such as children, elderly people and those with pre-existing medical disorders, may be more susceptible than others [2].

Aerosol sampling with electrospun substrates is a technique that uses electrospun fibres to capture and collect airborne particles for the analysis. Electrospinning is the most well-known and well-established technique for making nanofibrous scaffolds utilized in filtering applications. Due to the method of electrospinning, thin fibres with diameters in the nano- to micrometre range are created by drawing polymer solutions or melts through a tiny orifice using an electric field. Due to their high porosity, huge surface area to volume ratio, microscale interstitial gaps and interconnectivity, these fibres can be employed as a substrate for aerosol sampling [8, 9]. The electrospinning process can be optimized by varying the processing parameters, such as the solution concentration, applied voltage and flow rate. Even though electrospun nanofibres can be very fragile and may not have the necessary mechanical strength, the high surface area can lead to issues such as poor wettability or difficulty in handling and can be sensitive to the environmental factors,

such as humidity, temperature and air flow, which can make it difficult to achieve consistent results [10]. Due to the difficulties at nanoscale, including spherical or sphere-like particles, such as sodium chloride (NaCl) and dioctylpthalate (DOP), two alternative filtration test procedures have been applied. Simultaneously monitoring particle concentration at upstream and downstream locations, DOP delivered discrete penetration results utilizing monodisperse aerosols. Another test setup was created to quantify polydisperse aerosols (with a size range of 10–400 nm) both upstream and downstream using a scanning mobility particle sizer (SMPS) [11]. However, one of the most crucial applications of electrospun fibre is filtering. Due to distinctive qualities, such as significant surface-area-to-volume ratio, nano porous structures, low basis weight and ratio, the electrospun nanofibre materials of uniform size might be used for a large-scale application of air filtration [12].

A technique for 3D printing based on the electrospinning to create shape-variable, biodegradable mask filters were devised [13]. The application scenarios of electrospun filters were widened by [14] to include the industrial pollutants such as 3D printing. The design of experiments (DOE) was used to optimize the electrospinning procedure, resulting in the formation of PAN nanofibres without beads, 100 nm in diameter. The PAN membrane with a diameter of 77 nm was created and used to filter PM2.5 emissions from FDM 3D printing and demonstrated a filtration effectiveness of 81.16%. Numerous investigations on the 3D reconstruction of electrospun fibre membranes and direct electrospinning of nanofibre, including the use of 3D printed polymeric materials, such as PLA placed on graphene-based air filters [15], have recently been conducted by the researchers. In this study, a flexible free-standing air filter was created using 3D printing to effectively remove NO [16].

1.2. Polymer nanofibre materials used in aerosol sampling

1.2.1. Poly(1-acrylonitrile), $(CH_2CHCN)_n$

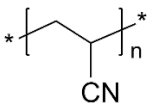

Fig. 1.1. Chemical structure of poly(1-acrylonitrile)[17]

It is commonly acknowledged that PAN is a superior polymer precursor to produce nanofibres. This is mainly attributable to its outstanding chemical stability and practical processability. Fig. 1.1 shows the chemical structure of poly(1-acrylonitrile). High heat stability and low electrical resistance in polyacrylonitrile fibres make them extremely useful in both industrial and medicinal settings. Due to its important characteristics, such as strong mechanical strength, plasticity and modest porosity values with larger surface area to volume ratio, PAN fibres make suitable electrospinning candidates [18]. The findings from the TOXNET database show that PAN has no recognized toxicities. Nitrile groups, which operate as hydrogen bonding acceptors and enable PAN membrane activity, make an excellent air filtering media

[19, 20]. PAN-based electrospun nanofibre membranes are receiving greater acknowledgement as cutting-edge materials in the field of air purification.

1.2.2. Poly(hexano-6-lactam), $(C_6HnNO)_n$

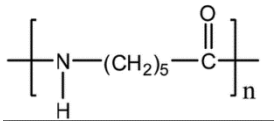

Fig. 1.2. Chemical structure of poly(hexano-6-lactam) [21]

According to [10], PA6 is one of the most often used engineering thermoplastics because of its high strength, strong fatigue resistance, good water absorption and chemical stability. Fig. 1.2 shows the chemical structure of poly(hexano-6-lactam). In industrial manufacture and applications, it is frequently referred to as nylon 6 or polycaprolactam. Caprolactam hydrolytic polymerization and anionic polymerization are the main methods for producing PA6. Due to its stability and controllability during polymerization, caprolactam hydrolysis polymerization is the preferred technique for the mass manufacturing of PA6. The molecular chain is generated by dehydration condensation of terminal carboxyl groups and amine groups during the hydrolysis and polymerization of caprolactam. Therefore, during the polycondensation process, it is crucial to keep the stoichiometric equilibrium of carboxyl groups and amine groups. When PA6 is modified through copolymerization, the modified polymer component that is added tends to influence the system's end group balance, which lowers the degree of polymerization. Therefore, current research focuses on copolymerization modification by adding various chain extenders to achieve copolymerization modification of PA6 [22, 23, 24, 25, 26].

1.2.3. Cellulose acetate, $C_6H7O_2(OH)_3$

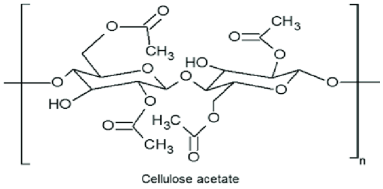

Fig. 1.3. Chemical structure of cellulose acetate [27]

Cellulose, being an abundant polymer, possesses exceptional electrospinning application. Cellulose acetate is generated from its acetate ester by acetylation process [28]. High porosity, elasticity with stiffness, high surface area to volume ratio and tensile resilience are the characteristics of CA fibre that lead to a variety of filtration applications [29, 28]. Fig. 1.3 shows the chemical structure of cellulose acetate. An environmentally friendly and biodegradable cellulose product is cellulose acetate (CA). It is easily made into fibres and films for different textile and biomedical applications as well as semipermeable membranes for separation processes [30, 31].

However, when CA films are made by using solvent casting, they tend to have poor surface stability and dense structure, leading to low chemical and thermal stabilities [31]. Nanotextures can be produced using electrospinning to enhance the structure and characteristics of conventional casting texture.

CA has a huge potential for the application in electrospinning due to its abundance and rank as one of the most common biopolymers on the globe. The researchers have investigated the deacetylation of incredibly small CA fibres, producing smooth nanofibres with diameters between 100 and 1,000 nm [32]. The average diameter of the CA nanofibres, which ranges from 160 to 1,280 nm, depending on the solvent composition, was electrospun from a mixture of acetic acid and water. Moreover, [33] investigated the effects of different solvent systems on the morphological appearance and size of the electrospun CA products, while [34] has suggested that ribbon-like porous CA fibres can be electro sprayed by using a mixture of acetone and dichloromethane with the amount of dichloromethane in the binary solvent system having a major effect on the fibres porous structure. Due to the increased volatility, fibres with greater porosity were created.

1.2.4. Poly[ε]caprolactone, $(C_6H_{10}O_2)n$

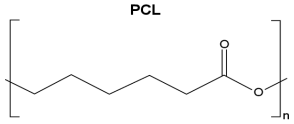

Fig. 1.4. Chemical structure of poly[ε]caprolactone [35]

Poly(ε-caprolactone), one of the most extensively researched biodegradable polymers, has the advantages of high mechanical strength, strong biocompatibility, suitable rate of biodegradation and the generation of non-toxic residues during hydrolytic decomposition [36]. PCL is broken down by hydrolyzing ester bonds to produce acid monomers [35]. Fig.1.4 shows the chemical structure of the chemical structure of poly[ε]caprolactone. Numerous researches have demonstrated that by combining PCL with natural polymers, the high crystallinity of PCL may be blended to overcome its strong hydrophobicity and slow degradation [37, 38]. Clinical and biological usage of PCL is not new. PCL has shown to be useful in a variety of in vitro and in vivo applications in addition to being a biomaterial [35, 39]. As previously mentioned, this polymer is used for purposes other than biomedical materials as well. The FDA-approved aliphatic polyester, poly(ε-caprolactone) (PCL), has garnered attention in numerous disciplines owing to its exceptional biocompatibility [40, 41]. Furthermore, prior research indicates that PCL breaks down at high temperatures and has one of the lowest melting points among hydrophobic polymers [42, 43, 44].

1.2.5. Poly(bisphenol A carbonate), $C_{15}H_{16}O_2$

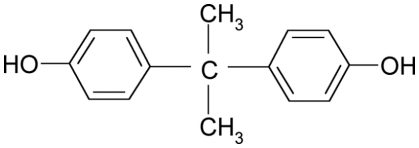

Fig. 1.5. Chemical structure of poly(bisphenol A carbonate) [45]

PC is a thermoplastic polymer that is known for its high strength, transparency and resistance to impact. These properties make it a suitable material for use in various applications, such as filtration, tissue engineering and drug delivery [46]. Fig. 1.5 shows the chemical structure of poly(bisphenol A carbonate). PC is a flexible material that has been used in a wide range of products, such as armoured vehicles, electrical equipment, load-bearing items, compact and digital video discs, sports safety equipment and transparent windows that can withstand bullets, train carriages and architectural projects. Moreover, PC fibres can be modified by incorporating various agents, such as nanoparticles, drugs or other polymers to enhance their properties and functionality [47].

One of the studies [48] discusses the development of PC nano fibres for particle filtration applications. The researchers were able to produce smooth and bead-free fibres with a diameter of 300 nm by adding CTAB to the solution during the electrospinning process. The combination of high specific surface area and polarity resulted in 100% filtration efficiency with a thickness of 32 mm and air permeability of 78.36 L cm2 h1. The conclusion of the study is that PC nano fibrous membrane has potential as a material for particle filtration applications. Similar study achieved high efficiency in the preparation of ultrafine PC fibres by adding hexadecyl trimethyl ammonium bromide (CTAB), resulting in an average pore size of 504 nm and an average diameter of 319 nm [49].

1.3. Fabrication techniques for nanofibrous filters

1.3.1. Electrospinning techniques

Electrospinning has been extensively investigated for more than a century with 1D fibres receiving a lot of interest. Over the years, electrospinning, a reliable, practical, affordable, environmentally safe and industrially sustainable method for making polymer fibres, has been essential in producing a range of polymeric fibres with diameters from nanometres to some micrometres. Even though there are several ways to make nanofibres, including self-assembly, vapor-phase method, solution-liquid-solid methods, template-directed methods and hydrothermal synthesis procedures. However, these methods produce a number of limitations, including expensive costs, a complicated preparation process and material limitations. However, electrospinning provides a continuous approach with a manageable morphology and outstanding diameter/length ratio [50, 51].

1.3.2. Solution electrospinning

A method for creating nanofibres or ultrafine fibres is electrospinning. Using a small nozzle and a strong electric field, the method pulls a polymer solution or melt towards a target where the charged droplets quickly solidify into fibres. Electrospun fibres are highly consistent in size and shape and can range in diameter from tens of nanometres to several microns.

Fluid dynamics, electrostatics and polymer science are all included in the theory of electrospinning. In a container with a high voltage applied between the nozzle and the target, the polymer solution or melt is put. The polymer cannot flow from the nozzle to the target due to a repulsive force that is produced by the electric field. A thin, charged jet of polymer is pulled from the nozzle at a particular threshold when the electric forces outweigh the surface tension forces. The stretching and alignment that the jet experiences as it flies results in the fibres getting finer and more uniform. The fibres become charged because of the stretching and alignment, which aids in stabilizing and preventing the fibres from collapsing onto themselves.

The charged fibres are drawn to the target, which is normally grounded, and become consolidated into nanofibres. By altering variables such as polymer concentration, the applied voltage and the flow rate of the polymer solution, the electrospinning process may be managed. Numerous products can be made with electrospinning, including filters, energy storage devices, wearable electronics and medical equipment. Electrospinning is a very promising technology with the potential to completely transform a wide range of industries due to its capacity to manufacture ultra-fine fibres with a high degree of consistency [52].

1.3.3. Melt electrospinning

A technique for creating nanofibres from polymer melts is called melt electrospinning. The process involves melting a polymer material, typically a thermoplastic, and then forcing the melted material through a small nozzle under high electrical potential. The electrical potential creates an electrostatic force that pulls the melted material into thin, continuous fibres. The fibres are then solidified and collected onto a collector surface to form a nonwoven web of nanofibres.

The theory behind the melt electrospinning involves several physical and electrical forces. The high electrical potential creates an electrostatic force that attracts the melted polymer towards the collector surface. The molten polymer's viscoelastic characteristics, such as its viscosity and surface tension, as well have an impact on the nanofibre web's final fibre diameter and structure. The final fibre structure is influenced by the material's velocity as it is driven through the nozzle and the separation between the nozzle and the collector. The controlling of numerous factors that affect the electrospinning process, such as the electrical potential, polymer viscosity and surface tension, flow rate and nozzle-collector distance, is crucial in order to achieve reliable and uniform nanofibre production. It is possible to create nanofibres with ideal diameter, strength and orientation by adjusting these variables for a certain purpose. As it can create fibres with a consistent diameter and high aspect ratio (length-to-diameter ratio), melt electrospinning has gained popularity as a

method for creating nanofibres. This method yields nanofibres that have a wide range of uses in such industries as filtration, energy storage, tissue engineering and medication delivery [27].

1.3.4. Principle scheme of electrospinning equipment

The method of electrospinning uses the electrostatic forces produced by a high-voltage source to propel the spinning of melts or droplets of polymer solution coming through a small aperture. This method, which was first patented in 1902, has its origins in Lord Rayleigh's nineteenth-century studies on the electric fields (US Patent 692,631). Formhal did not realize its potential for processing textile yarns until 1934. Theoretical insight into how an electric field impacts a small liquid volume was made possible by Taylor's work. A liquid droplet that has been exposed to the electric field develops an electrostatic charge near the tip of the droplet. The shape of the droplet changes from a nearly spherical surface to an elongated cone shape, which is later referred to as a Taylor cone, as a result of this charge repulsion counteracting the surface tension. A jet is then released from the capillary spinneret afterwards. Although the direction and electric charges of this jet are complex, in the absence of a viscous polymer solute, the liquid will finally fragment into tiny droplets, resulting in the electro spraying process [64]. Fig. 1.6 shows an electrospun polymer fibre's internal structure and X-ray patterns with a high degree of crystallinity.

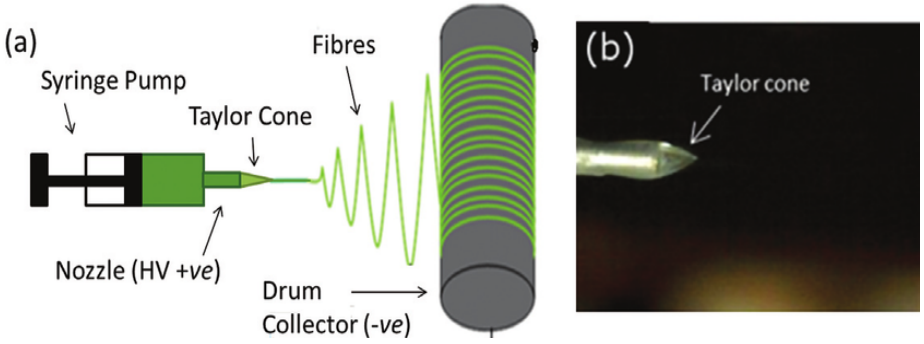

Fig. 1.6. (a) Diagram illustrating the experimental configuration employed for the fabrication of polystyrene micro-fibres and (b) a detailed view of Taylor cone [65]

However, the viscosity of the polymer must be taken into consideration as well when the liquid has it as a solute. If the viscosity is high enough, it prevents the jet from breaking up into droplets. As an alternative, a thread of polymer solution develops and exhibits the same electrical instability as pure liquid. These instabilities, which entail bending or whipping motions, might cause the polymer solution to travel down a convoluted course. The polymer thread elongates as a result of this action and stretching because solvent is being drained from it. The creation of fibres with sub-micron diameters depends on this elongation process. Although necessary for achieving severe fibre elongation, the whipping process distinguishes this method from other fibre production methods [37].

1.3.5. Equipment for laboratory-scale electrospinning

A high-voltage power source, a syringe pump and a collector, which can be as easy as a sheet of aluminium foil, are the three main pieces of equipment needed for this process. Alternative arrangements are possible though.

Coaxial electrospinning is an innovative version of needle electrospinning that occasionally uses two concentric needles of differing diameters. Core-shell fibres, which can be created using this method, have an inner core that is different from the fibre's outer shell. There have been several technological improvements in electrospinning system design in recent years.

An array of aligned fibres may be required in many applications and for some characterisation techniques in place of a random mat of fibres. This need can be satisfied in several ways. Utilizing a rotating collector, which results in aligned fibres, is one straightforward technique. One crucial component of control is preparing aligned fibres, but there is as well a need for precise nanofibre deposition to produce patterned nanostructures. Several methods can be used to achieve this. For instance, in order to produce patterns, near-field electrospinning shortens the distance between the collector and a solid probe [66]. If this technique is to be employed for continuous fibre creation, the adjustments are required.

Large-scale fibre production, which is frequently required for considerable commercialization in a variety of applications, is not appropriate for the system. The multi-needle system is one simple method; however, needles are prone to clogging, and it requires careful spacing of needles to prevent interference between the surrounding fields [67]. The investigation of needleless techniques has been prompted by these difficulties. In such procedures, numerous jets are produced by a revolving cylinder that is only partially submerged in a polymer solution. Elmarco has secured a patent for this method, which is marketed under the name "Nano spider". The adoption of a stationary wire electrode system is a more recent development [68]. Other methods include using a revolving cone and pressurized air to create bubbles on the surface from which several jets can be generated.

1.3.6. Application areas

The study on fast filter sampling showed that glass fibre filters with porous morphology results in multiphoton ionization with fast conductance application [69]. It has been used as a collection of dust system in industrial scale. Hot air circulation and air conditioning systems are used in workplaces and residential places for providing air quality. In addition, they provide microbial contamination protection. The panel filter has a list of air cleaning systems, which includes pleated filters, reusable filters, pleated filters, deep pleated filters, electronic aerosol cleaner and electret filters. Following indoor air filter types were identified by Duran [70], such as melt blown, fibreglass, spun bond bi-component, polyester/cotton, high loft polyester, fibrillated film, needle felt.

Respirators and face masks are used to protect from the environmental pollutants. Two types of respirators include air purifying and air supplying respirators. These were very well used in Covid-19 pandemic, which shook humankind.

Healthcare and surgical face masks are used to protect from blood splatters and colloidal microorganisms during surgical procedures. It has 5 performance characteristics: i) flammability resistance, ii) penetration of fluid resistance, iii) breathing comfort, iv) bacterial filtration and v) sub-micron particle filtration. Air purifiers or room cleaners are residential, portable and can remove particulate matter and odour. Two types of air demisters are used in industrial, residential and commercial scale for removing moisture and hydrocarbon and oil mist from the air. International standard ISO 14644-1 defines cleanrooms, which need to have controlled air borne particles and controlled temperature, pressure and humidity environment. These cleanrooms are used in hospitals, genetic research, biomedical research, pharmaceutical, food processing, laboratories, universities, semiconductor, industrial processing sectors [70].

1.4. Filtration mechanisms and modelling

1.4.1. Airborne particle sampling

Human lung surface area is approximately 80 m2, which is the same as the tennis court surface area [53]. This illustrates how human lung acts as a major pathway for particulate matter and various gaseous contaminants [54]. Aerosol is a term used to describe a suspension of solid and liquid particles in a gaseous medium that can be quantified. The investigations on the health impacts of aerosols have evolved since the 1950s. One of the earliest and most popular methods for achieving ambient concentration were described in [55, 56, 57]. In recent times, more research efforts were put on the natural and synthetic aerosols leading to global warming. Generally, aerosol particle size ranges from 0.001 to 100 μm. Particle behaviours are administered by physical laws, as various size particles behave differently in distinct ranges. The intrinsic properties and motion of gas suspended depends largely on the particle behaviour inside an aerosol. Mass concentration is the most important aerosol property to be measured for the environmental and health effects. The mass concentration of suspended particles worldwide is measured through an efficient particle air filter by allowing quantifiable air volume for a period of 24 hours. Filters were weighed before and after particle sampling in a laboratory setting with regulated humidity and temperature. Then the particle mass concentration is determined by dividing deposit volume by sample volume [58]. Commercially available aerosol filters provide filter material selection, which includes pore size, shapes and collection characteristics. The main parameters to be noted while selecting aerosol filter are collection efficiency, pressure drop and compatibility with sampling conditions including cost. The substrate filter, size-selective inlet, filter holder, flow controller and flow mover are all components of the aerosol sampling system [59, 60]. Most used filter samplers in the earlier days were cellulose fibre membrane, cellulose acetate membrane, glass fibre filters and PVC (polyvinyl chloride). However, after significant research about the desorption and adsorption of water at various relative humidity, sample efficiency variability and contaminants, particulate matter in the atmosphere can as well provoke genotoxicity in addition to cytotoxicity to human

beings, which is investigated by the gel electrophoresis and cell culture techniques. This topic covers aerosol sampling filters/membranes including:

1. Classification of aerosol sampling filters;
2. Methods for filter analysis;
3. Aerosol particle post processing methods: gravimetric, spectroscopy, chromatography and toxicity assessment;
4. Areas of application.

1.4.2. Classification of aerosol sampling filters

Aerosol filters can be logically classified based on their structure characteristics. As a result, there are five different types of aerosol sampling filters: straight through pore membrane, fibrous, granular bed, porous foam and porous membrane filters. Fig. 1.7 shows the classification of aerosol sampling filters. The selection of air sampling filter is based on certain criteria, which includes collection efficiency, availability, cost, analytical procedures requirement and filter's ability to retain physical integrity and collection properties under ambient sampling conditions [60].

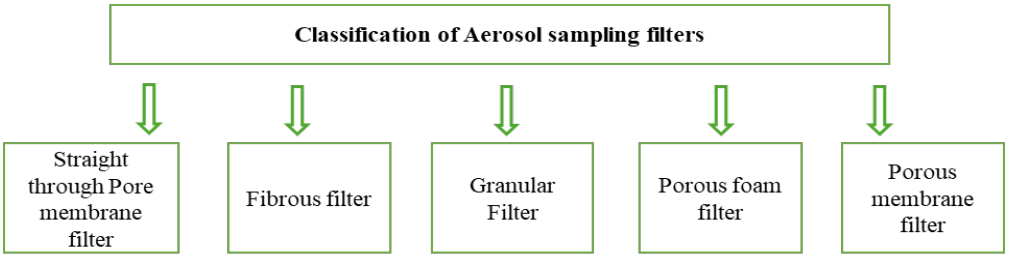

Fig. 1.7. Classification of aerosol sampling filters

1.4.3. Fibrous filters

Individual fibre mats form a fibrous filter. The diameter of fibres ranges from less than 1 mm to several hundred micrometres. Usually, fibrous filter porosity is high, which ranges from 0.6 to 0.999 μm. Typically, porosity of less than 0.6 μm is not found due to the difficulty of obtaining thin smaller layer of component fibres by compressing procedure. Table 1.1 shows the air sampling filter characteristics. Usually, the filters are fabricated with binder material for holding fibres together. In aerosol filters, binder free materials are used due to their interference caused organic binders in it. Most widely used general purpose air filter is cellulose fibre filter. Its advantages include: cost effective nature, various size availability, characteristics of high mechanical strength with low pressure drop. Certain limitations include low filtration efficiency for sub micrometre particles and moisture sensitivity.

Table 1.1. Characteristics of air sampling filters

Filters	Pore size	Porosity	Available filters	Collection efficiency	Pressure drop
Straight through pore membrane filter	0.1–8 µm	5–10%		High	Significantly higher
Fibrous filter	0.1–100 µm	60–90%	Cellulose, glass, polymer fibre and quartz filters	High collection efficiency requiring low air velocity	Lowest
Granular bed filter	200 µm	40–60%	-	High granular size results in low collection efficiency	-
Porous foam filter	10–50 µm	<97%	Fibrous and membrane filters	Low	-
Porous membrane filter	0.02–10 µm	<85%	Sintered metal, polymer and ceramic microporous filter	High	High

1.4.4. Glass fibre filter

This filter is used for air samplers with high volume as filter media standard. Considering paper filters, glass fibre filter has a higher pressure drop and filtration efficiency of more than 99%, which are lesser than 0.3 µm. Compared to cellulose fibre filters, glass fibre filters are less affected by the moisture. Another way of overcoming the setbacks of glass fibre filters is by coating Teflon, which provides less moisture sensitivity and is passive to chemical transformation catalysing. Glass fibre filters are depth filters consisting of compressed glass fibres that form an asymmetric three-dimensional network with numerous interspaces. As a result, particles are caught both on the surface and farther into the filter structure. Glass fibre filters have a great ability to capture dust and have good adhesive characteristics. They have good wet strength and can handle large flow rates.

Due to lesser contamination level of trace elements and inert ability, quartz fibre filters are widely used in air samplers with high volume. Polystyrene fibre filter has limited sampling applications. Nevertheless, its filtration efficiency is comparable to that of the glass fibre filters. Quartz fibre filter contains quartz filaments made of tightly woven mat. Positive bias to gravimetric measurements is obtained by the adsorption of organic vapours [61, 62]. Compared to glass fibre filters in terms of sampling, quartz glass fibre filters serve as depth filters. Due to their incredibly low and consistent blank values, they are especially helpful for analysing metal components in dusts. Nevertheless, the existence of soluble silicates may still obstruct the analysis when employing the AAS graphite furnace method. Numerous varieties of quartz glass fibre filters could be mechanically delicate, which could be problematic for gravimetric analysis.

1.4.5. Porous membrane filters

Colloidal solution results in a gel called membrane filters. Teflon, polyvinyl chloride, sintered metal and cellulose ester are commercially available membrane filters and are most widely used. It has intricated and homogenous microstructure providing a path of air flow irregularly. Depending on the manufacturing technique, this complex structure has a series of layers stacked by various process. Even for smaller pore size particles, the particle collection efficiency and pressure drop are very high. Due to the impact of inertial mechanism and Brownian motion principle, using filter structure particles are trapped by surface. Teflon coated glass fibre filter application involves polycyclic aromatic hydrocarbon analysis (PAH) and weighed accordingly [63].

1.4.6. Straight through pore membrane filters

Uniform sized, straight through pore, consisting of polycarbonate membrane are straight through pore membrane filters. The manufacturing process involves neutron bombardment of polycarbonate membrane with etching process resulting in membrane with uniform pore size. Bombardment time can be manipulated for pore number, and the etching process determines the pore size. Particle analysis often uses this filter.

1.4.7. Granular bed filters

Air sampling with specialized applications can utilize packed or granular bed filters. Filtration is achieved by passing aerosol particles through granular bed and using extraction steps to recover aerosol in the later steps. The recovery of aerosol from granular filter media is often done for the chemical analysis by using volatilization, washing and use of specific solvents. The collection of both gaseous and particulate matter pollutants can be collected simultaneously with desirable filter media selection that is distinguishing application of granular bed filters.

1.4.8. Porous foam filter

Using an instrument, which is simple, less expensive and compact, size dependent particle penetration characteristics can be achieved using porous foam filters. Filter formation is done by using polyethylene or reticulated polyurethane containing bubble matrix structure pierced at point of contact and connected short elements with three-dimensional lattice. Geometrical parameters determine the foam structure.

1.5. Methods for aerosol filter analysis

Techniques for filter analysis for aerosol deposited can be categorized into three, which includes gravimetric, microchemical and microscopic.

1.5.1. Gravimetric analysis

Aerosol mass concentration is measured after specified sampling period by weighing the increase in filter weight. The method involves higher efficiency aerosol

filter collection; thus, an increase in weight attributes directly to the collected aerosol. The following parameters must be independent of temperature, humidity and age of the filter weight. This analysis is considered to be more sensitive to the buildup of static charge, moisture and humidity. Water vapor uptake by the filter material leads to moisture retention and aerosol sample hygroscopicity. Cellulose quartz and glass fibre are less susceptible to moisture absorption than cellulose fibre filters. Interference of relative humidity with the filter can be minimized by equilibrating at constant temperature and humidity for 24 hours. Homogeneity is not considered important for certain filter analysis and gravimetric analysis. Operating procedure for gravimetric analysis is provided next.

New filters are stored in equilibrium trays at controlled temperature and humidity for at least 4 weeks in order to avoid the change in the blank filter weight from the production process and outgas any residues. Field-exposed filters are balanced in the same environment for 24 hours, allowing soluble deposits to reach equilibrium. Unexposed filters were divided into 150 mm diameter Petri culture dishes so that all the surfaces could establish an equilibrium environment. In order to achieve equilibrium environment, Petri dishes with filters are placed in laminar air flow hood with the lid slightly open. Each filter is inspected by placing it on the light table surface, and the flat tip of the sterilized forceps was used. In order to prevent contamination, non-powdered latex gloves were used.

1.5.2. Microscopic analysis

Physical characteristics, such as morphology, size and composition, are measured by using electron or light microscopy for the aerosol particle analysis. Straight through pore membrane and polycarbonate filters are suitable for microscopic applications because they are flat, smooth and have relevant surface collection. The selection of a filter for sampling airborne microorganisms, such as bacteria, fungus and viruses, necessitates counting the number of viable microorganisms or colony forming units under a microscope. During this process, the loss of moisture may be caused by the loss of viable microorganisms by filter surface collection. Thus, filter surface collection for these kinds of microorganisms is limited and thus transferred after the collection to proper growth media.

1.5.3. Microchemical analysis

The chemical analysis of filter media collection of particles is widely used for the application of air quality monitoring. The 2 main factors to be considered while selecting filter media for this analysis involve blank filters background response arising due to the interference minimization that occurs during the particulate matter quantity analysis and chemical transformation forming artefacts during and after filter sampling. Due to the low pressure drop and high-volume sampling, certain filters are suitable for microchemical analysis of aerosol particles, such as Teflon coated glass, cellulose, glass and quartz fibre. Aerosol extraction can be done with cellulose filter papers but has low particle collection efficiency. Quartz fibre, glass and Teflon coated

glass needs acid leaching for recovery but has higher particle collection efficiency, whereas glass fibre filter undergoes positive mass artefact in ambient air sampling due to the presence of slight alkalinity. Due to the low elemental blank concentration and low uptake of water vapor, quartz fibre filters are widely used in the microchemical analysis of aerosol sampling.

1.6. Cytotoxicity evaluation of aerosol particle

1.6.1. The overall structure of respiratory tract

The lungs are made up of a complicated network of different cell types, communications and uncontrollable movements. Designing in vitro models to investigate the health impacts of inhaled aerosols relies heavily on this substance's structure. With the help of millions of alveoli, a tree-like network of branching airways is connected to the trachea, and the lung's fundamental role of facilitating gas exchange between the air and venous blood [71, 72]. In pulmonary aerosol administration methods, non-cellular barriers, such as mucus and surfactant layer that shield the respiratory system from dangerous and harmless xenobiotics, must be taken into account [73, 74]. The trachea/bronchi and smaller bronchioles have pseudostratified epithelium, smaller bronchioles have cuboidal epithelium, and alveoli have squamous cells. The epithelial tissue of the lung develops from a single anlage but changes as the airways deepen. In fact, 95% of the surface of alveoli are lined by alveolar type I epithelial cells, which as well line pulmonary capillaries and share a basement membrane with them. Lung surfactant is secreted by the alveolar type II epithelial cells to avoid alveolar collapse [75, 76]. The intricacy of the lung epithelium is influenced by at least 40 different cell types, including epithelial cells, endothelial cells, fibroblasts, nerve cells, lymphoid cells, gland cells, dendritic cells and macrophages. All four areas of the respiratory tract contain components of lymphatic tissue. There are ongoing efforts to locate and examine specific lung cells, including cutting-edge cell types, such as pulmonary ionocytes that are important for comprehending disease causes [75, 77, 78].

1.6.2. Aerosol dynamics and lung dosimetry

The way in which aerosols interact with the structure of the lungs is a subject of great interest in the respiratory research. This includes being aware of the location and manner in which aerosols settle as well as the potential for inducing clearance systems. [79]. In order to establish the amount of aerosol that a biological model can absorb, it is critical to comprehend the physicochemical properties of aerosols, i.e., from production to characterization. Understanding the physicochemical properties of aerosols, from production to characterization, is essential for figuring out how much aerosol, a biological test model will absorb, which is known as dosimetry. Dosimetry is particularly important for pharmacology testing and has been discussed in studies involving nanoparticles and liposomal ciclosporin A [80]. Concentration, shape, solubility, size and density of aerosols are crucial factors to consider when detecting and measuring deposition in specific lung compartments [81, 82]. The nasopharyngeal cavity may filter out aerosols larger than 10 micrometres, while smaller aerosols are

deposited in the lung through sedimentation, diffusion or inertial impaction [83]. Aerosols must have a diameter of 0.01 to 0.1 μm to reach the lower airway. Clearance processes can be classified into physical and chemical clearance [73], the surfactant film, aqueous surface lining layer, mucociliary escalator, macrophages, epithelial cellular layer and dendritic cells are just a few of the cleaning structures that make up the lung's barrier [84].

1.6.3. Types of nanoparticles utilized for the clinical purposes

The use of nanoparticles in the medical applications, such as the delivery of medicines and genes, fluorescent labelling and contrast agents, shows great promise [85, 86]. At least one dimension of the material must fall within the range of 1–100 nm for it to be considered a "true" nanoparticle. Due to their capacity to more effectively target cancer cells, increase efficacy and lower toxicity in the body, nanoparticles are being used more frequently as medication carriers, notably for chemotherapy treatments. Gold nanoparticles (AuNP) are a great option for creating nanocarrier systems because of their advantageous properties, such as a non-toxic and biocompatible metal core [87]. Among a few metal oxide nanoparticles that have received therapeutic use approval, there are superparamagnetic iron oxide nanoparticles (SPIONs). They are used in a variety of biomedical contexts, including magnetic resonance imaging (MRI) [88], drug delivery [89], gene delivery [90] and destroying the tumour tissue with hyperthermia [89]. The characteristics of superparamagnetic iron oxide nanoparticles have many advantages. They can be directed by an external magnetic field, which can be utilized to direct medication delivery or target locations for imaging. Second, they may generate cytotoxic heat when exposed to alternating magnetic fields, which can have uses in the treatment of cancer [88]. Metal oxide nanoparticles can as well be found in externally applied goods, such creams and sunscreen lotions that contain titanium dioxide and zinc oxide NPs [91]. The ability of these NPs to penetrate into deeper epidermal layers, causing absorption to the bloodstream and accumulation in tissues, must be investigated. Nano scaled AgNP, which has exceptional antibacterial qualities, is widely used in medicine for a variety of applications, including bone prostheses, surgical equipment and bandages for wounds.

1.6.4. Innovative approaches to aerosol particle cytotoxicity assessment

Fine particles suspended in ambient air (aerosol particles) are known to cause adverse effect to human health. Depending on their size, they penetrate human airways and get settled in the upper respiratory tract (referred to as inhalable aerosol fraction), the middle respiratory tract (thoracic fraction) and the lower respiratory tract (respirable fraction). The latter fraction of aerosol particles is of special importance, since due to a small size, it reaches the lungs, enters the alveoli, and subsequently, bloodstream. The prevalence of several diseases, including cancer, cardiovascular disease and asthma, is increased by the aerosol particles. Therefore, it is crucial for the current human exposure studies to understand the reasons behind the negative

health impacts [136]. In vitro assays serve as a cost-effective, ethically favourable, and informative analysis for the observation and estimation of toxicity and its effects on cells [137]. Typically, in vitro assays rely on two main approaches, i.e., indirect (submerged exposure) and direct (air–liquid interface) [138]. Direct methods involve the deposition of aerosol particles directly onto cultured cells via a specially prepared membrane (i.e., air–liquid interface), allowing to physiologically mimic the inhalation process over a defined period. However, the direct air–liquid interface method mostly aims to quantify inhalation toxicology endpoints, as opposed to the general cytotoxicity. The method is based on directing aerosol stream onto monolayer of specially cultivated cells, placed in a specific exposure chamber. Such method provides a toxicological response to the real-time unaltered aerosol particles. The international patent application WO2011094692A2 is titled "Systems and methods for collecting and depositing particulate matter onto tissue samples". Direct aerosol in vitro exposure systems and methods are disclosed, and they are based on the electrostatic charge of the particles. Without pre-concentration or additional collection procedures, such as using water or a filter, these devices can be utilized to collect and deposit particle materials onto the tissue. An air-containing-particulate-matter input, a container for holding one or more tissue samples, a porous membrane supporting the air–liquid interface of the tissue sample and an area for electrostatic precipitation can all be found in the system. The air received at the input can have particulate particles in it that can be electrically charged at the electrostatic precipitation area and flow over the tissue sample where they are collected and measured. The US patent application US2018171280A1 "Cell culture exposure system (cces)" describes an air–liquid interface (ALI) exposure of cultured cells using a direct aerosol in vitro exposure method. A process for determining the impact of a polluting airstream includes the following steps:

1) Exposing cells to a membrane until adhesion of the cells has occurred,
2) Feeding cells periodically until there is a confluent monolayer of cells on said membranes,
3) Aspirating off non-adherent cells, applying fresh media,
4) Exposing the cells to over-head stream containing pollutants,
5) Removing the cells from the membranes that have been exposed to the over-head stream,
6) Measuring the cells' response to toxins in the over-head stream.

The indirect method is based on the following sequence of operations:

1) Collecting aerosol particles onto sampling substrates or filters,
2) Recovering aerosol particles from a filter by using extraction to a liquid (usually phosphate buffer solution, methanol or Gamble's solution),
3) Filtering the extract from remaining insoluble particles,
4) Placing extract into culture medium containing cells,
5) Recording the cell response.

This (indirect) method is comparatively simpler than the direct method since it does not require specific equipment for exposing cells. A major drawback of the

indirect method is that it only indicates the toxicity of soluble particles that dissolve in the liquid media during the extraction process. This causes the level of toxicity to be underestimated [79, 139].

In the Chinese patent application CN102346147A, the phrase "Method for Detecting Difference of Cell Toxicity Between Atmospheric Nanoparticles and Industrial Nanoparticles" refers to a deceptive approach for determining the difference in cell toxicity between the air nanoparticles and industrial nanoparticles. The steps in the procedure are as follows:

1) Creating a cell suspension in a culture medium, placing the cell suspension in a cell culture dish and incubating the culture dish for 24 hours,
2) Producing a contaminated solution by combining a prepared particulate matter solution with the culture medium, cleaning the cells with a D-hank's balanced salt solution, contaminating the cells and then cultivating the contaminated cells for four hours in the incubator,
3) Mixing the culture media with a DCFH-DA fluorescent probe, closing the container and wrapping it in tin foil paper before incubating the mixture for 0.5 hours,
4) Using an inverted fluorescence microscope to observe the fluorescence intensity and distribution while taking pictures,
5) Using fluorescence analysis software to process photos to get preliminary data, analysing and contrasting.

According to the method, the preparation of the cell section is quick and easy, and it is simple to obtain raw material. By using the cell detection method, the result is accurate, the influence factor is reduced, and multiple nanoparticles can be detected at once. The method does not include the procedure for the collection of aerosol particles. It may be assumed that this procedure involves the collection on certain filter and subsequently extracting particles into a solution, which makes it a classical indirect method. The above presented information indicates that the determination of aerosol particle cytotoxicity is a complex multistage procedure, both by indirect and direct methods; thus, the simplification of this procedure is highly appreciated [136].

Current direct methods involve deficiencies including:

1) Cytotoxicity determination based on the inhalation toxicology endpoint only,
2) Preparation of cell monolayer is complicated and time consuming,
3) Costly method due to the requirement of specific equipment, i.e., exposure chambers.

Current indirect methods involve deficiencies including:

1) A long aerosol particle collection time, usually, high-volume sampling is necessary, i.e., at least 900 m^3 of air is needed to collect enough fine particulate matter to result in a toxicological response.
2) Transfer of particles from a filter substrate by solvent extraction, dissolve and filter residual particles: such sequence requires the utilization of time and equipment. Moreover, due to the partial solubility of particulate matter in a selected solvent, only partial information of particle cytotoxicity is obtained [140].

1.6.5. In vitro cytotoxicity evaluation technique

It is possible to evaluate the lung toxicity of airborne NPs by using both in vitro and in vivo models. In order to evaluate the toxicity of NPs in commercial applications, in vitro assays are thought to be less complex, quicker and more affordable [141, 142]. Since it might be difficult to mimic particle–cell interactions in vivo, in vitro models have the benefit of allowing in-depth studies by using human lung cells [143]. NPs are typically dissolved in the culture media before being administered as a suspension to the lung cells. However, this method may result in changes to the characteristics of NPs as a result of interactions between the particles and with other elements of the medium. Despite the fact that the alveolar epithelium, which has a huge surface area and a thin barrier thickness, is where most inhaled NPs enter the body [144, 145], because there is no suitable mechanism for exposing NPs to cells, it is still unclear exactly how NPs interact with alveolar epithelial cells. Therefore, an ideal in vitro testing system should have a number of essential components, including the ability to accurately measure cellular dose, simulate the aerosol deposition mechanism to mimic actual lung conditions and use cell types that accurately represent those targeted by NP exposure routes.

1.6.6. Viability assay (LDH release)

Numerous techniques are widely used to evaluate cell viability. Cell viability is typically assessed by using tetrazolium reduction tests, LDH assays, immunohistochemistry apoptosis biomarkers and comet assays for genotoxicity [146]. Electron microscopy is used for NP intracellular localization. In order to determine cell toxicity in laboratories, the LDH test is frequently employed. These assays include the incubation of a reagent with a cell culture; the live cells then transform the reagent into a coloured or fluorescent product, which is subsequently identified by using a plate reader. No colour or fluorescence is produced by non-viable cells since they are unable to convert the reagent. However, NPs' distinctive physicochemical characteristics can interact with assay components or obstruct the readout, which could result in inconsistent results. Carbon nanomaterials, for instance, have been observed to exhibit such effects [147, 148, 149, 150].

A more modern method that involves minimally invasive real-time cell-microelectronic sensing has been used to assess the cytotoxic effects of NPs. Additionally, because of their inherent optical characteristics, NPs themselves can interfere with the readout directly, increasing light absorption, as it was seen with sodium titanate NPs. The LDH assay has been frequently used to evaluate the cytotoxicity of NPs, including those consisting of silica, iron oxide, titanium oxide and zinc oxide, since the release of a sizable amount of LDH from the cytosol occurs following cellular necrosis [151]. However, the scientific community is concerned with the LDH assay's consistency. According to reports, LDH activity sharply declines in low pH environments while becoming unstable in high pH environments [152].

1.7. Summary of literature review

Aerosol particles are small, suspended particles that are known to have a negative impact on human health. They enter human airways and settle in the upper respiratory tract, known as the inhalable aerosol fraction, the middle respiratory tract, known as the thoracic fraction, and the lower respiratory tract, known as the respirable fraction. Due to its small size, the latter portion of aerosol particles is especially significant since it can enter the bloodstream after entering the alveoli and reaching the lungs. The prevalence of several diseases, including cancer, cardiovascular disease and asthma, is increased by the aerosol particles. Therefore, it is crucial to understand the root causes of negative health impacts for current human exposure investigations.

Among the most popular techniques for sampling aerosols is the collecting of aerosol particles on a filtering substrate. The varieties of membranes, foams and fibrous matrixes make up the filtering substrates. Two groups of membrane filters are often distinguished:

a) Porous membranes with intricate structures and winding passageways through the filter material; these membranes are known to be made of polytetrafluoroethylene or cellulose-esters;

b) Alternatively, capillary pore filters made of polycarbonate, polyethylene terephthalate, etc. have straight through pores throughout the membrane.

Membrane filters are highly stable and effective at capturing particles. However, they do offer a significant pressure drop within the filtering membrane layer's thickness. Large-pored volume mesh is how foam filters are made, and this allows to capture of course (respirable) particles. These filters are made of stainless steel or polymer (polypropylene).

The building blocks of fibrous matrices are dense meshes of fibres with erratic orientations. Within the depth of the filtering layer, they gather aerosol samples, offering great filtration efficiency with a relatively small pressure drop. Typically, cellulose or natural materials, such as glass or quartz, are used to create fibrous matrixes.

Although fibrous filters are among the most used substrates for aerosol sampling, they have a number of shortcomings: a) as filters have a wide surface area, substances with a higher volatility that are present in the measured particles, such as certain PAHs or organometallic compounds, evaporate from the filter over time; b) mineral fibre blank values may have an impact on the following chemical analyses (aerosol particles, such as metals); c) some formulations of pure mineral fibres (such as Quartz) are mechanically fragile and break apart when handled. There are limited possibilities for fibrous aerosol sampling filters due to their chemical makeup and fibre shape (porosity, fibre size and pore size). Additionally, a variety of chemical analysis techniques and recently created methods for chemical analysis of the collected particles need the creation of unique filters with unique chemical compositions. When chemical characterisation is required, sampling on a variety of substrates is typically necessary because no one filter medium is adequate for all intended chemical tests.

The number of fibrous aerosol sampling filter options is limited based on their chemical composition and fibre morphology (porosity, fibre size, pore size). At the same time, the broad variety of chemical analysis methods as well as emerging new methods for chemical analysis techniques of collected particles require the creation of bespoke filters having unique composition. No single filter medium is appropriate for all desired chemical analyses, and it is often necessary to sample on multiple substrates when chemical characterization is desired. The present invention allows the fabrication of bespoke aerosol sample collection filters using several techniques of electrohydrodynamic polymer processing from the plurality of polymers (benefiting the selection for subsequent chemical analysis of the collected particles) and obtaining plurality of surface morphologies (benefiting the selection for sampling particles of various sizes and shapes).

Fine particles suspended in ambient air (aerosol particles) are known to cause adverse effects to human health. Depending on their size, they penetrate human airways and get settled in the upper respiratory tract (referred to as inhalable aerosol fraction), the middle respiratory tract (thoracic fraction) and the lower respiratory tract (respirable fraction). The latter fraction of aerosol particles is of special importance, since due to small size, it reaches the lungs, enters the alveoli, and subsequently, bloodstream. Aerosol particles increase the incidence of various diseases, such as asthma, cardiovascular, cancer and others. Therefore, understanding the causes of the adverse health effects is of paramount importance in current human exposure studies. In vitro assays serve as a cost-effective, ethically favourable and informative analysis for the observation and estimation of toxicity and its effects on the cells.

Typically, in vitro assays rely on two main approaches, i.e., indirect (submerged exposure) and direct (air–liquid interface). Direct methods involve the deposition of aerosol particles directly onto cultured cells via a specially prepared membrane (i.e., air–liquid interface), allowing to physiologically mimic the inhalation process over a defined period. In this way, the method is more advantageous than the indirect method, since the dose of particles can be determined more precisely. However, the direct air–liquid interface method mostly aims to quantify inhalation toxicology endpoints, as opposed to the general cytotoxicity. The method that was used is based on directing aerosol stream onto monolayer of specially cultivated cells, placed in a specific exposure chamber. Such method provides a toxicological response to the real-time unaltered aerosol particles.

In order to observe and estimate the toxicity and its effects on cells, in vitro experiments offer a practical, ethically acceptable educational approach, especially since it involves an in vitro method where the sacrifice of rats or mice is not necessary.

The contribution of the author of this dissertation is focused on researching the current state of knowledge regarding nanofibre filtering material production via solvent electrospinning and its implications for cytotoxicity evaluation. The author has provided comprehensive insights into the optimization of production parameters, highlighting the need for further research to enhance material quality and performance. Additionally, the author of the dissertation has emphasized the importance of developing advanced cytotoxicity evaluation techniques tailored to

nanofibre materials to ensure higher filtration efficiency, lower pressure drop and estimate toxicity in vitro. Overall, the contribution aimed to provide a thorough understanding of the key challenges and opportunities in this field, laying the groundwork for future research endeavours.

2. MATERIALS AND METHODS

2.1. Materials

2.1.1. Polymers

Poly[ε]caprolactone (PCL, Mw~80,000, Product No. 440744, Sigma-Aldrich), cellulose acetate (CA, Mw~30,000, Product No. 180955, Sigma-Aldrich), poly(1-acrylonitrile) (PAN, Mw~150,000, Product No. 181315, Sigma-Aldrich), poly(bisphenol A carbonate) (PC, Mw~45000, purity 100%, CAS no. 25037-45-0) and poly(hexano-6-lactam) (PA6, Mw~100,000, Product No. 181110, Sigma-Aldrich) were used as polymer materials for fibre production. Polyethylene glycol (PEG, Mw~400, CAS no. 25322-68-3) from Panreac and Scharlau provided the potato dextrose agar used for solvent casting. All polymers were completely soluble in the solvents selected for each layer of the filter.

2.1.2. Solvents

Formic acid (98%, Product No. F0507, Sigma-Aldrich), acetone (99.8%, Product No. 34850-M, Sigma-Aldrich), glacial acetic acid (99.5%, Product No. A6283, Sigma-Aldrich), N, N-dimethylformamide (DMF) (99.8%, Product No. 227056, Sigma-Aldrich), dichloromethane (DCM), purity 99%, Cat. No. 24233-M, Sigma-Aldrich, and N, N-dimethylacetamide (DMA) (99.8%, Product No. 271012, Sigma-Aldrich), tetrahydrofuran (THF) (99.8%, Product No. 102391) were used as polymer blending solvents. Hexadecyl trimethyl ammonium bromide (CTAB), ≥98% CAS no. 57-09-0, a cationic surfactant, was used to achieve bead free fibres, and all were purchased from Sigma-Aldrich, USA.

Sodium chloride (NaCl) and bis(2-ethylhexyl) sebacate (DEHS) (Cat. No. 290831, Technical grade 90%) were used for the creation of test aerosols; they were both acquired from Sigma-Aldrich, USA. Electrospun nanofibres were fabricated by using all materials without undergoing any purification process.

Table 2.1. Electrospinning solvent properties [153]

Solvents chemical formula	**Boiling point (°C)**	**Surface tension/ (m Nm^{-1})**	**Dielectric constant (ε)**	**Density (g cm^{-3})**
Formic acid: CH_2O_2	101	-	57.9	1.22
Acetone: C_3H_6O	56	25.20	20.7	0.791
Glacial acetic acid: $C_2H_4O_2$	118	27.10	6.15	1.050
Dichloromethane: CH_2Cl_2	40	28.1	8.93	1.325
N, N-dimethylacetamide: C_4H_9NO	166	36.70	37.8	0.937

N, N-dimethylformamide: C_3H_7NO	153	37.10	36.70	0.944
Tetrahydrofuran: C_4H_8O	65	26.40	7.58	0.885

2.1.3. Culture of cells

An immortalized human bronchial epithelium cell line, BEAS-2B, was used in the investigations. The cells were grown in Nutrient Mixture Kaighn's Modification Medium (F-12K Nut Mix, Gibco), supplemented with 10% fetal bovine serum (FBS), 1% penicillin (100 U/mL)/streptomycin (100 g/mL) (P/S) and 0.4% amphotericin B (Gibco) and incubated in a humid incubator at standard temperatures (5% CO2 at 37 °C). At 80% confluence, the cells were collected with a 0.25% trypsin-EDTA solution. BEAS-2B cells from passages 5 through 13 were employed. Every 2 to 3 days, the medium was replaced.

2.1.4. Nanoparticles

The following nanoparticles have been used: silver nanoparticles, 99.5% trace silver base, size <100 nm, PVP as dispersion, Cat. No. 576832, Sigma-Aldrich, number CAS 7440-22-4; copper nanoparticles, Cat. No. 774103, Sigma-Aldrich, 60–80 nm, >99.5% trace copper basis, number CAS 7440-50-8; 12–20 sheets of graphene oxide with a 4–10% edge oxidation, contains 50% ≥ carbon, 5% water and ≤11% oxygen, Cat. No. 796034, Sigma-Aldrich.

2.2. Design of experiments

This project aims to create and validate nanofibrous filters with 3-layer for collecting aerosol particles. It involves designing and characterizing these filters, exploring their performance under different airflow conditions and validating them as platforms for cytotoxicity analysis.

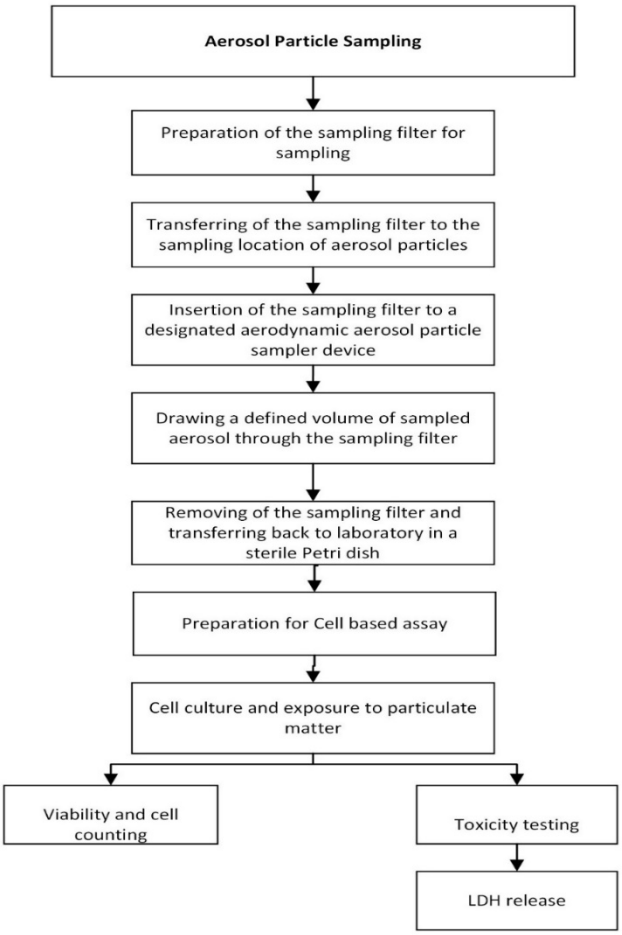

Fig. 2.1. The procedure of utilizing composite fibrous aerosol particle sampling filter for the collection and in vitro toxicity testing of aerosol particles

2.2.1. The fibrous matrix usage as an aerosol particle sampling filter

The design of the aerosol sampling filter described in this thesis presents an approach aimed at optimizing the key operational parameters that are crucial for effective particle collection. This filter configuration comprises a 2D composite filter with a minimum of three layers of non-woven fibrous matrices. The layered structure is carefully engineered to ensure superior mechanical stability, high particle collection efficiency and an optimal pressure drop across the filter layer. Layer 1, positioned at the base, consists of a microfibre network that provides robust mechanical support for the upper layers. Layer 2, situated centrally, comprises larger nanofibres to facilitate binding between the top and bottom layers while offering additional mechanical reinforcement. Layer 3, the uppermost layer, acts as the primary collection surface for aerosol particles. The thickness ranging between 50 and 150 micrometres, depending on the materials employed, the composite filter operates primarily as a surface filter,

capturing particles above the fibres through mechanisms such as impaction, interception and diffusion. Sized according to the standard diameters for sampling devices, the filter discs typically measure 25 mm, 37 mm or 47 mm with provisions for customization. The production of this composite filter involves the integration of two modifications of the electrohydrodynamic polymer processing technique, i.e., melt electrospinning and liquid–solution electrospinning. This filter is made to have numerous important characteristics including:

1) It must efficiently capture aerosol particles (>99.5% for respirable aerosol particles);

2) It must have enough mechanical rigidity to keep its shape while being handled, sampled for particles and used in in vitro cell seeding procedures;

3) It must be non-cytotoxic and biocompatible;

4) The aerosol sampling filter is built as a composite filter disc with at least three non-woven fibrous layers, and it must enable cell attachment and growth for at least 72 hours.

2.2.2. Electrospun nanofibres on 3D printed PC for aerosol filtration

The substantial surge in industrialization has now led to a decrease in the quality of air, thereby increasing health problems. Air filtration has been recognized as an operational way to reduce PM pollution for decades. Nanofibrous filtration is regarded as an effective substitute for well-known technology due to its governable morphology with exceptional diameter/length ratio in a continuous method. The experimental design model for each PC electrospun nanofibre included the following parameters: nanofibre collection time, solvent ratio, deposition voltage, tip-to-collector distance and polymer concentration. The study focused on determining the media's average fibre diameter, shape, filtering effectiveness and pressure drop. The nanofibrous layer exhibited a fibre diameter ranging from 0.19 ± 0.04 μm to 0.56 ± 0.14 μm. This unique morphology enabled the filters to consistently achieve an efficiency of particle collecting between 98.4 and 99.9%. Using the experimental results, the response surface plots were generated to visually represent the relationship between various factors and the desired characteristics of nanofibre media, including fibre diameter. Building upon the modelling outcomes, nanofibre filter media were subsequently fabricated. Such filtering media allowed for reaching high filtering efficiency (99.9%) with reasonable pressure drop.

The research aimed at developing high efficiency air filtration media: a series of experiments were conducted by using solution electrospinning. Seven distinct polycarbonate nanofibre layers were electrospun onto a 3D printed polycarbonate support layer, which prevents breakdown during low-pressure sampling, and to collect aerosol particles on the top electrospun nanofibrous layer. The morphology of the surface, the fibres' typical diameter was carefully examined: consistently smooth and free of beads nanofibres were further analysed for filtration capabilities.

2.2.3. The fibrous matrix usage as a 2D cell cultivation platform and for the cytotoxicity testing of aerosol particles

These fibrous matrixes are used in the current procedure as substrates for in vitro cell cultivation as well as scaffolds or membranes. The three-layer structure ensures fibrous 2D cell cultivation surface's key operational characteristics for in vitro cell culture, including no intrinsic cytotoxicity, low surface roughness, small pores and good mechanical stability during handling and when submerged in cell cultivation media. Human non-tumorigenic lung epithelial cell line (BEAS-2B) has been used to demonstrate the substrate's use as a fibrous 2D cell growth platform. The cells were cultured for a predetermined amount of time on a clean substrate using the procedure described below, after which Real-time-Glo MT Cell Viability Assay (Promega) measurements were made. By measuring the amount of light released by the cells after the exposure to a cell-permeant form of the Glo reagent, this technique calculates the vitality of the cells. The amount of ATP produced by the cells is directly measured by the luminescence signal, which is proportional to the quantity of live cells. As a result, higher luminescence signals and lower luminescence signals imply higher and lower cell viability, respectively. Beas-2B cells luminescence signal grew with time, indicating proliferation and vitality on all types of membranes that were examined. The membrane with a polyamide 6 top layer had the lowest luminescence signal, which indicates the lowest proliferation rate among the investigated matrixes. The membrane with a cellulose acetate-made top layer produced the highest proliferation/metabolic activity.

This technique reduces the steps needed for sample extraction, dissolution and transfer to cells (in the case of an indirect method) or avoids a difficult sampling setup (in the case of a direct method) and instead provides an optimized method based on a single integrated platform for aerosol particle collection and cell cultivation. The technique may be used to assess the cytotoxicity of aerosol samples taken from a range of sizes, including but not limited to indoor work environments, indoor homes, indoor hospitality settings, indoor public spaces and atmospheric urban and rural air. The suggested technique enables the assessment of the cytotoxicity of a wide range of aerosol particles, such as combustion aerosol and designed nanoparticles, combustion aerosol particles, secondary organic aerosol particles or tobacco product aerosol particles.

The study introduces an innovative integrated platform aimed at bridging the gap between in vitro cytotoxicity testing and aerosol sampling.

The study's distinctiveness is evident in several key aspects provided below.

Unified platform design: a significant breakthrough lies in combining aerosol collection and in vitro cytotoxicity analysis on a single platform. This approach overcomes the limitations of separate procedures, reducing the risk of particle loss or alteration and ensuring that the tested particles closely mimic those present in the original aerosol.

Versatile sample filters: the research presents novel multipurpose sample filters designed for aerosol collection. These filters enhance the reliability and relevance of

toxicological data by effectively capturing a wide range of aerosol types and facilitating subsequent cytotoxicity studies.

Cutting-edge in vitro cytotoxicity assessment: within the same platform used for aerosol collection, the study integrates state-of-the-art in vitro methods for cytotoxicity investigation. This approach minimizes uncertainties stemming from storage and transportation processes, streamlines the workflow and enables immediate cytotoxicity analysis.

Comprehensive toxicity profiling: the platform is designed to provide a multi-parameter toxicity profile that considers genotoxicity, oxidative stress, inflammation and cell viability. Beyond traditional cytotoxicity assessments, this thorough analysis offers valuable insights into potential health risks associated with the aerosol exposure.

2.3. Aerosol particle three-layer sampling filter

2.3.1. Manufacturing of the filter substrate

The electrohydrodynamic polymer processing technology known as electrospinning was used to create the fibrous aerosol particle sampling filter material. In order to create the final structure of the filter, two variants of this technique were used.

To begin with, micro fibrous layers were created using a combination of melt electrospinning and fused deposition modelling. The 3D Fibre Printer (3Df-01C, Bious), used to do this, is a proprietary device.

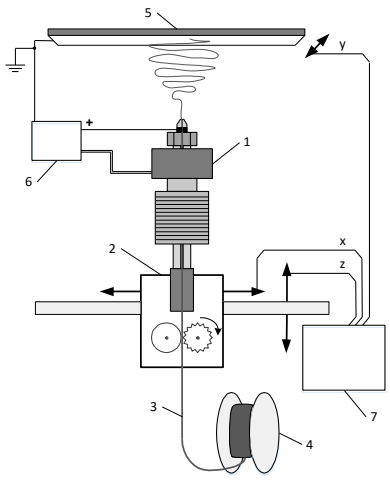

Fig. 2.2. An illustration of the 3D-printing setup using fibres: nozzle heating, a filament extruder, a filament, a filament coil, a grounded collection plate, a high voltage supply and an axis control are all included in the diagram

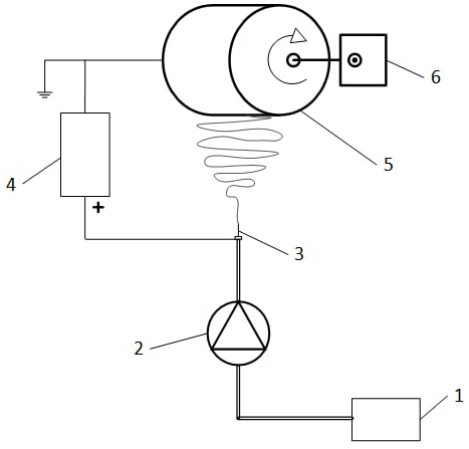

Fig. 2.3. An illustration of the setup for solution electrospinning solution reservoir: syringe pump, metal needle, high voltage supply, grounded rotating collector and rotation motor are shown in the diagram above

It operates on the same principle as a fused deposition 3D printer (Fig. 2.2), in which a polymer filament (in this case, PCL) is fed through an extruder to a hot end, melted and then deposited on a collector with the help of high voltage between the hot end and collector surface with the latter being positioned in three dimensions by a computer algorithm [154]. Through this process, a layer of non-woven, randomly or semi-randomly oriented microfibres is produced that has a homogeneous structure, high porosity and is suitable for supporting nanofibrous layers due to its moderate mechanical stability.

Solution electrospinning is a different method that can create fibres with a sub-micrometre diameter. The primary components of the fabrication setup (Model SE-01C, Bious Labs, Lithuania, Fig. 2.3) are as follows: 10 ml of the polymer solution in a plastic syringe, a syringe pump, a metal needle with a blunt tip, a revolving metal collector and a high voltage source attached to the metal needle and the rotating collector are shown in Fig. 2.3. While a revolving collector is grounded, a needle attached to a positive electrode of a high DC voltage source is used to force the polymer solution through. A dense filtering layer is created by the production of nanofibres on a collector surface as a result of high voltage electrical field [155].

As stated in the results sub-section (3.1), the fibrous layers created using both approaches were combined to create a single product. Following completion, the substrates were allowed to dry for 12 hours in a vacuum room with the goal of cleaning any remaining solvents from the solution electrospun membranes. Until further testing, the membranes were kept at 40 °C in sealed polypropylene bags. Sharp chisels were used to cut the filter substrate samples to diameters of 25 mm or 37 mm.

2.3.2. Efficiency of filtering out simulated aerosol particles

In a specifically made testing device (Fig. 2.4), aerosolized NaCl and DEHS particles were used to challenge the filters' ability to filter out the particles. The NaCl solution in deionized water (0.1% w/v), and DEHS were supplied via a collison nebulizer (Model CN 6 J, BGI Inc., USA) and diluted with dry air in a porous tube diluter to produce polydisperse aerosol. An 85Kr bi-polar neutralizer (3054 A, TSI Inc., USA) was then used to achieve charge equalization. Filter holders were filled with samples of filters that had a diameter of 37 mm. An illustration of the fibre-based 3D printing setup is provided. It includes a grounded collection plate, a high voltage source, a filament extruder, filament and filament coil as well as nozzle heating. Both upstream and downstream particle concentrations were monitored using the electrical low-pressure impactor (ELPI +, Dekati Ltd., Finland). With a face velocity of 5.3 cm/s, a pressure sensor (Model P300-5-in-D, Pace Scientific Inc., USA) first monitored the pressure drop before and after the sample medium, and then at intervals between 3 and 20 m/s.

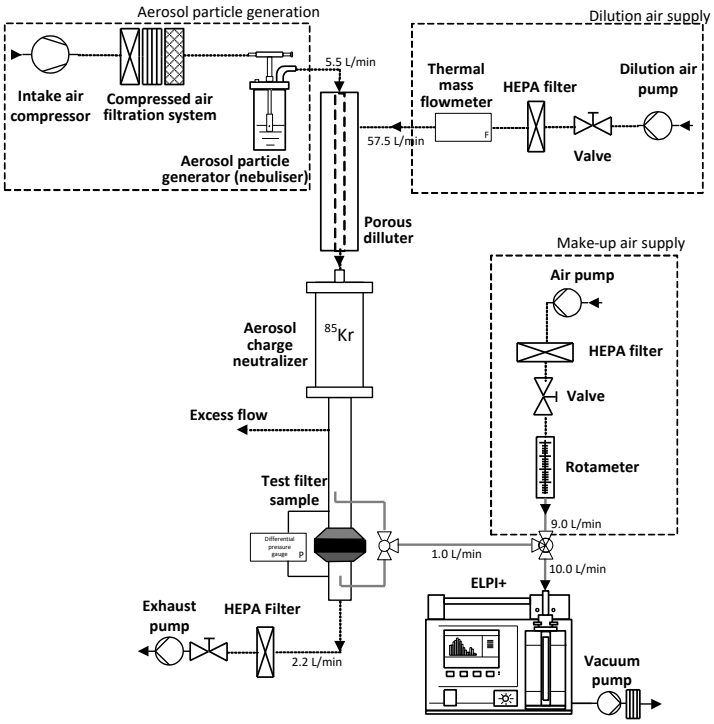

Fig. 2.4. Filter material testing setup for particle collection efficiency and pressure drop

2.4. Electrospun PC nanocoating on 3D printed support

2.4.1. Preparation of polymer solutions

In order to electro spin PC, the solvent was carefully chosen, as it needs to be able to dissolve the PC and not evaporate quickly enough that it would not interfere with the electrospinning process. DMF and THF were chosen to dissolve PC for producing nanofibres. Polycarbonate (wt%) and CTAB (wt%) with varying concentration was dissolved in a mixture of N, N-dimethylformamide, tetrahydrofuran in a 7:3 (v/v) ratio to achieve homogeneous solutions. This dissolution process involved mechanical stirring at a temperature of 55 °C. It is worth mentioning that DMF has a comparatively higher boiling point of 153 °C compared to THF, which has a boiling point range of 65–67 °C. The PC concentrations in the solutions varied between 14%, 17% and 20% (wt/v), while the concentrations of CTAB ranged from 0.2 to 0.8% (wt%) relative to PC.

The 3D printed PC support fabricated in the lab (Bious Labs, Lithuania) was used for collecting electrospun nanofibres. Mesh-type polycarbonate supports (size of 80 x 50 x 0.4 mm, mesh size of 0.786 x 0.786 mm) were made using commercial 3D printer. Polycarbonate filament (P51, Sigma-Aldrich) with diameter of 1.75 mm were extruded using 0.4 mm nozzle at a temperature of 235 °C. Printing pad temperature was kept at 85 °C. The mesh structure was formed using G-code made by slicing

software. Manual calibration was followed by the air cooling and winding up of the filaments. These concentration ranges were the experimental design followed a MODDE 7 software (Umetrics AB, Sweden) developed D-optimal-interaction model, ensuring the formation of well-defined nanofibres.

2.4.2. Electrospinning process and filter material development

The process of electrospinning begins by exposing PC solution to high DC voltage of 22 kV based on the flyback principle across a capillary containing 10 ml syringe with 21 size needle gauge, and the solution was delivered at a flow rate of 0.5 mL/h with tip to collector distance of 15 cm. The rotation was set at a linear speed of 150 cm/min, equivalent to the rotation frequency of 6 rpm. The electric field causes the solution to be pulled through the capillary tip, forming a thin jet. The temperature and humidity of the apparatus was maintained at 250 °C and 50% throughout the experiment. The jet is then collected on a 3D printed substrate attached to the grounded collector where the solvent evaporates, leaving behind the PC fibres. The fibres are collected on a 3D printed polycarbonate substrate and used for further characterization. Pressure Drop of PC filters at Various Flow Rates for Different PC and CTAB Concentrations is tabulated in Table 2.2, where PC1, PC2, PC3, PC4, PC5, PC6 and PC7 corresponds to PC14%, CTAB 0.2%, PC14%, CTAB 0.8% PC17%, CTAB 0.5% PC17%, CTAB 0.5%, PC17%, CTAB 0.5%, PC20%, CTAB 0.2%, PC20%, CTAB 0.8%. The manufacturing apparatus was used (designated as Model SE-01C and manufactured by Bious Labs in Lithuania) [155].

Table 2.2. Pressure drop of PC electrospun filters at various flow rates for different PC and CTAB concentrations

PC and CTAB concentration (%)	**Pressure drop (Pa)**	**Pressure drop (Pa)**	**Pressure drop (Pa)**	**Pressure drop (Pa)**
Flow rate (l/min)	1.7	2.5	4.4	11.2
PC1	436.3	650.3	1,212	2,390.7
PC2	242.3	361.3	667.3	1,877
PC3	119.3	158	292.3	808
PC4	87	126.7	234.7	652.3
PC5	222.7	415.7	593	1,610.3
PC6	175.3	257.7	458.3	1,208.7
PC7	225	332	602	1,651

The modde generated parameters for forming polycarbonate nanofibre using the electrospinning process are shown in Table 2.3. The electrospinning was conducted within a Plexiglas chamber at normal environmental conditions. The properties of the resulting fibres can be altered by adjusting various factors, including the characteristics of the polymer solution, applied voltage (V), needle gauge (n), flow rate (Q) and distance (d). In order to minimize the impact of air currents on the path

of the electrospun jet, the needle, electrode and grounded target are all contained within a chamber.

2.5. A single platform for both aerosol particle collection and cytotoxicity in vitro

2.5.1. Fabrication of a nanofibrous sampling platform

A melt 3D printer was used to create the polycaprolactone microfibre layer (substrate, bottom layer, Fig. 2.5 a) on which the micro- and nanofibre layers were created (Bious Labs Tech & Life, https://tech.biouslabs.com/). The macrofibre layer was a 5 x 10 cm in size. Polycaprolactone filament was dried at 35 °C for 12 hours before manufacturing. The polymer filament supply speed was 1.5 mm/min, the supply head to collector distance was 2 cm, the voltage was 12 kV, and the sample formation time was 1 h. The production chamber's ambient temperature was 20 °C, and the relative humidity level was 30%. In order to lessen imperfections and improve uniformity, the samples of the produced macrofibre layer were pressed for 20 seconds at a force of 20 kN.

The middle microfibre layer in Fig. 2.5 b was created in the manner described below. In order to create a CA platform, a solution of CA was created by dissolving 2.5 g of CA in a mixture of solvents (3:2, 6 ml of acetone and 4 ml of DMA) to create a 25% w/v CA solution, a magnetic stirrer running for 24 hours at 250 rpm and 25 °C (cat. no. 06-SH2-4C; ChemLand, Poland). A PCL solution was created for the PCL, PA6 and PAN platforms by dissolving 3.0 g of PCL in a solvent mixture (2:3, 6 ml of acetone and 9 ml of DMF) to create a 20% w/v PCL solution, utilizing a magnetic stirrer (ChemLand, Poland, Cat. No. 06-SH2-4C) at 350 rpm and 60 °C for 24 h.

As shown in Fig. 2.5 b, the top layer of the nanofibrous layers was created. Thus, 1.7 g of CA was dissolved for the CA nanofibrous layer in a 2:1 solvent mixture (6.7 ml of acetone and 3.3 ml of DMA) to produce a 17% w/v CA solution. A magnetic stirrer (Cat. No. 06-SH2-4C, ChemLand, Poland) was used to stir the mixture for 24 hours at a temperature of 25 °C and 250 rpm. In order to prepare PCL at a 20% w/v concentration, 3.0 g of PCL was dissolved in a mixture of solvents (2:3), including 6 ml of acetone and 9 ml of DMF, at 350 rpm and 60 °C, stirring with a magnetic stirrer (Cat. No. 06-SH2-4C, ChemLand, Poland) for 24 h.

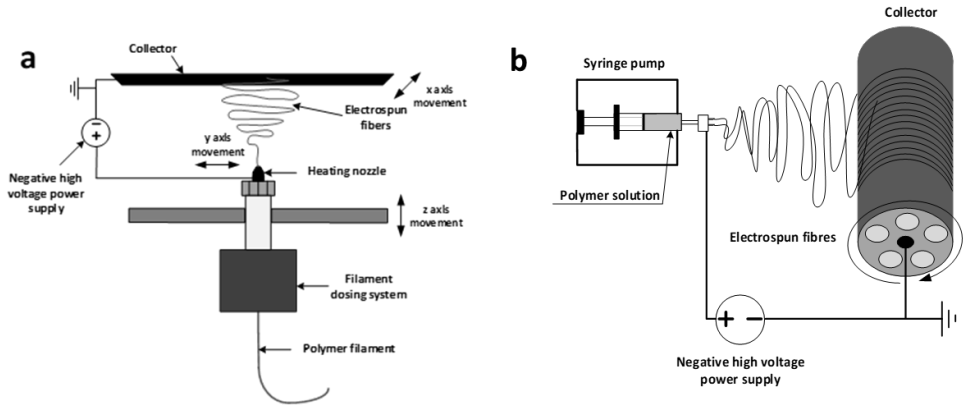

Fig. 2.5. Setup schemes of electrohydrodynamic processes: melt based fibre printing process (a) and solution based micro and nano fibrous layer formation process (b)

An electrohydrodynamic procedure (solution electrospinning) was used to create nano- and micro fibrous layers on top of the macro fibrous substrate (Bious Labs Tech & Life (https://tech.biouslabs.com/), the company that produced the solution electrospinning device). The needle was 15 cm from the collector, the voltage was 22 kV, the needle ID was 0.7 mm, and the flow rate of the polymer solution was 2 ml/h. The relative humidity in the formation chamber was 45%, and the temperature was 30 °C. The sample formation took place for 60 minutes.

2.5.2. Nanofibrous aerosol sampling and testing platform

The platform has three layers, each with a distinct function, as depicted in Fig. 2.6. During the manufacturing process, these layers are produced one on top of the other. Large diameter linked PCL threads make up the microfibre layer. This layer gives the platforms for sampling and measuring mechanical strength and stability. Having less flow resistance, it has big pores. The platform's midsection had a microfibre layer on it. Since the creation of nanofibres on the microfibre layer is unsuitable due to the macroscopic pores, which result in irregularities and flaws; this middle macrofibre layer serves as the foundation for the formation of the nanofibre layer. Microfibres with a diameter of typically less than 10 micrometres are incredibly small fibres. Often utilized in garments and cleaning products, they are recognized for their resilience, suppleness and capacity to wick away moisture. However, macrofibres are found in conventional textile materials, such as cotton and wool, and have bigger diameters, more than 10 micrometres, and are used for a variety of applications, including apparel and building materials.

Low aerosol particle retention efficiency is a characteristic of the microfibre layers, which are meant to create an environment conducive to the stability and effectiveness of the nanofibre layer. A nano diameter PCL fibre network with tiny, linked pores make up the nanofibre layer. This three-layer platform was created to efficiently collect aerosol particles on its surface and perform cytotoxicity studies on cells directly on the nanoparticles they had collected. The platforms for sampling and

testing must exhibit excellent aerosol particle collecting efficiency, stability, mechanical toughness, non-toxicity and biocompatibility with the research cells.

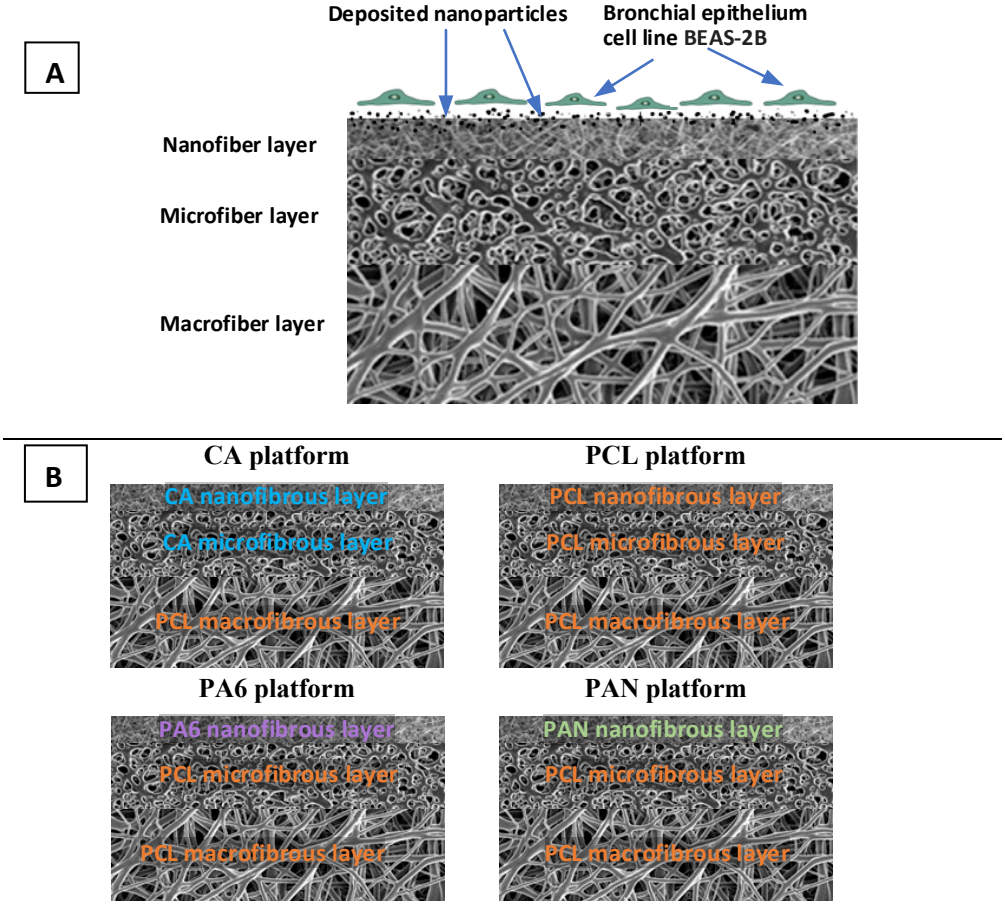

Fig. 2.6. Principal scheme of the cross section of nanofibrous sampling and testing platform (A), types of produced nanofibrous sampling and testing platforms: CA, PCL, PA6 and PAN (B)

In this investigation, four different platform types were created and put to the test (Fig. 2.6). The ability of PCL to form macro-sized fibres (diameter 10–100 µm) in materials with large (diameter 20–200 µm) linked pores is what causes the macro fibrous layer of all products produced from the PCL. The CA platform's nano- and micro fibrous layers were made from CA. A natural polymer created from cellulose by acetylation is cellulose acetate. According to [156], cellulose acetate is a biodegradable, renewable, non-corrosive, non-toxic and biocompatible substance; for these reasons, it was chosen as one of the alternatives.

Polycaprolactone, which is widely used in medical applications, such as tissue engineering and drug delivery systems, was used to create the nano- and micro-layers

of the PCL platform, because it is extremely biocompatible [157]. Although its use may necessitate surface alterations to improve tissue integration, the nanofibrous layer of the PA6 platform was created from polyamide 6, which demonstrates moderate biocompatibility and is acceptable for some medicinal applications [158]. As polyacrylonitrile, which is used to create the nanofibrous layer of the PAN platform, is typically thought to have low biocompatibility, its usage in medical applications is restricted without modification or coating to enhance its interaction with biological tissues [159]. The nanofibrous layer (top layer), on which aerosol particles are collected and to which cells are exposed in vitro, is the most significant layer of all sampling ant testing platforms.

2.5.3. Analyses of developed nanofibrous platforms

Using a scanning electron microscope (SEM; S-3400N, Hitachi, Germany) fitted with a cold-field emitter operating at an accelerating voltage of 2 kV, the structural morphology of the nanofibrous layer was examined. Using an energy-dispersive X-ray spectroscope (Bruker Quad 5040, Hamburg, Germany), elemental mapping analysis was carried out. ImageJ software (National Institutes of Health, USA) was used to analyse SEM pictures.

2.5.4. Aerosolized nanoparticle deposition

After the use of a microbalance (MXA5; Radwag, Poland), the nanoparticles were weighed. A 20 ml glass container with the weighted nanoparticles in it was then filled with 20 ml of deionized water. A homogenous dispersion of Ag, Cu and graphene oxide nanoparticles in deionized water was accomplished during the sample preparation procedure by using an ultrasonic bath (CK 3, SPIN, Italy). In order to achieve thorough dispersion, the vial was then placed in an ultrasound bath set at a frequency of 40 kHz and a temperature of 25 °C and ultrasonically processed for 30 min. The efficacy of the dispersion technique was validated by ultrasonication, and the suspensions were then used right away for subsequent size and zeta potential studies using a Delsa Nano C particle analyser (Beckman Coulter, Inc., USA).

The same experimental setup from Fig. 2.4 has been used and shows the system's schematic for gathering aerosolized particles on the platform samples. A collison nebulizer (Model CN 6 J, BGI Inc., USA), which produces aerosol at a flow rate of 5.5 lpm, was used to aerosolize the suspension of nanoparticles. This suspension was then diluted with dry air (57.5 lpm) in a porous tube diluter, and charge equalization was then performed using an 85Kr bi-polar neutralizer (3054 A, TSI Inc., USA). A holder held platform samples with a diameter of 37 mm, and the air with aerosolized particles (2.2 lpm) was filtered through the platform media. Since each type of nanoparticle suspension produced a steady amount of aerosol, the length of deposition could be adjusted to control how much material accumulated on the platforms. The aerosol's lifetime for particle deposition ranged between 10 and 40 s.

Gravimetric analysis was used to determine the collected mass of aerosol particles from samples taken from the platforms before and following the collection of the produced aerosol particles. Prior to the gravimetric analysis, the platforms were

conditioned for 24 hours in an atmosphere with a relative humidity of 40% and temperature of 22 °C. A microbalance (MXA5, Radwag, Poland) was used to weigh the platform sample and determine its mass according to a predetermined technique. Using a scanning electron microscope (SEM; S-3400N, Hitachi, Germany) with a cold field emitter running at an accelerating voltage of 2 kV, the deposited nanoparticles were examined. Since each type of nanoparticle suspension produced a steady amount of aerosol, the length of deposition could be adjusted to regulate how much material accumulated on the platforms. The deposition of aerosol particles lasted between 10 and 40 seconds. Energy dispersive X-ray spectroscope (EDS, Bruker Quad 5040, Hamburg, Germany) was used for the elemental mapping analysis. ImageJ software (National Institutes of Health, USA) was used to analyse SEM pictures.

Table 2.3. The experimental plan of three types of engineered nanoparticles at three concentrations tested for the two sampling and testing platform materials

Sample no.	Platform material	Type of nanoparticles	Mass of nanoparticles per sample, µg	Surface concentration of nanoparticles, µg/cm^2	Sample no.	Platform material	Type of nanoparticles	Mass of nanoparticles per sample, µg	Surface concentration of nanoparticles, µg/cm^2
PCL-Ag1	PCL	Ag	66.0±35.9	6.49±6.49	CA-Ag1	CA	Ag	4.58±6.13	4.99±0.60
PCL-Ag2	PCL	Ag	185±36.0	18.2±18.2	CA-Ag2	CA	Ag	164±9.25	16.1±0.91
PCL-Ag3	PCL	Ag	300±14.1	29.5±29.5	CA-Ag3	CA	Ag	290±37.6	28.5±3.70
PCL-Cu1	PCL	Cu	44.4±10.2	4.37±4.37	CA-Cu1	CA	Cu	42.5±6.08	4.18±0.60
PCL-Cu2	PCL	Cu	10.8±4.22	1.07±1.07	CA-Cu2	CA	Cu	11.4±0.82	1.13±0.08
PCL-Cu3	PCL	Cu	5.67±0.88	0.56±0.09	CA-Cu3	CA	Cu	5.45±1.11	0.54±0.11
PCL-GO1	PCL	GO	2.66±0.59	0.26±0.05	CA-GO1	CA	GO	3.26±0.58	0.32±0.06
PCL-GO2	PCL	GO	17.1±4.19	1.68±0.10	CA-GO2	CA	GO	15.5±0.95	1.53±0.09
PCL-GO3	PCL	GO	25.1±2.46	2.47±0.24	CA-GO3	CA	GO	27.1±3.72	2.67±0.37

PCL-0	PCL	None	0.00±0.00	0.00±0.00	CA-0	CA	None	0.00±0.00	0.00±0.00

2.5.5. The process of preparing the electrospun membranes for cell seeding

The author of the dissertation has worked with various kinds of 3D electrospun membranes in sterile circumstances and with an air flow beneath the hood. Utilizing a stainless-steel hole puncher that had been disinfected in ethanol and a hammer, 11 mm membrane discs were made. A 24-well plate cell culture insert (CellCrownTM 24NX, Scaffdex) was affixed to the prepared membrane discs in a cell culture laminar hood. The cell culture media was poured into the inserts in 12-well plates while they were in the "upside-down" position, such that it touched the membrane from below. In accordance with the conventional procedures, the cells were seeded on top of the membrane and left there overnight in a humid incubator in order to facilitate cell adhesion. The following day, the medium was taken out, the inserts were relocated to a 24-well plate, turned around so that the cells faced down normally, and 1 ml of the same culture was supplied. The previously indicated cell incubator was used to continue cultivating under the same circumstances.

2.6. Procedure for determining the particle toxicity in vitro

2.6.1. Evaluation of cell adherence to electrospun membranes

Using the EVOSTM M7000 imaging system (InvitrogenTM, Thermo Scientific), the cell adhesion to four different types of 3D electrospun membranes/scaffolds was evaluated. The cells were stained with calcein green AM dye (Invitrogen, Thermo Scientific) on day 5 following seeding in accordance with the manufacturer's instructions. In order to examine the non-specific interaction of the dye with the scaffolds, the scaffolds devoid of cells were stained as well.

2.6.2. Test for cell viability and proliferation

On 3D electrospun scaffolds, cell viability was tracked by using the RealTime-GloTM MT Cell Viability Assay (Promega). The cell proliferation/viability assay was carried out by using a continuous read format. According to the manufacturer's instructions, the reagents were added to the cells 18 hours after seeding, and the luminescence signal was monitored for 48 hours with a SpectraMax® i3 spectrophotometer (Molecular Devices, LLC, Sun Rose, CA). Twenty thousand cells were put into each well of a 24-well generic plate as a control, cytotoxicity assay (LDH).

Utilizing the CyQUANTTM LDH cytotoxicity assay from thermo scientific, the release of lactate dehydrogenase (LDH) was quantified. One day following cell seeding, the scaffolds were moved to a fresh 24-well plate for the same purpose as for the viability assay. A 24-well generic plate with 20,000 cells per well was seeded and used as a control. After 48 and 72 hours from planting, the LDH assay was carried out in accordance with the manufacturer's instructions. Using a SpectraMax® i3 spectrophotometer (Molecular Devices, LLC, Sun Rose, CA), the absorbance was measured at 490 and 680 nm (490–680 nm subtraction). The cells on the scaffolds

were lysed with the lysis solution at the conclusion of the experiment (5 days), and the quantity of LDH was assessed, indirectly indicating the number of the cells on the scaffold.

2.6.3. BEAS-2B exposure to nanoparticles of Cu, Ag and GO

To begin with, 100 µl of culture media and 6,000 BEAS-2B cells per well were planted onto 96-well plates. The following day, fresh cell culture medium containing scattered nanoparticles of copper (Cu; Sigma-Aldrich, 774103), silver (Ag; Sigma-Aldrich, 484059) and graphene oxide (GO; Sigma-Aldrich, 796034) was created. Thus, 1,000, 250, 62.5, 15.63, 3.9, 0.98 µg/ml six replicate wells for each type of particle and concentration were created by aspirating the medium from the plate containing the planted BEAS-2B cells and adding nanoparticle-conditioned media to each of the six wells. Using the RealTime-GloTM MT Cell Viability Assay (Promega) and a Live/Dead staining kit (Invitrogen) in accordance with manufacturer's instructions, the viability of the cells was assessed 24 hours later. Gene expression study was performed on the cells exposed to the nanoparticles at concentrations lower than 62.5 µg/ml. The cells were lysed for this purpose by using 200 µl of QIAzol (QIAGEN) and then kept at -20 °C for RNA extraction.

2.6.4. Exposure to Cu, Ag and GO nanoparticles as "cells on particles"

There has been selected the PCL type of membrane based on the membrane and BEAS-2B viability on various 3D electrospun membranes, as well as the physical characteristics of the membranes and their practical handling during processing before cell seeding and their performance in cell culture for the proof-of-concept experiments. When the membranes were cut off or punched into specific-sized discs for cell seeding and during the cell culture period, there were no degradations or detachments of the "nanofibre" layers.

The membranes that had nanoparticles gathered on top of the "nanofibre" layer were processed with sterile equipment in sterile settings. A hole-puncher was used to create discs with an approximate diameter of 6.4 mm, which were then placed on the bottom of the 96-well opaque white plate. Thus, 6,000 BEAS-2B cells/well in 100 µl of culture media (at least 5 well replicates per position) were used as the seeding density. The cells were seeded after processing control membranes devoid of particles in the same manner. As "blanks" for viability measurements, the membranes with and without the particles were exposed to the medium containing the reagents but devoid of cells in order to rule out any potential interference. After 24 hours, the cells were lysed in the same manner as before for the RNA extraction and subsequent gene expression analysis.

2.7. Characterization of the filter substrate

2.7.1. Distribution of fibre diameter and morphology

The morphology of nano and micro layers was assessed with the use of a scanning electron microscope (SEM S-3400N, Hitachi, Krefeld, Germany). The sizes

of fibres and pores were calculated using ImageJ software from the National Institutes of Health in the United States.

2.7.2. Pore size distribution

The porous size of the composite filter material was evaluated using a capillary flow porometer (CFP-0410, Bious Labs, Lithuania) and the bubble point method [160], and 25 mm filter disks were wetted with wetting fluid (Porofil Wetting Fluid, Anton Paar QuantaTec Inc., USA). In order to verify the device's functionality, commercial polycarbonate filter membranes with 0.4, 1.0 and 2.0 um pore sizes (Cyclopore, Whatman Inc., USA) and PTFE filter membranes with a 1 um pore diameter (Porafil, Macherey-Nagel GmbH, Germany) were utilized. The instrument, CFP-0410 from Bious Labs in Lithuania, uses a capillary flow porometer to measure the distribution of pores between 0.4 and 10 mmm, and 25 mm diameter filter disks were wetted using a wetting fluid called Porofil by Anton Paar QuantaTec Inc. in the USA. Commercial aerosol sampling filters (PTFE filter membranes with a 1 um pore diameter (Porafil, Macherey-Nagel GmbH, Germany)) and polycarbonate filter membranes with 0.4, 1.0 and 2.0 um pore sizes (Cyclopore, Whatman Inc., USA) were used to test the operation of the equipment. The device could measure the distribution of pores between 0.4 and 10 mm.

2.7.3. Wetting properties

The hydrophobicity of the filter sample surface was evaluated with the use of an optical tensiometer (theta lite TL 101, made by Finnish company Biolin Scientific) and the One Attention v1.0 program. A 20-liter drop of pure water was deposited on the composite filter's top layer, and the contact angle was measured after 10 seconds.

2.7.4. Weight stability

The samples were examined for gravimetric analysis stability before being put through filtration efficiency testing on the manufactured filtering substrates. The analyses were carried out in the order listed below:

1) The samples were examined for electret removal and charge. Following the production process, including electrospinning, fibrous nonwoven materials often have an electret charge. Therefore, electric charge was evaluated by using an electrostatic field metre (FMX-004, Simco-Ion, USA) in static charge reading mode. The field metre was mounted in a stationary position, and the samples were placed 25 mm in front of the measuring element. The values were recorded after 10 seconds, and the procedure was then carried out three times. After the charge had been balanced using an in-house built corona discharge bipolar ion generator, the method for measuring the electric charge was repeated.

2) Prior to the gravimetric analysis, the filter samples were conditioned at a temperature of 22 °C and a relative humidity of 40%. Using a microbalance (MXA5, Radwag, Poland) and a predetermined weighing methodology, the initial filter mass was calculated.

3) Using the reference method's technique, the stability of the filter weight was evaluated (Office of the Federal Register, 2001). The filter was put inside a cassette

(Clear Styrene, 37 mm, SKC Inc., USA), dropped from a height of 25 cm to the top of a lab table, picked up from the cassette and weighed once again.

4) Weighed filters were placed in an oven set at 40 °C for 48 hours to test the stability of the filters' temperature. After conditioning, the filters were weighed again.

2.7.5. Morphology of micro/nanolayer

The shape and structure of the nanolayers were statistically determined through scanning electron microscopy (using a Hitachi SEM S-3400N located in Germany). The size of the fibres was calculated using ImageJ software developed in the United States by the National Institutes of Health.

2.7.6. Viscosity and conductivity analysis

The viscosity of polymer solutions with a weight percentage between 10 was measured at 28 °C using a Brookfield digital viscometer (Model DV-E). The conductivity of each solution was assessed five times at 25 °C, and their average was determined using a conductivity metre (COND 340i, WTW Ltd., USA), respectively.

2.7.7. Filtration efficiency and pressure drop

The filtration efficiency of filters was tested against simulated aerosol particles of NaCl using a specifically developed testing rig [6]. The understanding is that the spherical particles exhibit greater filtration efficiency when compared to the cubic particles [161]. As a result, NaCl was chosen as the testing material to assess filtration efficiency, since its aerosol form consists of cubic particles that possess rounded edges.

Due to its intermediate shape, NaCl is considered suitable for measuring the average filtration efficiency. The NaCl solution was aerosolized utilizing a collison nebulizer (Model CN 6 J, BGI Inc., USA), and dry air was diluted in a porous tube dilator. The charged particles were balanced with the aid of an 85Kr bi-polar neutralizer (3054 A, TSI Inc., USA). Filter samples with a diameter of 37 mm were put in a filter holder and exposed to the test aerosol. The Finnish company Dekati Ltd.'s Electrical Low-Pressure Impactor (ELPI+) was used to monitor the particle concentrations both upstream and downstream. A pressure sensor (Model PCE-PDA 1L, PCE GmbH, Germany) was used to measure the pressure drop before and after the sample medium at face velocities of 5.3 cm/s and at intervals between 3 and 20 m/s. The results of the filtration efficiency tests were used to determine the overall performance of the filters and identify any limitations in their ability to capture particles.

2.8. Statistical analysis

Origin 2021 (Origin Labs Inc., USA) and Microsoft Excel (Microsoft Corp., USA) software were used to statistically process the data generated throughout the analyses. If not stated otherwise, the provided average data are presented as mean

standard deviation and were obtained from measurements that were performed in triplicate.

GraphPad PRISM software was used to analyse biological data. In order to identify statistically significant differences between groups, two-way ANOVA or multiple comparison t-tests were utilized. A difference was deemed statistically significant when $P<0.05$.

3. RESULTS AND DISCUSSION

3.1. Fibrous three-layer (all three layers from nonwoven fibres) aerosol sampling filter design, morphology and characterisation

Because of a number of advantageous characteristics, including a dense network of nanoscale fibres, tiny pore diameters and low specific weight, the design of an aerosol sampling filter based on a nanofibrous network depends on the ability of such a matrix to retain aerosol particles with high efficiency. Both inferior mechanical performance and a very significant pressure drop are the major limitations of the nanofibrous layer. The mechanical fragility is a significant barrier, even though the latter is expected when sampling filters have small pores, and it is not thought to be a serious shortcoming. It can be fixed by adding stronger support layers below the nanofibrous layer or supporting the nanofibrous layer with a support ring, as in the case of PTFE membranes. Following the latter approach, first, there was added a commercially available woven microfibre support to the nanofibre layer. Considering the woven matrix's rather high surface roughness and the layers' tendency to separate during handling due to a lack of chemical similarity and an excessive variation in fibre size, this strategy eventually seemed to be practically unworkable after several tests. Thus, a different strategy has been chosen to create the support layer utilizing 3D printing on a comparable material. Although the chemical compatibility between layers was resolved, the mechanical stability of the nanofibre support on the microfibre was still to be improved.

As a result, the final particle sample media had a three-layer structure with a gradient in fibre and pore diameter (Fig. 3.1). Layer 3 served as the base layer at the bottom of the three-layer composite, providing mechanical support for the fragile top layers. Layer two (the middle layer) served as a binding layer between macro fibrous layer one and layer three, ensuring the best adherence and preventing nanofibrous layer three from disintegrating during low pressure sampling. The third layer, which is the top layer, served as a surface for collecting nanofibrous 2D aerosol particles. The phrase "2D surface" in relation to layer 3 describes its function as a planar aerosol particle collection surface rather than its actual physical dimensionality in the strict physics context. Dimensionality is not the same as layers: particle mobility freedom within a material is related to dimensionality. In order to create a composite construction, various material sheets are stacked to create layers. This differentiation makes it clear how the filter functions and what advantages it has over single-layer nanofibre membranes. The term “nanofibrous 2D aerosol particles” refers to aerosol particles that have a nanofibrous structure (fine fibres at the nanoscale) and are collected on a two-dimensional surface (the nanofibre layer). The term "2D" in this case pertains to the surface where the particles are collected, not to the particles themselves being flat.

Layer 3 was applied to the collector surface before layer 2 and layer 3 formation started, while layers 1 and 2 formed later. Table 3.1 lists the technical specifications for fabricating layers 2 and 3. In order to achieve good chemical compatibility and

adhesion, layers 2 and 3 were constructed from the same polymer (apart from PAN). The variation in polymer content in the starting solution and the adjustment of other parameters to produce uniform layer morphology were largely responsible for various sizes of fibres. Four different kinds of three-layered composite aerosol sampling filter substrates compared with commercial filters were listed in Table 3.2.

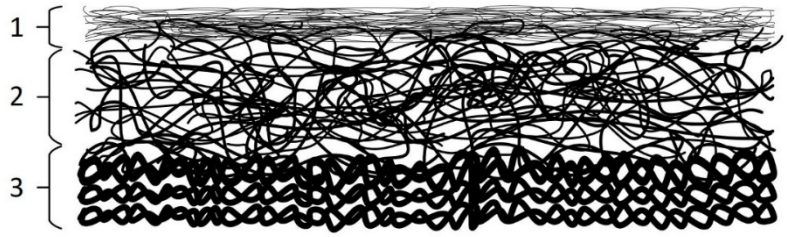

Fig. 3.1. The cross-sectional layout of three-layered substrate for the aerosol sampling filter: layer 3 is macrofibre providing mechanical support for the fragile top layers, layer 2 is microfibre served as a binding layer between micro fibrous layer 1 and layer 3, and layer 1 is nanofibre served as a surface for collecting nanofibrous 2D aerosol particles

Table 3.1. The composite aerosol sampling filter substrates' fabrication characteristics

Type of filter	**Layer no.**	**Polymer**	**Concentration of polymer in solution, %w/v**	**Solvent mixture**	**Voltage, kV**	**Tip-to-collector distance, cm**	**Polymer supply rate, g/h**	**Needle gauge**	**Ambient conditions, °C, % RH**
PCL	L3	PCL	10.0	6:4, DCM: DMF	22.0	19.0	0.20	25	25, 35
	L2	PCL	20.0	2:3, Acetone: DMF	22.0	15.0	0.40	21	30, 40
	L1	PCL	Melt of pure PCL		7.7	12.0	0.29	-	-
CA	L3	CA	17.0	2:1, Acetone: DMA	20.0	15.0	0.51	21	20, 55
	L2	CA	20.0	2:3, Acetone: DMF	22.0	15.0	0.40	21	30, 40
	L1	PCL	Melt of pure PCL		7.7	12.0	0.29	-	-
PAN	L3	PAN	10.0	DMF	20.0	15.0	0.10	21	22, 40
	L2	PCL	20.0	2:3, Acetone: DMF	22.0	15.0	0.40	21	30, 40
	L1	PCL	Melt of pure PCL		7.7	12.0	0.29	-	-
PA 6	L3	PA6	13.0	2:1, Formic acid: Glacial acetic acid	26.0	15.0	0.26	21	30, 35
	L2	PCL	20.0	2:3, Acetone: DMF	22.0	15.0	0.40	21	30, 40
	L1	PCL	Melt of pure PCL		7.7	12.0	0.29	-	-

Table 3.2. Compared commercial filters and their described properties

Sample	Thickness, µm	Fibre diameter [a] (mean, SD), nm	Pore diameter [a] (mean, SD), µm	Basis weight, g/m^2	Weight stability (loss at 40 °C), mg	Wetting properties, WCA [a]	Filtration efficiency at MMPS, % (NaCl)	Filtration efficiency at MMPS, % (DEHS)	Pressure drop, Pa (at face velocity of 10 cm/s)
PCL	480	0.42±0.022	1.20±0.06	92.9±1.9	9±3	96.9 ± 4.4	99.4±0.07	98.5±0.13	2,304±13
PAN	400	0.37±0.068	0.93±0.02	87.6±1.8	8±6	83.3 ± 1.2	99.5±0.31	99.5±0.88	1,478±15
CA	470	0.42±0.083	2.83±0.35	72.5±1.4	15±6	38.7 ± 7.7	99.4±1.3	99.0±1.50	476±3
PA6	390	0.086±0.019	0.46 ±0.04[d]	73.8±1.5	14±4	90.6 ± 4.4	99.9±0.1	99.7±0.13	2,159±16
PTFE	140[b]	-	2 [b]	70.9±1.1	<20	105.1 ± 4.7	99.9±0.45	99.8±0.54	526±12
QMA[162]	475	0.86±0.059	2.2 [b]	86.3±1.485 [b]	<20	0.0±0.0	99.97 98.0[c]	99.4±0.95	1,510±15
TQ[163]	432[b]	0.73±0.047	N/A [b]	52.0±1.758 [b]	<20	0.0±0.0	99.9 99.9 [c]	99.8±0.45	>2,500
MCE[164]	150[b]	-	0.8[b]	42.9±2.1	<20	0.0±0.0	99.98±0.03	99.8±0.52	>2,500

[a] Property reflecting primarily layer 1.
[b] Manufacturer's information.
[C] Manufacturer's information presented according to ASTM D 2986-91, [0.3 mm].
[d] Maximum pore size, estimated average size ca 0.2 mm.

PCL was used to create layer 1 with the average fibre diameter of 40.0±7.3 µm. The 3D fibre printing technology has the ability to create fibres with a highly predictable morphology. In this instance, the fibre structure was designed to be controlled by two mechanisms, i.e., direct writing and limited polymer whipping, resulting in a semi-random network (Fig. 3.2, layer 1 SEM images). The straight fibres in this structure gave it mechanical stability and endurance, while the randomly oriented fibres gave it a surface on which to build a second layer. Due to the regulated temperature regime below the polymer's thermal degradation threshold, the chemical composition of PCL was unaffected throughout the operation [154].

Layer 1 was used as a substrate for the solution electrospinning, while layer 2 was produced directly on top of layer 1. PCL solution served as a foundation for constructing layer 2 in the cases of PCL, PAN and PA6, resulting in an average fibre diameter of 2.80±1.31 µm (Fig. 3.1 and Table 3.1, layer 2). In the case of the CA sample, layer 2 was made with CA solution that had a 20% polymer concentration,

resulting in fibres that were 0.71±0.22 µm in diameter, which is three times smaller than PCL but larger than the top CA layer, which was made with CA solution that had a 17% polymer concentration. After it became apparent that CA nanofibres do not efficiently cling to PCL middle layer, CA was chosen as the middle layer.

Directly on layer 2, PCL, CA, PAN and PA6 polymer solutions were used to create layer 3. As a result, the samples were given names based on the top layer polymer. With average diameters of 0.42±0.21 µm for PCL, 0.42±0.08 µm for CA, 0.37±0.07 µm for PAN and 0.086±0.02 µm for PA6, the sub-micrometre fibres were successfully produced (Fig. 3.2, layer 1, SEM images). The fibre network was randomly oriented in all the samples, which is a frequent result of the solution electrospinning procedure.

As the primary filtering layer, the top layer of nanofibre was supposed to deposit accumulated particles on top of the substrate. The thick network of these nanofibrous filters might prevent particles from penetrating the deeper layers, making them more similar to solution cast filtering membranes than (micro)fibrous filters, which deposit particles at different depths in the filtering layer.

The composite filters' overall thickness, which ranged from 390 to 480 µm (Table 3.2), was higher than that of the commercial sample filters (140–475 µm). A relatively thick filter is produced by the composite layered structure; however, this should not prevent it from being used in most sampling devices.

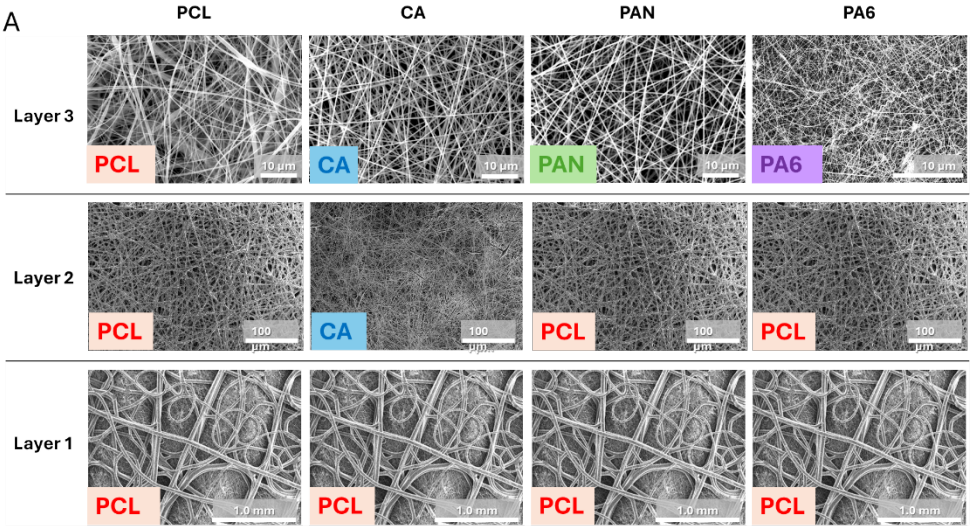

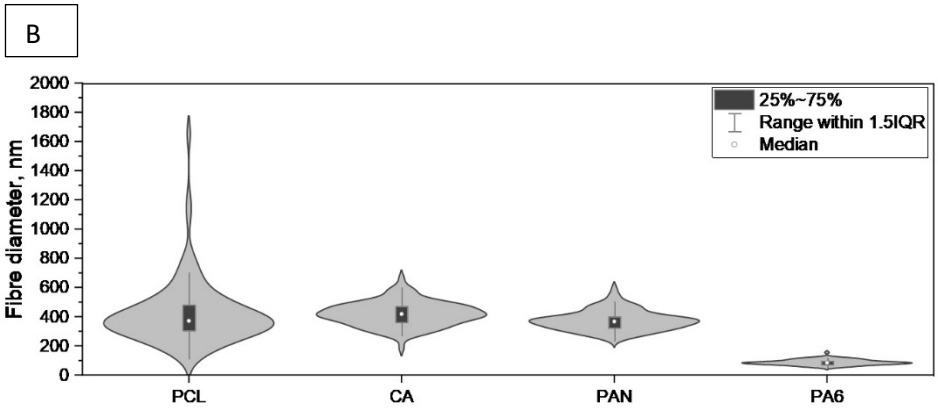

Fig. 3.2. A. SEM photos of the substrate layers for the aerosol sampling filter. B. The box and whisker graph below shows the top layer's fibre size distribution

3.1.1. Distribution of pores

The average size of the pores on the manufactured substrates ranged from 0.4 μm (PA6) to 2.83±0.35 mm (CA). It is well known that the diameter and length of the fibres determine the pore size of nanofibrous membranes [160]. The basic weight of the membrane, which has a negative impact on the pore size, is another determining factor. This could account for the difference in pore size fibre size between PCL and CA, while PCL had fibres of comparable size to CA, the latter's average pore size was twice as large while its basis weight was 20% lower (Table 3.2). SEM photos reveal the same thing, showing that the CA fibre packing was "looser". On the other side, PA6 has the tiniest fibres and pores. The relationship between these observations and the filtering efficiency and pressure drop will be revealed in sub-sections 3.1.4 and 3.1.5. In the electrospinning process, the polymer content in the solution can be changed (the thinner the solution, the smaller the fibres) as well as the electric field strength (the stronger the field, the smaller the fibres). Basis weight can be effectively managed in relation to the process duration. It is challenging to directly regulate pore size; therefore, it is advised to extend the electrospinning time if even higher level of efficiency is required to produce aerosol sampling filter substrates made by using this technique.

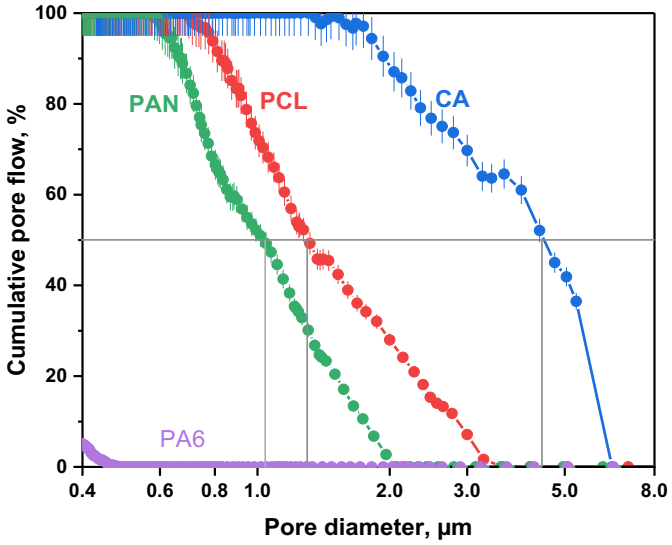

Fig. 3.3. Pore diameters and cumulative pore flow of aerosol sampling filter substrates; mean pore size is indicated by the grey lines

3.1.2. Stability of weight

The substrates for the aerosol sampling filters were suitable in terms of weight stability. The filter mass barely changed because of the test against loose surface particles. Pure polymers were used to create the filters reported there, which were then transformed into an inert nonwoven fibrous network. This network has a reputation for having a mechanically sturdy structure that resists chipping, flaking or shedding. The resultant fibres are lengthy and knotted, and they carry the initial polymer's elastic properties along their length. Electrospun filters are similar to the polymer membrane filters, such as PTFE, MCE, or PC, in that regard.

Specifically, if the filter is utilized as respiratory protection equipment, a concern has been raised about the release of nanofibres (as nanoparticles) from the body of nanofibrous air filters under passing airflow [165]. Since most experts believe there is a low possibility that nanofibres will be released from the fibre network, the data on this phenomenon is quite scant. No discernible release of fibres was observed in research with PAN nanofibres, or only at extremely high face velocities (30 cm/s) [166]. A gravimetric examination of the collected particles would not be considerably impacted by such minute shedding on the bulk of the sampling filter. However, it should be highlighted that the passing air testing would be more advantageous and the existing standard approach for loose particle testing by dropping may not accurately reflect the particle release potential from the nanofibrous filters. The electrospinning technology offers a chance to create filtering materials with sorptive qualities by incorporating nanoparticles into the material. Depending on the nanoparticle grafting technique, such a product may be susceptible to mass loss when dropped, although it is unlikely to be utilized especially for the gravimetric analysis.

Under thermal treatment at temperatures up to 40 °C, no appreciable weight loss was seen. The thermal characteristics of precursor polymers, which are often capable of retaining mass until the temperature of breakdown (>250 °C), are typically present in electrospun nonwoven mats. The evaporation of the leftover solvent, which is retained in the nanofibrous matrix due to partial evaporation during the solution electrospinning, is another, possibly more likely, source of mass loss. While the leftover solvent on the surface of the fibre may aid in the network's creation by fusing some of the fibres together and producing a mechanically stronger network [167], in order to prevent the solvent from having an adverse influence on the collected particles or from interfering with future chemical analysis, it must be eliminated after the spinning process. According to the obtained matrix, the vacuum drying process was introduced, which eliminates most solvent residuals [168].

3.1.3. Wetting attributes

Since water does not normally encounter the surface during sampler operation, the wetting characteristics of the aerosol sampling filter material are not of the utmost concern during the sampling. However, the wetting qualities of the materials have been evaluated, because the provided method is most useful when particles are analysed afterwards, where elution of particles may be required.

Virgin PCL, PAN and PA6 with WCA near to 90 °C are among the tested polymers that are intrinsically hydrophobic, whereas CA is hydrophilic. However, (nano)fibrous materials wetting characteristics may differ from those of their film compared to the other materials [17]. A water droplet's interaction with a fibrous material is governed by the processes called capillary sorption, adhesion, spreading and immersion [169].

PCL 102.1± 4.4°, PAN 85.3 1.2°, PA6 97.6 ±4.4° and CA 52.7 ±7.7° were the first WCAs of the produced nanofibrous filters (Fig. 3.4). This number represents the angle of water contact between a small drop of water and the surface of the item being examined [170]. The drop enters the fibrous matrix after placement, and the pace at which this happens is influenced by both the substance and the architecture of the nanofibrous network. This characteristic is maintained by the hydrophobic PCL, PAN and PA6, which is accounted for by the fact that nanofibrous layers have minute pores that are difficult for liquids with high surface tension to pass through. Due to the presence of carboxy groups in the polymer chain, CA as well efficiently carries water to nanopores.

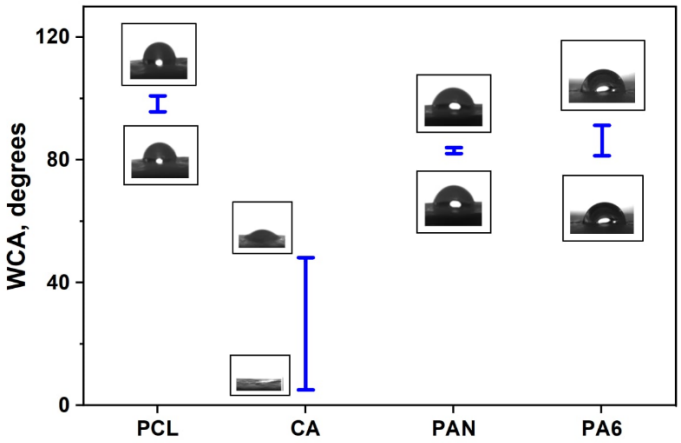

Fig. 3.4. Water contact angle (WCA) as a measure of the wetting characteristics of aerosol sample filters; the range shows the value at the beginning (0 s) and the value at the end (9 s)

3.1.4. Filtration efficiency

High retention efficiency of fine particles, such as 99.5% for the respirable aerosol fraction, is a key design factor for aerosol particle sampling substrates [171]; [172] performed a thorough evaluation of many commercially available standard sampling membrane filters. Most polymer-based membranes with pores smaller than <2 mm demonstrated great collection efficiency of >99%, supporting information provided by the manufacturers. Additionally, it has been observed that, as expected by a capillary tube model, filter membranes with straight through pore structures give reduced collection efficiency [173]. The proximity of composite layered nanofibrous membranes to membrane substrates where air is forced to travel through many layers of random pores increases the likelihood of particle–fibre contact, even in the range of ultrafine particles [174].

The average retention efficiency inside the developed substrates came close to the anticipated 99.5% efficiency in the case of solid NaCl aerosol. PCL and CA samples were close to the critical value at the most penetrating particle size (ca. 99.3–99.4%). Such high values, which mostly depend on the shape of the fibre network and basis weight, are not exceptional for nanofibrous networks used for the air filtration [107, 51]. In this instance, the porosity and fibre size of the morphology were closely related to the efficiency values. Average pores in cellulose acetate were the greatest (1–5 mm), whereas those in PCL were marginally smaller (0.7–3 mm). In addition, the central layer of CA, which had a structure that was relatively denser than that of PCL, may have contributed to the similar collection efficiency of CA and PCL. The PA6 and PAN membrane with its tiniest fibres (<0.1 mm) and holes (<0.4 mm) offered almost 100% collection efficiency for all particle sizes.

A slightly decreased collection efficiency, particularly for CA and PCL, was caused by the difficulty that the designed sampling filters had with the liquid DEHS aerosol. The monodisperse distribution of DEHS aerosol results in greater count

median diameter of particles (Fig. 3.5) that are closer to the size of the most penetrating particle and carry various properties of particle charge, maybe even after the charge equalization [175]. It has been demonstrated that DEHS particles penetrate high-efficiency micro fibrous filter media more deeply [176]; nonetheless, the stated efficiencies in the case of nanofibrous networks are comparable [107, 51]. It was not possible to pinpoint the exact causes of the differences in filtration efficiency between the two types of aerosols due to the wide range of influencing factors that are present in testing setups and filtration media, but it appears that increasing the specific weight of the upper layer may be necessary to achieve the highest possible collection efficiency.

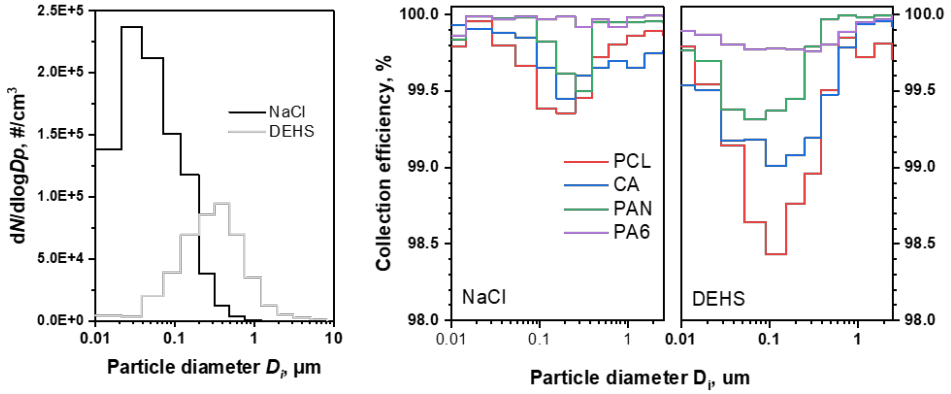

Fig. 3.5. Size distribution of NaCl and DEHS aerosol particles on nanofibrous filtering substrates (left) and collection effectiveness (right)

3.1.5. Pressure drop

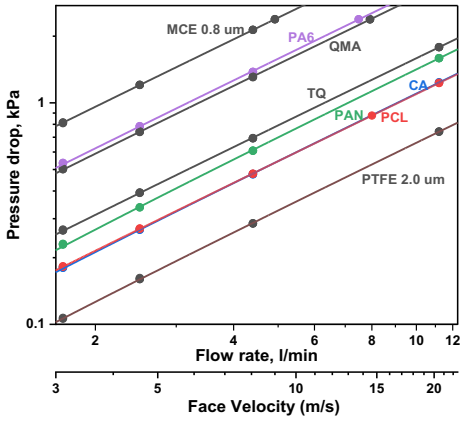

Fig. 3.6. Pressure drop in relation to the sample flow rate of the filter: PTFE 2.0 m (SKC), QM-A – quartz filters (Whatman Inc.), TQ – tissue quartz filters (Pall Corp.), MCE 0.8 mm – mixed cellulose ester membranes, pore size 0.8 mm (SKC Inc.) are given as reference filters

While the primary objective of the aerosol particle sample filters is to ensure high collection efficiency, the pressure drop that naturally happens across the filter is concerned as well because it raises the possibility of sampling equipment failures and necessitates overall higher investments and energy costs. The factor for filter quality [155] or Fig. of merit [173] have been employed as pressure drop ratio and particle filtering efficiency since they are connected. In choosing media appropriate for a particular sampling device, the fluctuation of pressure drop with sampling flow rate is much more crucial in the case of aerosol particle collection filters. As a result, the analysis was conducted as described by [177] who correlated sampling flow rate, pressure drop and pore diameters for different commercial filters. Fig. 3.6 shows the examination of these filters created in this study. In general, the location of filters is in good agreement with the porosity and filtration efficiency values; PA6 has the maximum pressure drop, while CA and PCL have nearly equal values across the investigated flow rates. The fibrous membranes, which had pores with an average size of < 0.8 mm, were positioned quite well among the commercial filters at the same time. Even though PA6 membrane has pores with a diameter of about 0.2 mm, it can operate with high efficiency and a relatively narrow pressure drop range, making it a valuable platform in situations where high-performance sampling is required.

3.1.6. Summary of research

The melt or solution electrospinning tests were conducted under specific conditions tailored to each polymer and desired filter properties. The selection of these conditions was based on factors, such as polymer type, concentration in the solution, solvent mixture, voltage, tip-to-collector distance, polymer supply rate, needle gauge and ambient conditions. For example, in the case of PCL, electrospinning was performed using a concentration of 10.0% w/v PCL in a solvent mixture of 6:4 DCM:DMF with a voltage of 22.0 kV, a tip-to-collector distance of 19.0 cm and a polymer supply rate of 0.20 g/h. Similar parameters were adjusted for other polymers, e.g., CA, PAN and PA6, to optimize the electrospinning process and achieve uniform layer morphology. Numerous experiments were conducted to optimize the process conditions and obtain filter materials with the desired properties. Different sets of conditions were tested for each polymer, varying the parameters such as polymer concentration, solvent mixture, voltage and needle gauge. Through systematic experimentation and adjustment of these parameters, the author aimed to achieve uniform fibre morphology, appropriate pore size distribution and high filtration efficiency. The optimization process involved iterative testing and refinement until satisfactory results were obtained, ensuring the production of high-quality filter materials suitable for aerosol sampling applications. The final composite filters comprised three layers, each serving a specific function in the filtration process. Layer 1 provided a surface for collecting nanofibrous 2D aerosol particles, while layer 2 served as a binding layer between the macro fibrous layer 1 and layer 3, ensuring optimal adherence and preventing disintegration during sampling. Layer 3 acted as the base layer, providing mechanical support for the fragile top layers.

Incorporating both micro fibrous support for mechanical stability and nanofibrous membranes with strong particle-catching capabilities, nanofibrous aerosol sampling filter substrates were developed. These substrates featured diverse morphologies and were crafted from four distinct polymers (PCL, CA, PAN, PA6) with pore sizes ranging from 0.2 to 3 mm and fibre diameters less than 5 mm. Compared to commercial filter substrates, they demonstrated competitive pressure drops, excellent collection efficiency (>99.4% with NaCl aerosol at MPPS) and stable weight. Electrospinning proved effective in substrate production, and further enhancement can be achieved by increasing the top layer's basis weight by 10–20% to achieve collection effectiveness above 99.5% for all polymers. Mechanical performance can be enhanced through alterations in the support layer and polymer selection. Particle loading should be considered, especially for smaller pore matrices (e.g., 0.4 mm), as it may increase pressure loss due to blockage.

Technical problem: the technological issue of an effective aerosol particle sampling is resolved by the study that is being presented. Currently, only a few materials (such as quartz or cellulose) can be used as fibrous aerosol sampling filters, making it impossible to use these materials for applications in subsequent chemical analyses that call for a specific composition of filter material that does not interfere with a particular method of chemical analysis. Although fibrous filters have favourable efficiency and a relatively low pressure drop, the fabrication methods are restricted, making it impossible to produce the custom sampling substrates required for a given sampling technique and subsequent physico-chemical/toxicological treatment.

Solutions: the process for creating fibrous aerosol particle collection filters from a variety of polymers is described in the research, which provides a platform for aerosol sampling for multiple post-sampling analyses. The chemical composition, fibre and pore sizes, pressure drop and filtration efficiency of the fibrous sampling media produced by this technology will all be under control. The fibrous particle sample filter will have a high rate of particle retention, exceptional mechanical stability and a custom chemical composition for post-processing by a variety of chemical analysis methods. The electrohydrodynamic processing of polymer melts and solutions is the basis for the suggested fabrication approach, which yields a nonwoven plurality of randomly oriented fibres with diameters ranging from 1E-7 to 1E-4 metres and pores with diameters between 1E-7 and 1E-6 metres. The variety of polymers and fibre morphologies described in the study gives air quality specialists and scientists the chance to choose sample substrates for the unique requirements of their work, considering further processing of collected aerosol particles. The fibrous filter is intended for use in filter-based aerosol samplers, where it is placed in a holder and exposed to the sampled air flow for a predetermined amount of time. Aerosol particles are kept in the upper layer of the air flow and can be moved there for gravimetric, spectroscopic, chemical or toxicological examination.

Advantageous technical effects: the process for making fibrous aerosol sampling filters has the following positive technical effects. 1) In terms of variety of

polymers available for such production, it enables control over the chemical composition and purity of fibrous membrane. Chemical composition is crucial for the further processing of collected particles by destructive and non-destructive methods, such as chromatography and toxicology. Non-destructive methods include microscopy and spectroscopy. 2) It allows to manage the fibrous filter's overall morphology including the diameter of fibres, the size of pores, the gradient of pores, the packing density and the specific weight. 3) It offers improved mechanical qualities through the use of a gradient layering method that uses layers with various fibre diameters.

Industrial applications of the sampling filter and production method: the installations in aerosol sampling devices in occupied, indoor and outdoor areas by the users of aerosol particle sampling equipment are the practical applications of the manufactured filter disc. In the frameworks of the official air monitoring initiatives, the highest volumes of such sampling filters are used. The primary use of such sample filters in scientific research, notably the creation of new aerosol particle analysis methods, is due to the possibility of manipulating the surface morphology of the particle collection and the precursor polymer. The various machines listed in this patent will be used to manufacture these filters on an industrial basis. As the upscaling production could change the morphology of filtering layers and, in turn, the qualities of the finished product, it is important to carefully examine the size of the production scale.

3.2. Two-layer (3D printed support with nanofibre nonwoven layer) composite nanofilter for aerosol particle filtration

The research examined the complex interactions between variables that affect the production and functionality of polycarbonate nanofibrous air filter substrates. Notably, the polymer solution's conductivity and viscosity were both increased when CTAB was added, i.e., two important factors influencing the electrospinning process. The generation of bead-free nanofibres with different sizes was successfully demonstrated by the SEM pictures, indicating the effectiveness of CTAB in improving solubility and encouraging fibre formation. The relationships between CTAB concentration, polymer concentration and fibre characteristics were clarified using process parameter modeling, offering important insights for the optimization. Additionally, the tests of filtration effectiveness demonstrated that the substrates could achieve high rates of particle retention, which were ascribed to both increased fibre accumulation and reduced fibre sizes. The PC composite filters demonstrated improved air flow despite greater pressure drop.

3.2.1. Viscosity

Increasing the CTAB amount from 0.2 to 0.8% led to a decrease in viscosity for the PC 14% solution from 50.7 to 32.2 mPa.s, and similarly for the PC 20% solution, from 185.3 to 111.5 mPa.s. The inclusion of CTAB caused a significant rise in conductivity and a reduction in the viscosity of the solution. The range of the concentrations that yield continuous fibres in electrospinning is determined by the

viscosity of the solution. The formation of continuous fibres is the result of the abundant chain entanglements within the polymer solution.

3.2.2. Conductivity

It should be noted that the conductivity of the DMF and THF in their original state was checked before preparing polymer solutions to ensure that there were no alterations to the solvent's conductivity over time. The conductivity showed a direct correlation with the amount of CTAB added, as the increase in CTAB content led to a proportional increase in conductivity. This can be attributed to the linear rise in ionic concentration. This finding suggests that the conductivity of the PC solution has been greatly influenced by the addition of CTAB. One of the studies on solvent conductivity on polystyrene electrospun fibres explains that electrospun uniform fibres are a result of high conductivity of solutions and vice versa [178]. It is widely recognized that surface tension and electrostatic forces compete during the electrospinning process. Hence, the enhanced conductivity likely enabled the solution to carry a greater charge, leading to an increased electrostatic force that could effectively counteract surface tension [179]. Additionally, the viscosity may have decreased as well. Therefore, the solution's conductivity is an extremely important parameter in the formation of bead-free nanofibres, particularly when low polymer concentrations are employed in this case. The nature of one of the solvents in the polymer solution exerts a significant influence on the solution's conductivity. Therefore, the changes in solution conductivity can result in observable alterations in surface morphology. In conjunction with other electrospinning parameters, solution conductivity plays a crucial role in fabricating polymer nanofibres with the desired morphology [45]. Overall, the combination of increased conductivity and reduced viscosity resulted in a substantial decrease in the diameter of the PC nanofibres. Table 3.3 shows rheology measurements of PC solution and the characteristics of nanolayer material. The viscosity of all PC solutions was measured using a Brookfield Viscometer with Spindle number L2 at a speed of 20 rpm.

Table 3.3. Properties of PC solution used in electrospinning and characteristics of produced nanolayer material

Solution mixture	Viscosity (mPa. S)	Conductivity (µs/cm)	Fibre diameter mean (µm)	Pore diameter mean
PC14%, CTAB 0.2%	50.7	36	0.323	1.321
PC14%, CTAB 0.8%	32.2	141	0.563	0.999
PC17%, CTAB 0.5%	64	96	0.497	1.146
PC17%, CTAB 0.5%	60.8	92	0.328	1.119
PC17%, CTAB 0.5%	62.1	100	0.374	1.132
PC20%, CTAB 0.2%	185.3	52	0.19	1.024
PC20%, CTAB 0.8%	111.5	124	0.538	1.058

3.2.3. Morphology

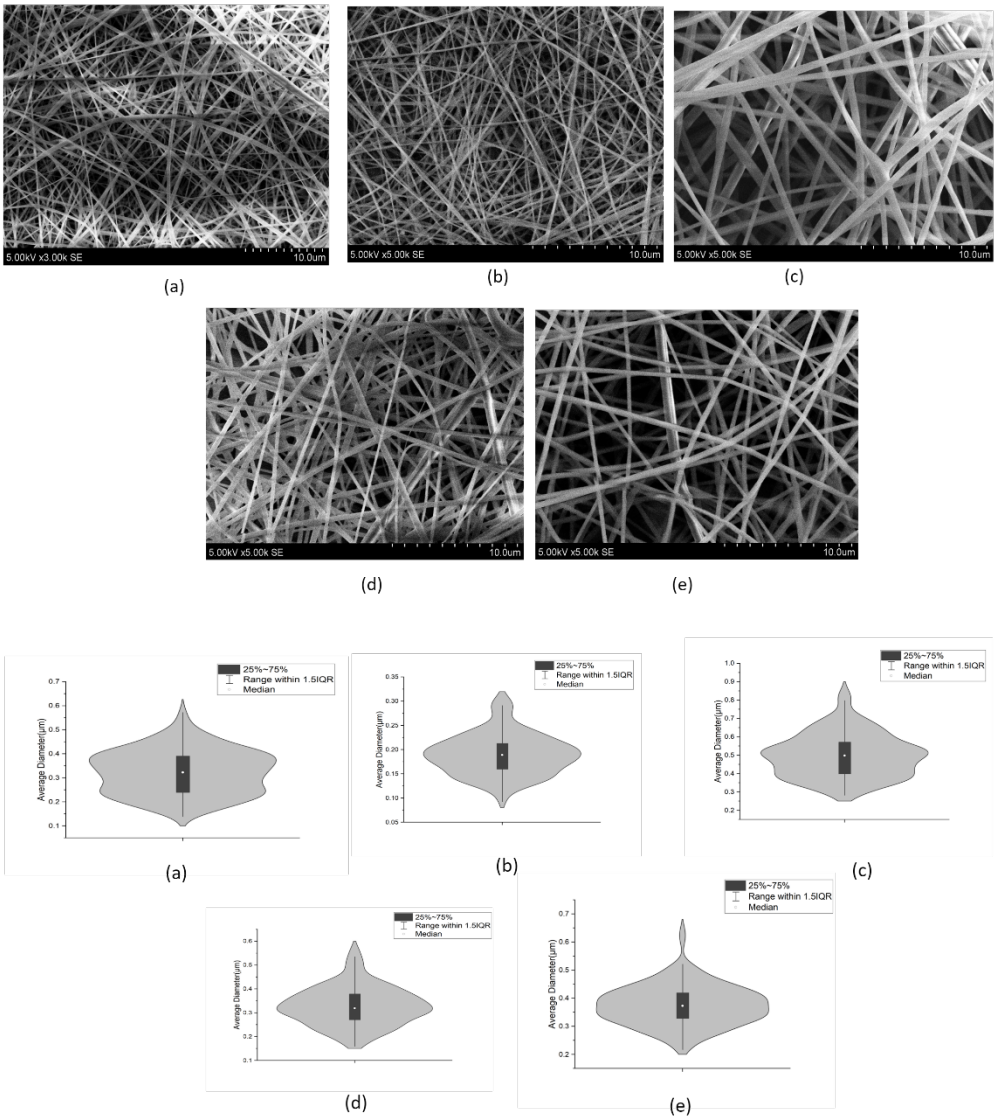

Fig. 3.7. SEM images show the polycarbonate nanofibres deposited layers of the filter used for aerosol sampling: (a) PC14%, CTAB 0.2%, (b) PC14%, CTAB 0.8%, (c) PC17%, CTAB 0.5%, (d) PC17%, CTAB 0.5%, (e) PC17%, CTAB 0.5%, (f) PC20%, CTAB 0.2%, (g) PC20%, CTAB 0.8%; the size distribution of the nanofibres is depicted in a box and whisker plot below

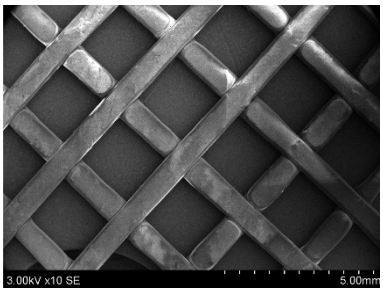

Fig. 3.8. 3D printed polycarbonate support

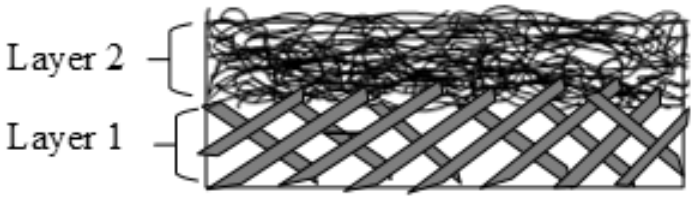

Fig. 3.9. The cross-sectional view of 2-layer air filtration substrate: layer 1 – 3D printed polycarbonate support, layer 2 – electrospun polycarbonate nanofibrous layer of varying concentration

All PC solutions yielded bead-free fibres with average diameters as follows: 0.32µm, 0.19µm, 0.56µm, 0.54µm, 0.50µm, 0.33µm and 0.37µm. Fig. 3.9 shows the SEM images of polycarbonate nanofibres deposited layers of the filter used for aerosol sampling. The solubility of PC was greatly enhanced by the addition of CTAB to the solution. CTAB, a cationic surfactant, enhances its conductivity, resulting in the successful production of ultra-fine PC fibres without any beads. In order to ensure optimal chemical compatibility and adherence, each of the 7 polycarbonate (PC) concentrations were electrospun onto a base layer consisting of a 3D printed polycarbonate substrate. The PC fibres demonstrated desirable morphology characteristics, including a smooth surface and a lack of beading, as indicated by their diameter. The formation of smooth fibres without beads was attributed to achieving a balance between many electrospinning variables, including viscosity, concentration and applied voltage, in relation to surface tension. However, the impact of solvent evaporation on fibre morphology changes was identified as significant. Solvent evaporation during the electrospinning process led to the occurrence of droplet coagulation at the needle tip, as observed. Other factors caused changes in fibre morphology were influenced significantly by either the viscosity or the concentration of the polymer. Usually, the solutions with a high viscosity had a greater tendency to overcome surface tension, causing the droplets to form a continuous jet under the influence of the applied voltage. However, it was observed that as the concentration increased, the uniformity of the produced fibres decreased, and with a longer receiving time of 60 minutes of PC, nanofibres exhibited a denser configuration. In order to

achieve a successful preparation of ultrafine bead-free fibres with the lowest average diameter, it is imperative to maintain a systematic control over a range of spinning parameters and carefully select appropriate solvents and solution parameters.

The plan generated by the Modde was adjusted until the complete dissolution of PC concentration with CTAB was achieved. Increasing the CTAB concentration for PC 14% resulted in a decrease in fibre size from 0.32 to 0.19 µm. However,, further increases in CTAB content for PC 20% had limited influence on the fibre diameter.

3.2.4. Process parameter modelling

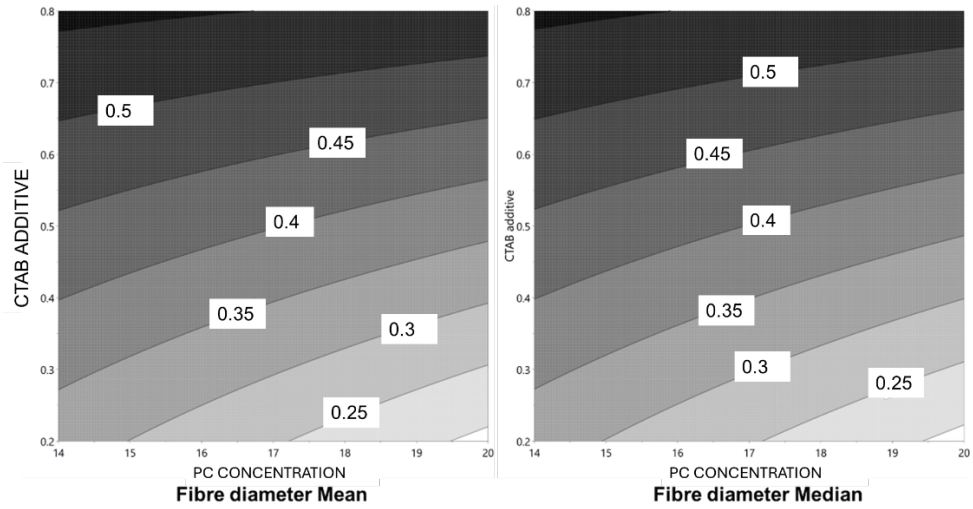

Fig. 3.10. Surface plots of PC concentration with CTAB additive over fibre diameter mean and median

The data obtained from the experimental runs were used to generate surface response plots. These plots aimed to establish a relationship between the factors, such as CTAB and PC polymer concentration, and the corresponding responses of the nano spun fibres, including fibre diameter mean, standard deviation (SD) and interquartile range (IQR). Fig. 3.10, 3.11, 3.12 show the response surface plots depicted for respective parameters. The observed trends in the graphs generated from process parameter modelling provide valuable insights into the intricate relationship between the CTAB additive and various key properties of the solution. In the fibre diameter mean vs. CTAB additive graph, the variability in fibre diameter suggests a discernible influence of CTAB concentrations. This is likely attributed to the surfactant-polymer interaction and the potential formation of micelles, wherein higher CTAB concentrations may lead to either an increase or decrease in fibre diameter mean.

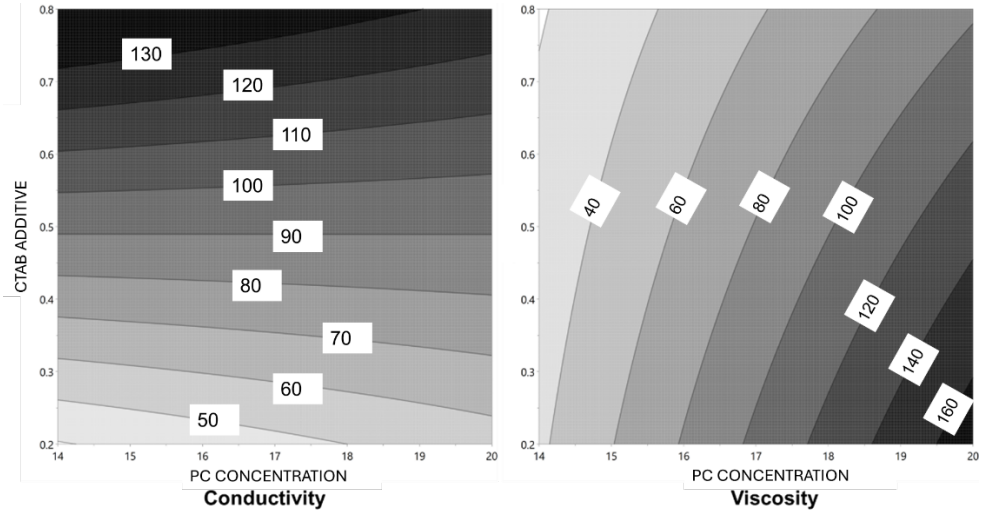

Fig. 3.11. Surface plots of PC concentration with CTAB additive over conductivity and viscosity

The conductivity vs. CTAB additive graph reflects the impact of CTAB on the electrical properties of the solution. The observed trend is indicative of the surfactant's role in enhancing ion mobility and, consequently, the electrical conductivity of the solution. Additionally, it is clear that both PC concentration and CTAB additive directly affect the dispersion of fibre diameters. Lastly, in the viscosity vs. CTAB additive graph, the variations in viscosity point towards the complex interplay between CTAB and polymer, where micelle formation and surfactant-polymer interactions will likely contribute to the changes in solution viscosity. Understanding these associations is crucial for optimizing the manufacturing process, as the physics behind these phenomena shed light on how CTAB concentrations influence the solution's structural and rheological properties.

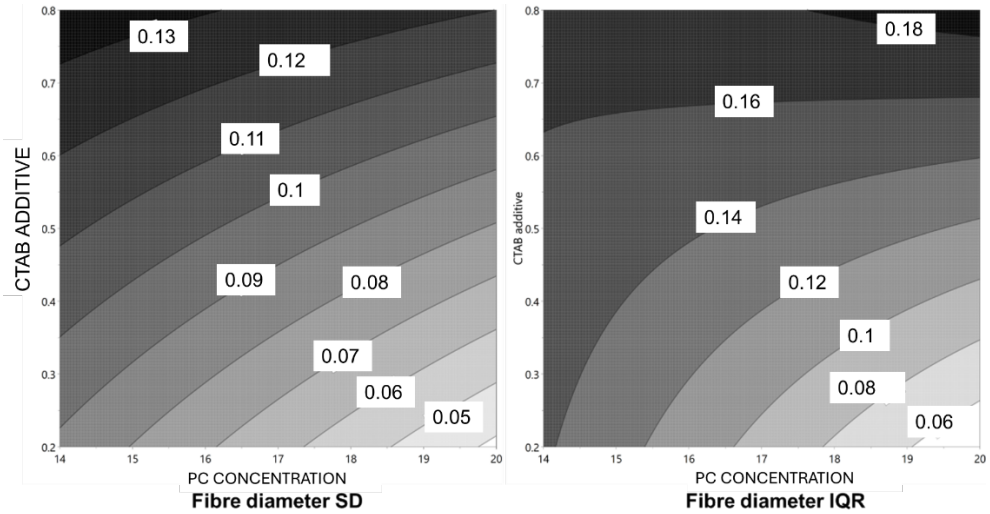

Fig. 3.12. Surface plots of PC concentration with CTAB additive over fibre diameter SD and IQR

The examination of fibre diameter standard deviation (SD) and interquartile range (IQR) in relation to the CTAB additive concentration provides additional insights into the structural consistency and variability of the solution during the manufacturing process. In the fibre diameter SD vs. CTAB additive graph, the observed variations in fibre diameter standard deviation highlight the sensitivity of the fibre-forming process to the changes in CTAB concentrations. This variability may be attributed to the stability of micelles formed by the cationic surfactant, wherein different CTAB levels contribute to varying degrees of dispersion in fibre diameters. Meanwhile, the fibre diameter IQR vs. CTAB additive graph sheds light on the range within which the central 50% of fibre diameters lie. The graph may reveal how the addition of CTAB affects the uniformity of fibre diameter distribution.

3.2.5. Filtration efficiency

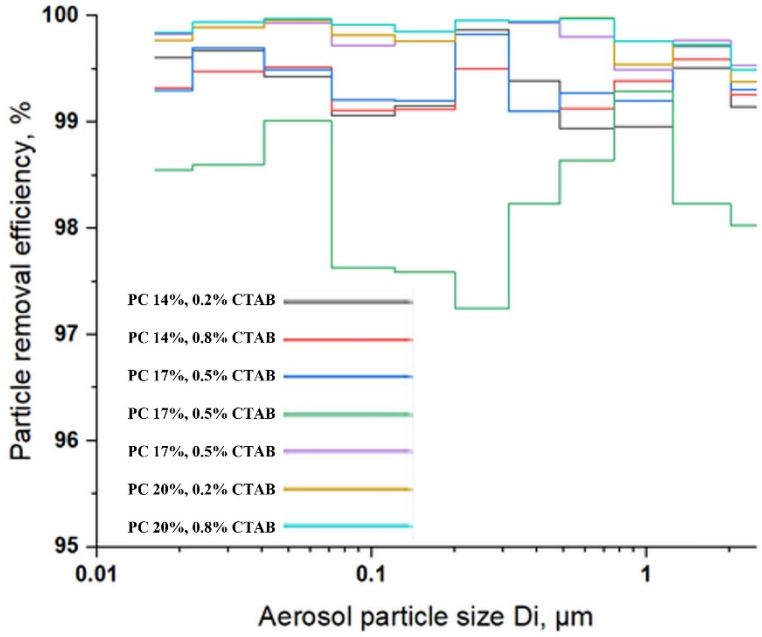

Fig. 3.13. NaCl aerosol particle collection efficiency of 7 nanofibrous polycarbonate air filtration substrates

The author utilized optimized results to create nanofibre filter media on 3D printed substrate samples. These samples were then subjected to testing in the experimental filtration setup outlined in sub-section 2.3.2 and Fig. 2.4. The filtration efficiency and pressure drop of seven PC nanofibre filter media samples were measured. The filtration performance with NaCl particles in the most penetrating particle size range was evaluated by using the electrical low-pressure impactor (ELPI+, Dekati Ltd., Finland). The primary focus of the analysis of fibrous filter's filtration efficiency was on the impact of inertia and diffusion induced by Brownian motion on the particles with minimal attention given to the effects of the particles' interaction with electric field force and gravity [180]. The PC substrates that were developed achieved an average retention efficiency that approached the desired 99.9% for solid NaCl aerosol particles. The greater filtration effectiveness can be attributed to the greater accumulation of fibres, because of the elevated polymer concentration in the solution. When the solution contains a higher concentration of polymer, the solvent in the jet is comparatively less volatile, leading to a greater rate of polymer accumulation and increased density of the resulting filters [181]. The smaller fibre diameters have been attributed to an increase in filtration efficiency. However, this may as well result in a decrease in air permeability. PC1-PC6 demonstrate excellent overall filtration efficiency over 99%. However, PC 7 may have a slight disadvantage in terms of efficiency for certain particle sizes.

In general, when the particle diameter is greater than that of the fibres, fibrous filters achieve filtration efficiency primarily through interception. Fibrous filters employ three primary filtration mechanisms to capture particles, namely interception, inertial impaction and diffusion, depending on the size of the particles. Interception and inertial impaction are responsible for capturing larger particles with a diameter above 0.4 mm. Diffusion and interception work together to capture medium-sized particles ranging from 0.1 to 0.4 mm in diameter. Smaller particles below 0.1 mm in diameter are captured primarily through diffusion. When particulate matter (PM) diffuses onto the fibre surface, the fibres exhibit strong adsorption. The adsorbed particles can vary in size, either being smaller than or equal to the diameter of the fibre or larger. The internal structures of the filters may be attributed to solvent evaporation and shear forces occurring during the electrospinning process [182]. However, in this study, the mechanical filtration was used, which allowed the use of nanofibrous membranes with pore sizes much smaller than those of common filters to block particles smaller than 2.5 µm [155, 183].

When the fibre diameter is small, the specific surface area-to-volume ratio is high, resulting in a greater probability of particle contact with the fibre and leading to high filtration efficiency. Recent studies have shown that combining or layering large and small fibres can help to reduce the resistance while maintaining filtration efficiency [184].

The concentration of the polymer solution used in the electrospinning process had an impact on the fibre diameter, which in turn could affect the filtration efficiency. It was concluded that the designed structure significantly improved the overall filtration performance of the filter that was prepared. Increasing the duration of fibre collection leads to a denser nanocoating on 3D substrate and positively impacts the filtration efficiency.

3.2.6. Pressure drop

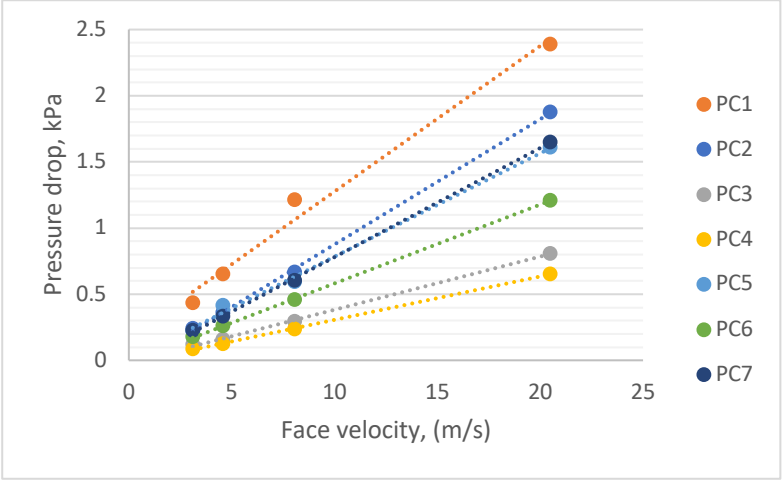

Fig. 3.14. Pressure drop through the filter as a function of face velocity

At the face velocity of 5.3 cm/s, the pressure drop across the seven nanocoating ranged from 201.5 to 721.5 Pa. This velocity is considered standard when researching high-efficiency filters. Fig. 3.14 shows the pressure drop at different face velocities for the filter. The pressure drop differences in PC1-PC7 are primarily influenced by the variations in the flow rate and unique characteristics of each membrane. Higher flow rates generally result in increased pressure drops, but the specific design, materials and properties of each PC membrane play a significant role in determining the magnitude of these differences. The pressure drop measurements of the nanofibre filters exhibited relatively high values. However, this comes at the cost of a higher pressure drop across the thickness of the filtering membrane layer. The distance between the nanofibres remained constant during the fabrication of the PC composite filter, which increased filtration efficiency with a smaller pressure drop. Low mass electrospun filters were effective at collecting particles, but they did that at the expense of a greater pressure drop per unit of filter thickness than the traditional filters [185]. The research shows that the fibres exhibit an evenly distributed pattern with smaller pore sizes. Additionally, due to the proximity of the fibres resulting from the shortened distances caused by the pores, there was an increase in pressure drop. Consequently, the PC composite filter demonstrated enhanced air filtration efficiency despite higher pressure drop.

3.3. Testing "cells on particles" concept

3.3.1. Assessing biocompatibility of nanofibrous sampling platform

Human bronchial epithelial cells from the BEAS-2B line were able to adhere to and develop on a variety of nanofibrous testing and sampling surfaces. After 48 hours of culture, there was seen a considerable rise in cell proliferation/viability (Fig. 3.15, A). Cells that expanded on the PA6 platform showed the least pronounced rise in the proliferation signal.

The release of LDH, which was correlated with the quantity of dead cells, was then assessed. There was no discernible difference in the amount of LDH released during the 72-hour culture of Beas-2B cells on various membranes compared to the same number of cells cultivated on the plastic surface of the 24-well plate (2D control) (Fig. 3.15, B). The total release of LDH, which represents the number of cells that developed on the substrate, was determined after 5 days of cell culture on nanofibrous sampling and testing platforms and 2D plastic surfaces (Fig. 3.15, C). When compared to the same number of BEAS-2B cells planted on a typical plastic 2D surface, the LDH release from cells growing on all platforms was more than two times higher. The cells cultured on the PA6 membrane had the lowest LDH release, and these findings are consistent with the lowest viability/proliferation signals from the same samples. As a result, it was determined that CA, PCL and PAN platforms were the best substrates for the development and cultivation of BEAS-2B cells. After staining with the live cell dye calcein AM after 7 days in culture, it was possible to confirm BEAS-2B growth and viability of all evaluated platforms. Depending on the type of material

being utilized as a substrate, the cells generate dense monolayers with various morphologies.

CA and PCL nanofibrous sampling and testing platforms were found to be the most promising based on the findings of cytotoxicity (LDH release and BEAS-2B vitality) tests with BEAS-2B cells. These platforms were then tested with designed silver, copper and graphene oxide nanoparticle.

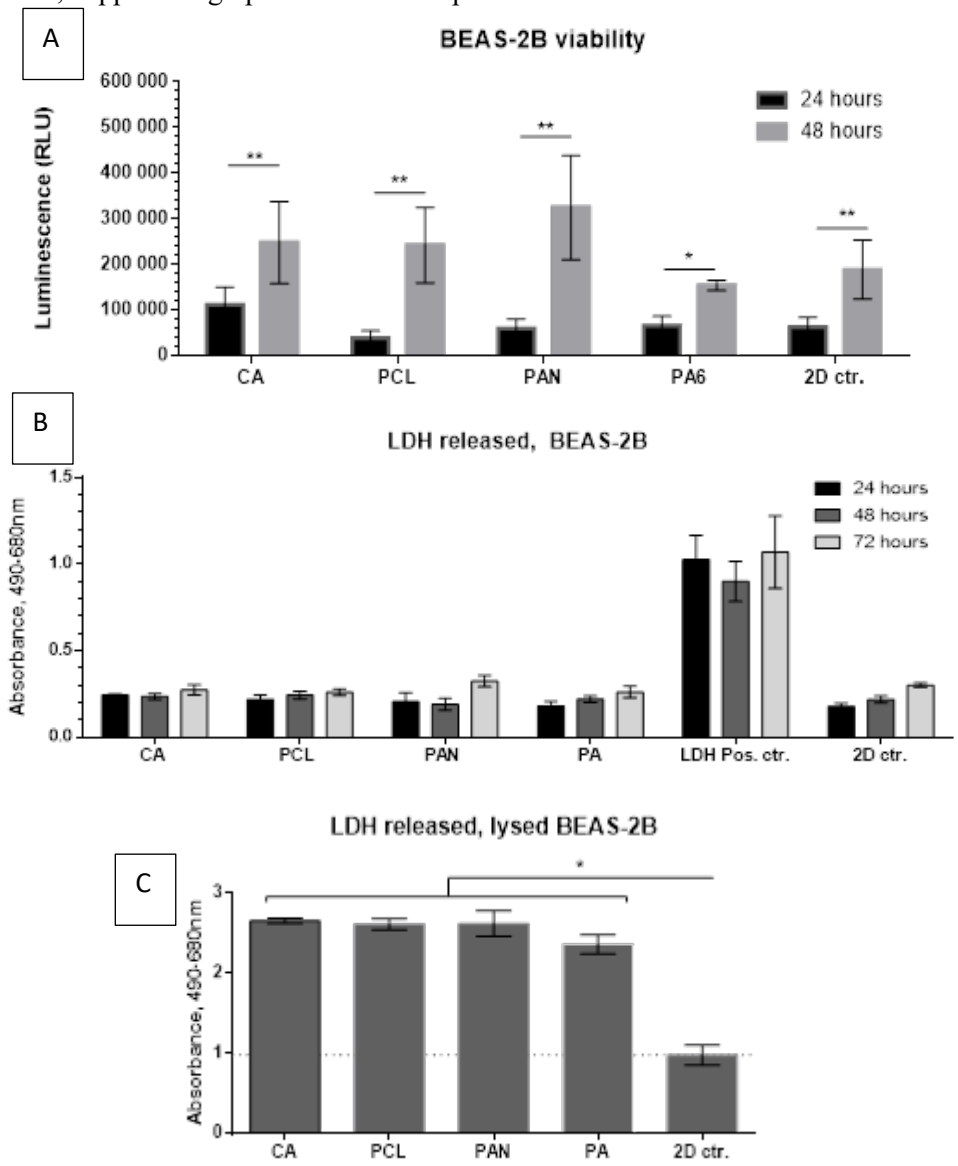

Fig. 3.15. BEAS-2B viability on a different type of platforms up to 48 hours: * – $p<0.05$, ** – $p<0.01$, 2D ctr. – BEAS-2B cultured on standard (2D) bottom of the 24-well culture plate (A), cytotoxicity of BEAS-2B cells measured as the lactate dehydrogenase (LDH) release

from dead cells during 72 hours of cultivation on different type of platforms (B), LDH release from the lysed BEAS-2B cells, cultured on different types of the platforms and on standard (2D) bottom of the 24-well culture plate, * – $p<0.05$ when compared to 2D control (C)

3.3.2. Characterizing particle deposition on nanofibrous platform

Silver nanoparticles had an average size of 60 nm in the study utilizing the DelsaTM nano C particle analyser with a size distribution of 20–110 nm and a zeta potential of –35 mV, indicating greater stability in deionized water. The copper nanoparticles had a positive zeta potential of +28 mV, varied surface characteristics and an average size of 85 nm with a size distribution of 55–115 nm. The highest average size of 250 nm, the widest range of sizes (45–655 nm) and a zeta potential (-24 mV) that was comparable to silver nanoparticles were all displayed by graphene oxide nanoparticles. The observed sizes and size distributions of silver and copper nanoparticles in the nanoparticle analysis performed using the DelsaTM Nano C particle analyser were found to be mainly consistent with the manufacturer's requirements. The AgNPs' average size was 60 nm, which was in good agreement with Sigma-Aldrich's stated size of <100 nm (Cat. No. 576832). The manufacturer's stated range of 60–80 nm (Cat. No. 774103) was significantly exceeded by the copper nanoparticles' average size of 85 nm. The manufacturer's requirements (Cat. No. 796034), which do not specify a precise nanoparticle size, cannot be directly compared with the graphene oxide nanoparticles because of their average size of 250 nm and wide distribution. The values of the zeta potential provide important information on the stability of nanoparticle suspensions. Zeta potential measurements of the AgNPs showed a value of -35 mV, indicating a stable suspension in deionized water. With a zeta potential of +28 mV, the copper nanoparticles showed fair stability as well. However, the zeta potential of the graphene oxide nanoparticles was -24 mV, which is less suggestive of a stable suspension and more likely to indicate particle aggregation. Overall, the results of zeta potential suggest that the suspensions of silver and copper nanoparticles are more stable than the suspension of graphene oxide in deionized water. Size, shape and surface charge, or zeta potential, of nanoparticles in suspension can all affect how stable they are. Higher absolute zeta potential values tend to improve stability by boosting electrostatic repulsion and lowering the chance of agglomeration. The stability may be impacted as well by the outside variables, such as pH, ionic strength and presence of stabilizing chemicals. Additional assistance in preventing agglomeration formation can come from mechanical techniques, such as ultrasonication. The stability of nanoparticle suspensions is ultimately determined by a combination of these elements.

The research team previously documented the fibre diameter, mechanical and physical characteristics and aerosol particle collecting effectiveness of the nanofibrous sampling and testing platforms [6]. The research team has created four multilayer composite filters utilizing two variations of the electrohydrodynamic (electrospinning) technique and a variety of polymers. In essence, these filters served as a 2D collection surface for the sampling of aerosol particles thanks to their layered

structure, which offered a gradient from micro to nanofibrous layers. The study discovered that these filters with a moderate pressure drop were able to obtain particle collection efficiencies for particles of size 0.3 µm ranging between 99.4 and 99.9%. According to the findings, these filters can be modified for certain physical, chemical or toxicological studies of the collected particles [6].

In this investigation, silver, copper and graphene oxide nanoparticles were employed. Three different amounts of these nanoparticles were placed on the nanofibrous sampling ant testing platforms' surfaces. Based on the findings of the initial cellular toxicity tests, nanoparticle doses were chosen. AgNP surface concentration ranged from 4.99 to 29.5 µg/cm2. The rigs' surface levels of copper nanoparticles ranged from 0.54 to 4.37 µg/cm2. The density of graphene oxide nanoparticles on the surface ranges from 0.26 to 2.67 µg/cm2.

Fig. 3.16 displays SEM pictures of the nanoparticles entrapped on the surface. On the nanofibrous surface, the particles were equally dispersed and adhered to the nano threads. Silver and copper have average particle sizes of 84–1,530 nm and 110–3,550 nm, respectively, while graphene oxide has an average size of 3,550 nm. The nanoparticle sizes that were disseminated in distilled water were a little bit larger than what the particle producer had claimed. The deposited and aerosolized particles on the sampling platform were much greater in size.

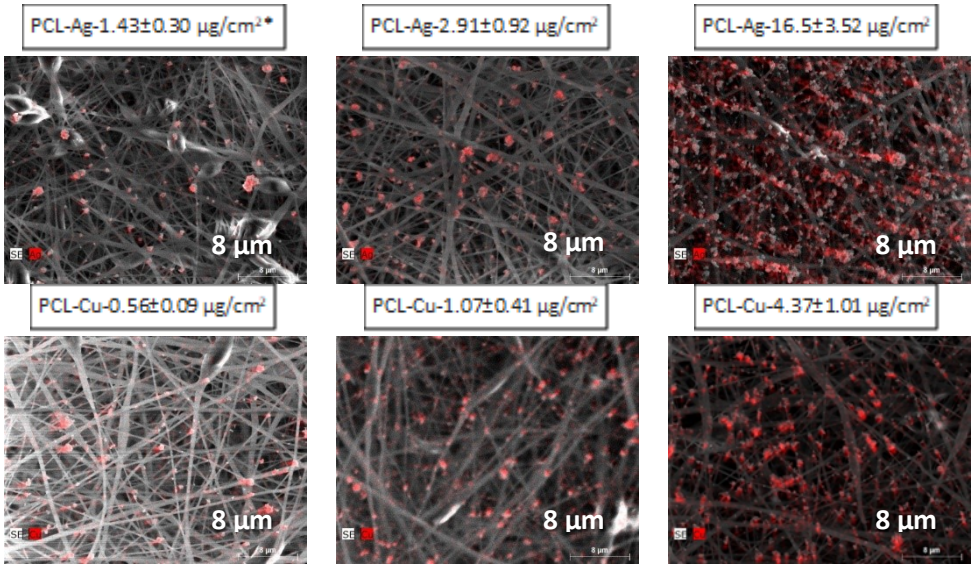

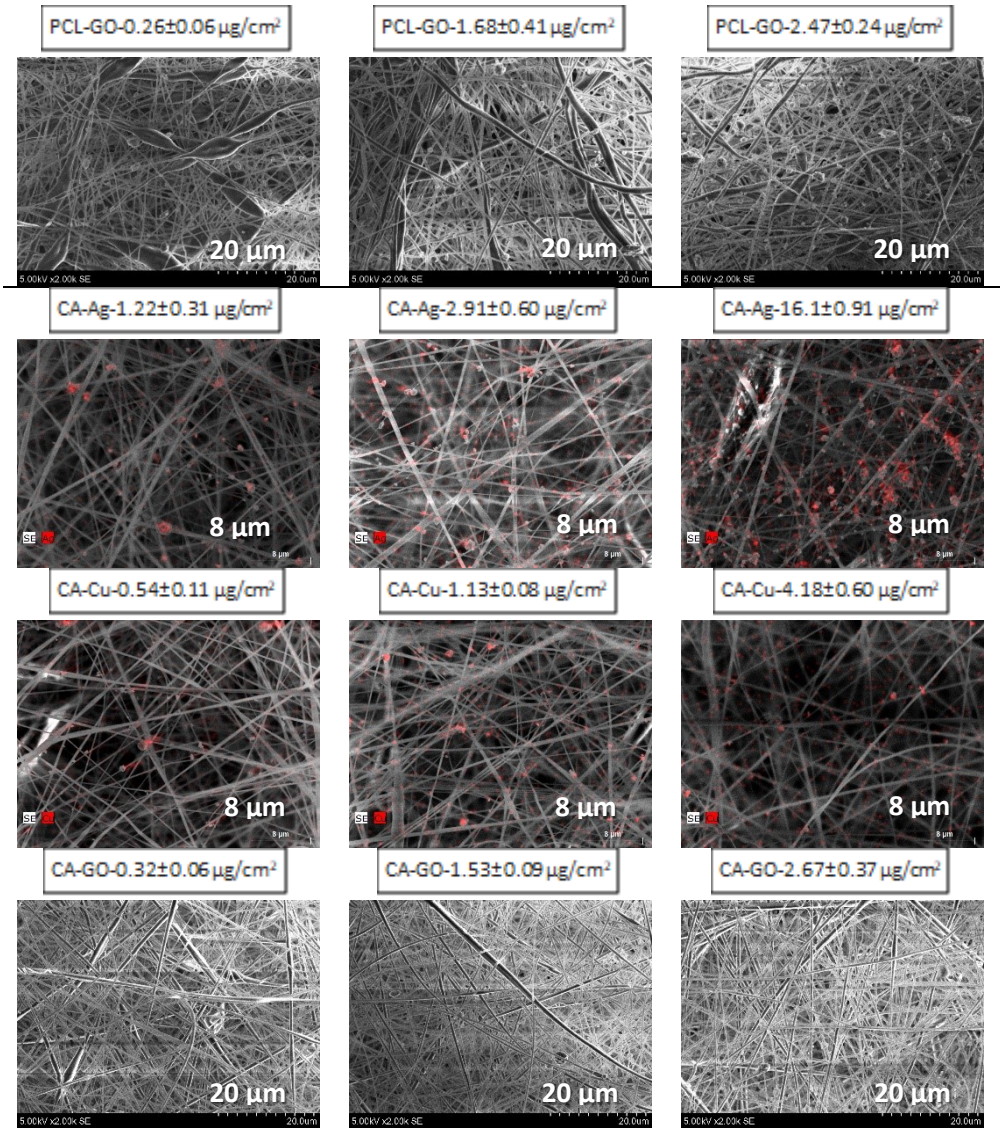

Fig. 3.16. SEM images of nanoparticles deposited on the nanofibrous platform, PCL nanofibrous platform, CA-cellulose acetate nanofibrous platform, Ag-silver nano particles, Cu-copper nanoparticles and GO-graphene oxide nanoparticles; in the SEM (EDS analysis) images, the silver and copper particles are coloured red

The aerosol particle formation method can be used to explain this occurrence. Using a collison nebulizer, which propels a suspension of nanoparticles into water under high pressure, aerosol particles were produced for this investigation. The created suspension's droplets were carried away from the nebulizer by airflow as the sprayed jets of the suspension struck the glass walls. The aerosolized suspension

droplets were then dried by dilution with dry air in the following phase. As the water in the suspension droplet progressively evaporated, its diameter did the same. The agglomerates are formed when individually isolated nanoparticles gradually come together. Due to potential lingering toxicological effects, the researchers decided not to apply any chemical additives to alter the size of the agglomerates throughout this study. In SEM EDS analysis, "SE" stands for secondary electrons, which are emitted from the surface of a specimen and are used to generate high-resolution images revealing surface morphology and topography details.

It may be concluded that the samples are appropriate and can be studied by using human epithelial cells because the collected nanoparticles were connected to the surface of the nanofibres and distributed equally on the surface of the nanofibrous platform.

3.3.3. Studying cellular response to Cu, Ag and GO NPs on PCL platform and discussion

Cells on particles and viability of BEAS-2B: different amounts of copper (Cu), silver (Ag) and graphene oxide (GO) were coated on the surface of a PCL-type platform, where BEAS-2B cells were grown for 24 hours. Less than 15% viability was found in the cells grown on membranes with 0.6 μg/cm2 copper and only 2.7% viability at a concentration of 3.2 μg/cm2 of copper. These relatively low concentrations of copper nanoparticles collected on the membranes had the greatest impact on the viability reduction. Less poisonous than copper, silver nanoparticles lowered cell viability to 68% at 1.4 μg/cm2, 37% at 2.9 μg/cm2 and 2.5% at 5 μg/cm2. Graphene oxide nanoparticles on PCL type platforms were the least harmful to BEAS-2B: their 0.33 μg/cm2 concentration only reduced viability to 96%, while 2.7 μg/cm2, to 54%.

In order to assess the biological impacts of aerosol particles, numerous in vitro systems have been created. Organ-on-chip models, cocultures of two or more cell types, 3D spheroids/organoids and monocultures of various respiratory epithelial cells can be used as in vitro testing methods [186]. In vitro cultures may be immersed in culture medium or of the air–liquid interphase (ALI) type, where the aerosol matter contacts the cells from the air in the exposure chamber, depending on how the cells are exposed to the aerosol particles [187]. There are benefits and drawbacks to these testing systems. One of the drawbacks of in vitro aerosol particle testing systems is the requirement to disperse or dilute the particles in the liquid carrier to be applied on the cells submerged in the medium, or the generation of dry solid particles by the dispersion of powders, the generation of aerosols by the dispersion of liquids, or the ablation from solid bulk materials (for ALI systems) [188, 189]. Depending on the particle density, they may remain suspended and/or interact with surfaces such as plastic where cells are seeded, which could have an effect on the actual dose to which cells are exposed [190]. In order to conduct further in vitro and in vivo toxicity testing, the extraction of ambient air aerosol particles collected on filters is required. Additionally, it has been demonstrated that different extraction techniques utilizing various solvents do not retain the chemical composition of ambient aerosol particles

and result in diverse toxicological reactions [191]. There was created and tested a novel kind of in vitro testing system that operates on the "cells-on-particles" principle, where cells are seeded on a biocompatible, cell-friendly nanofibrous sampling and testing platform. On a nanofibrous platform comprised of cellulose acetate (CA), polycaprolactone (PCL), polyacrylonitrile (PAN) and polyamide (PA), the growth and viability of BEAS-2B cells were examined. Although all of the investigated materials were found to be cell-friendly, the sampling platforms built of PCL and CA demonstrated the highest cell viability/proliferation. The PCL type platform performed better than the CA type platform among the two due to its decreased wettability and lack of detached nanofibre sheets that resembled "spiderwebs", unlike the CA type platform. As a result, a PCL-type platform was the optimum choice for substrate for ambient air filtration and particle collection as well as for cell attachment and growth. The PCL membranes have been frequently used in tissue regeneration research because of their biodegradability, biocompatibility and lack of toxicity of biodegradation products [192].

The chosen platform's suitability for ambient air filtration/nanoparticle buildup and subsequent use for direct impacts on cells were then put to the test. The effects on cells in vitro have been extensively demonstrated in several scientific studies; thus, it has been chosen to use commercially available copper (Cu), silver (Ag) and graphene oxide (GO) nanoparticles [193, 194]. The experiments were conducted by treating BEAS-2B cell cultures in conventional 96-well plates with serial dilutions of Cu, Ag and GO nanoparticles before testing by principle "cells on particles" with the PCL type platform. It was checked for cell viability as well as expression of the genes known to be responsive to the treatments with metal or GO nanoparticles (MT1X, MT2A, HSPA1A) [195, 196], stress-induced transcription factor ATF3 [197] and protection from oxidative stress and xenobiotics as well as NQO1 [198]. It has been demonstrated that all three types of nanoparticles significantly reduce the viability of BEAS-2B cells between doses of 15.63 and 62.5 μg/ml with EC50 values falling in the range of 20 to 24 g/ml for every type of nanoparticle studied. Muhamad et al. demonstrated that biogenic AgNPs caused cell death in A549 and BEAS-2B cell lines in a dose-dependent manner with IC50 values of 20–28 μg/ml and 12–35 μg/ml, respectively [199]. Human lung epithelial (A549) cells were demonstrated to be highly toxic to copper oxide nanoparticles with an IC50 value of 15 mg/L after 24 hours [200]. According to Gurunathan et al. findings on the cytotoxicity of graphene oxide in HEK293 cells, 50% of the cells die after being exposed to concentrations between 20 and 30 μg/ml [196]. It was possible to confirm the dose-dependent rise in the number of dead cells by staining the cells 24 hours after exposure using a Live/Dead staining kit. The BEAS-2B did not stain red (dead) or green (living) as much as those exposed to Cu or Ag when subjected to the maximum (1,000 g/ml) concentration of GO particles. The ability of GO nanoparticles to quench fluorescent light may help to explain this [201, 202].

The vitality of BEAS-2B cells grown on the PCL-type platform with nanoparticles was different because of the exposure tests based on the "cells on

particles" principle. Although it was not immediately apparent, there was clearly seen a dose-dependent and more crucially, NP-type-specific response when the exposure was carried out in a conventional 2D culture system. Comparing two systems when the exposure paths are different is challenging. In order to predict the concentration of nanoparticles covering the cell growth area surface, if all the particles in a medium sedimented on the bottom of the well, the specific exposure dose conversion was calculated (Table 3.4). As a result, it was possible to roughly translate the exposure dose from μg/ml to μg/cm2. The EC50 values in this scenario would be in the range of 6.25 to 7.5 μg/cm2 for 2D grown cells, which reacted similarly to various types of nanoparticles in culture media (EC50 range from 20 to 24 g/ml). Cu NPs were used to seed BEAS-2B cells on the PCL-type platform, and the 0.6 μg/cm2 concentration reduced cell viability to less than 15%, while 3.2 μg/cm2 concentration reduced it to less than 5%. AgNPs reduced cell viability to 68% at the concentration of 1.4 μg/cm2 and 37% at the concentration of 2.9 μg/cm2. A low concentration of GO NPs (0.3 μg/cm2) had no discernible impact on cell viability (96%), but a rise in particle concentration on a PCL-type platform to 2.7 μg/cm2 caused a discernible reduction in the percentage of viable cells (54%). It is possible to infer that the particles are gathered on a PCL-type platform, and the cells are seeded on top of it with the particles integrated. The significant reduction in cell viability is caused by much lower particle concentrations than in the model when particles dispersed in the culture medium are applied to the adherent cells. 2D cell culture typically refers to the cells that are grown in a monolayer on a flat surface, such as Petri plates. Both terms convey the idea of cells being cultured in a two-dimensional environment rather than in a three-dimensional structure.

Table 3.4. A conversion of the exposure dose values of 2D cell culture from μg/ml to μg/cm^2

Nanoparticle concentration in medium, μg/ml	1,000.00	250.00	62.50	31.25	15.63	7.82	3.91	0.98
Extrapolated concentration of nanoparticles on the surface of the well bottom if all sedimented, μg/cm^2	312.50	78.13	19.53	9.77	4.88	2.44	1.22	0.31

In the transformation from μg/ml to μg/cm2, the author calculated that the conversion from μg/ml (X) to μg/cm2 (Y) would be Y = X/3.2, assuming all of the solution's particles would settle on the bottom of the 96-well plate (0.32 cm2).

A novel method for evaluating aerosol particles was created and tested in this study. It has been demonstrated that pertinent information regarding the response of cells to aerosol nanoparticles can be collected on a PCL-type platform without the need for additional processing steps that require the aerosol particles to be dissolved in a solvent and put through various dilution steps before being applied to the desired

cell model in vitro. A similar response was seen when particles were put on top of the adherent cells, which were then seeded on top of the particles. If the exposure doses are changed from µl/ml to µg/cm2, it will be possible to hypothesize that cells are more susceptible to the aerosol particle exposure and are cultivated on a PCL-type platform with particles. This exposure concentration conversion is, in fact, only an approximation, since it ignores a variety of factors and situations, such as particle sedimentation time, interactions with polymers (PCL), adherence to well walls made of plastic and interactions with culture media proteins. The "cells on particle" testing method appears to be technically easier and quicker, because it does not require manipulations, such as particle extraction or solution preparation for cellular exposure (as in submerged culture or ALI systems). It is especially helpful for preliminary testing of nanoparticle toxicity.

3.3.4. Summary of research method for estimating aerosol particles cytotoxicity

In order to tackle aerosol particle toxicity testing challenges, there has been developed an innovative in vitro evaluation system called “cells-on-particles”. This system utilizes nanofibrous platforms made from biocompatible polymers, such as cellulose acetate (CA), polycaprolactone (PCL), polyamide 6 (PA6) and polyacrylonitrile (PAN), created through electrohydrodynamic processes. These platforms serve a dual purpose: efficient collection of aerosol particles and subsequent cytotoxicity analysis using BEAS-2B human bronchial epithelial cells. Most importantly, this approach eliminates the need for particle separation before in vitro investigation. The research revealed that these nanofibrous platforms are biocompatible with BEAS-2B cells, CA and PCL platforms showing superior cellular viability and reduced lactate dehydrogenase (LDH) release, making them ideal for further testing with engineered nanoparticles. There were used aerosolized solutions of silver (Ag), copper (Cu) and graphene oxide (GO) nanoparticles to mimic the environmental contaminants. The particles were evenly distributed on the nanofibrous platforms, despite some aggregation, likely due to the collison nebulizer aerosol generation method, supporting their suitability for subsequent biocompatibility studies. The “cells-on-particles” approach revealed a clear dose–response relationship, demonstrating heightened cellular sensitivity to lower particle concentrations during direct exposure. While this novel methodology provides a valuable tool for more accurate and realistic aerosol toxicity assessments, it requires a larger number of replicates due to the potential non-uniform particle distribution.

Technical problem: the background of the technical issue is that according to the state of the art, determining the cytotoxicity of aerosol particles requires an unnecessarily sophisticated technique that includes lengthy particle sampling, many processing steps or complicated exposure equipment.

Since the extracted suspension only contains a partial description of the particle's cytotoxicity, the methods for determining aerosol particle cytotoxicity that rely on the extraction of the particle from the sampling substrate run the risk of misrepresenting the true toxicity potential.

Solution: with the help of this discovery, it is now possible to assess the cytotoxicity of aerosol particles directly from filter medium where they have been collected. Additionally, it gives a better approximation of the cytotoxicity of the particles because the solvent extraction stage has no effect on the physical shape or chemical makeup of the particles. This approach for particle sampling/collection and subsequent cell growth is based on a single integrated polymer fibrous platform. Compared to in vitro models based on particle extracts or the air–liquid interface, this approach yields a simpler process, more representative results and a faster observation rate. By particularly constructing these filters to be employed in toxicological analysis of the collected particles and aerosol particle cytotoxicity studies, the innovation expands the utility of aerosol sampling filters. Three fibrous layers make up the fibrous platform: layer 1 is made up of microfibres at the bottom, supporting the top layers structurally; layer 2 is made up of nanofibres in the middle, ensuring good adhesion between the bottom and top layers; layer 3 is made up of nanofibres at the top, providing an effective 2D surface for gathering aerosol particles and cultivating cells to study the cytotoxic response. In this context, "2D surface" refers to the top layer of the matrix, layer 3, where cells proliferate and do not move into layers 2 and 1. During aerosol sampling, subsequent handling, and in vitro cell cultivation, the three-layer structure creates a fibrous matrix with great mechanical stability. The wide pores of the microfibre layer (layer 1) provide minimal barrier for culture medium to approach upper layers, ensuring good circulation of the media within the fibrous matrix and supplying nourishment to cells from the top as well as from the direction of attachment.

The described method and process offer a middle ground between the direct and indirect methods that are currently used to determine the cytotoxicity of aerosol particles. Aerosol particles are gathered on a filter similar to the direct technique; however, the extraction, purification and suspension processes of the gathered particles are skipped. The fibrous matrix with particles is immersed in a culture medium, and the cells are then added on top of the matrix, which is a feature that is similar to the direct technique. In contrast to the traditional direct technique, the cells now have a durable 2D support scaffold in which the collected particles remain on the surface of the fibrous matrix, ensuring more efficient contact with the cells.

Advantageous effects: the research offers a better and more straightforward approach for calculating particle cytotoxicity. The method's application simplifies the cytotoxicity testing process, since it offers a single platform (a fibrous matrix) for the collection of aerosol particles and the growth of the cells by allowing cells to be grown directly on the collected particles. This can be accomplished by employing an aerosol that has a special design. A three-layer composite sampling filter with a top nanofibrous layer that doubles as a scaffold for 2D-fibrous cell culture is as well as an effective filter for collecting aerosol particles.

The method produces a more accurate cytotoxicity assay because cells undergoing cytotoxicity testing are exposed closely and directly to both the undissolved collected aerosol particles and the dissolved aerosol particles in the water-based cultivation media. This contrasts with the traditional indirect testing, in which

cells are exposed to a solution of soluble aerosol particle fractions. Additionally, the technique expedites particle cytotoxicity testing, making it effective in terms of time and resource use. The indirect procedure's processes of particle extraction from the filter, dissolution, filtration and suspension are skipped as well as the direct procedure's steps of monoculture preparation and sophisticated setup. The method reduces the financial costs, and the environmental impact associated with the use of chemicals or laboratory supplies by saving materials that are applied routinely for aerosol particle cytotoxicity testing (such as extraction solvents, filtering media and syringe consumables).

Applications of the method: the method that is being discussed is the one that can be applied in environmental laboratories, businesses or health institutions where it is necessary to evaluate the toxicity of the components of ambient air. The applications of such are designed to determine the toxicity of the components of ambient air in studies and research on the environmental or occupational pollution.

4. CONCLUSIONS

1. The presented research demonstrates a successful development of three-layered composite aerosol sampling filter, which working layer was composed of polymer nanofibre matrix. Employing a combination of electrospinning techniques and material engineering, there were created substrates with gradient fibre and pore diameters, ensuring a superior particle retention efficiency and sufficient mechanical stability. The substrates, constructed from various polymers including PCL, CA, PAN and PA6, exhibited competitive pressure drops (ranging from 476 to 2,304 Pa at a face velocity of 10 cm/s) and excellent collection efficiencies (>99.4% with NaCl aerosol at MPPS). These substrates offer a customizable solution to meet the unique requirements of aerosol sampling across scientific and industrial domains through precise control over fabrication parameters and polymer selection.
2. This dissertation as well presents an attempt in the development of two-layer composite aerosol sampling filter constructed on 3D printed support and nanofibre working layer of polycarbonate (PC). The morphology of the nanofibrous layer was adjusted by optimizing hexadecyl trimethyl ammonium bromide (CTAB) addition to the PC solution. This resulted in bead-free nanofibre matrix that was capable in achieving high rates of particle retention approaching 99.9% for solid NaCl aerosol particles. Despite the increased pressure drop, the filters maintained improved airflow, highlighting their potential for high-efficiency filtration applications.
3. The application of nanofibrous aerosol sampling filters for evaluating the cytotoxicity of aerosol particles was demonstrated. The filters fabricated of biocompatible polymers, such as CA, PCL, PA6 and PAN, exhibited sufficient cellular viability and reduced lactate dehydrogenase (LDH) release. Specifically, LDH release from cells cultured on the PA6 platform was the lowest among the tested surfaces. A clear dose-response relationship was between Cu, Ag and graphene oxide nanoparticle concentrations and cellular viability. For example, at a concentration of 0.6 $\mu g/cm^2$, copper nanoparticles reduced cell viability to less than 15%, while at 3.2 $\mu g/cm^2$, the viability dropped to less than 5%. This method simplifies testing procedures, offers more representative results and expedites testing timelines.

5. SANTRAUKA

5.1. ĮVADAS

Remiantis „Global Burden of Disease“ tyrimu, palyginti su kitais sveikatos rizikos veiksniais, įskaitant sėdimą gyvenimo būdą, per didelį cholesterolio kiekį ir natrio vartojimą, aplinkos oro tarša yra susijusi su didesne mirtingumo tikimybe ir kelia didelių iššūkių visuomenės sveikatai. Vienas iš sudėtingiausių ir kenksmingiausių oro teršalų – smulkios kietosios dalelės – gali padidinti astmos riziką, sukelti bronchitą ir plaučių ligas, plaučių vėžį, aukštą kraujospūdį ir neurodegeneracines ligas [1, 203].

Siekiant išsiaiškinti smulkiųjų aerozolio dalelių koncentraciją patalpų ir lauko ore, jų šaltinius ir transformacijas aplinkoje, buvo vykdomi tūkstančiai mokslinių tyrimų projektų, aiškinamasi, kokie mechanizmai lemia žalingą jų poveikį žmonių sveikatai. Sukurta daug aerozolio dalelių koncentracijos aplinkos ore nustatymo metodų, įskaitant inercinį, gravitacinį, išcentrinį, terminį, optinį matavimą realiuoju laiku, aerodinaminio dydžio matavimą, elektrinio judrumo metodą, elektrinio aptikimo masių spektrometriją ir minėtų metodų derinius [3].

Vienas pirmųjų, žinomiausių ir dažniausiai taikomų aerozolių mėginių ėmimo metodų yra aerozolio dalelių rinkimas ant filtruojančio pagrindo. Pluoštinės matricos, membranos ir putos sudaro didžiąją dalį filtravimo substratų. Membraniniai filtrai (akytosios membranos, kapiliarinės membranos) yra labai stabilūs, efektyviai surenka daleles, tačiau dėl to filtravimo membranos sluoksnio viduje labai krinta slėgis. Jie gaminami iš polimerų (pvz., PTFE, celiuliozės esterių). Porėtieji filtrai gaminami iš neorganinės medžiagos (pvz., nerūdijančiojo plieno) arba polimero (pvz., polipropileno) ir veikia kaip didelių porų tinklelis stambioms dalelėms sulaikyti. Pluoštinių matricų sudedamosios dalys yra tankios, netolygios orientacijos pluoštų poros. Paprastai pluoštinėms matricoms kurti naudojama celiuliozė arba natūralios medžiagos, pavyzdžiui, stiklas ar kvarcas. Nepaisant to, kad pluoštiniai filtrai yra vieni dažniausiai aerozolių ėminiams imti naudojamų substratų, jie turi nemažai trūkumų: dėl didelio paviršiaus ploto mėginyje esančios didesnio lakumo medžiagos (pavyzdžiui, kai kurie policikliniai aromatiniai angliavandeniliai ar organiniai metalo junginiai), randamos paimtose dalelėse: a) ilgai laikomos išgaruoja iš filtro; b) turi įtakos cheminės analizės rezultatams (pavyzdžiui, metalai aerozolio dalelėse); c) mineralinio pluošto mechaninės savybės dažnai yra nepakankamos ir ėminių rinkimo procese filtrai gali suirti.

Pastaraisiais dešimtmečiais labai išsiplėtė aerozolių citotoksiškumo tyrimai, visų pirma susiję su nanodalelėmis. Šį padidėjusį dėmesį iš dalies sukėlė didėjantis susirūpinimas dėl galimo aerozolinių nanodalelių, kurios jau paplitusios daugelyje pramonės ir aplinkos atmosferų, poveikio sveikatai. Dėl šių dalelių savybių įvairovės ir sudėtingos jų sąveikos su biologinėmis sistemomis atlikti išsamų aerozolinių nanodalelių vertinimą tebėra sudėtinga užduotis, nepaisant gausėjančių mokslinių tyrimų. Šiuos tyrimus dar labiau apsunkina tai, kad nėra nusistovėjusių nanodalelių toksiškumo nustatymo metodų. Patikimų ir prieinamų nanodalelių citotoksiškumo

in vitro vertinimo metodų poreikis nuolat auga dėl didelės nanodalelių medžiagų ir jų galimo citotoksiškumo įvairovės.

Tačiau turimoje mokslinėje literatūroje vis dar tebėra atotrūkis tarp citotoksiškumo tyrimų ir aerozolio ėminių ėmimo. Vėlesnių citotoksiškumo vertinimų tikroviškumas ir tikslumas gali sumažėti dėl šio atotrūkio sukeltų dalelių savybių pokyčių ir galimų nuostolių jas tvarkant, sandėliuojant ir transportuojant. Naujausiuose tyrimuose skatinama taikyti integruotą strategiją, pagal kurią, siekiant įveikti šią problemą, aerozolio mėginių ėmimas *in situ* derinamas su vėlesniais toksiškumo *in vitro* tyrimais.

Siekiant išspręsti aerozolio mėginių ėmimo ir citotoksiškumo *in vitro* tyrimų skirtumus, šiame darbe pristatoma inovatyvi integruota platforma, paremta „Cells-on-Particles“ koncepcija, kurioje aerozolio dalelių surinkimas ir *in vitro* citotoksiškumo tyrimai sujungiami į vieną pluoštinę matricą. Tai padeda įveikti atskirų metodų trūkumus, sujungiant aerozolio mėginių ėmimą ir *in vitro* citotoksiškumo analizę vienoje platformoje, taip užtikrinant, kad įvertintos dalelės tiksliai atspindėtų originalaus aerozolio daleles, ir padidinant gautų toksikologinių duomenų svarbą.

Disertacijos tikslas

Disertacijos tikslas – sukurti nanopluoštinius aerozolio dalelių mėginių ėmimo filtrus ir apibūdinti jų savybes.

Uždaviniai

1. Suprojektuoti, pagaminti ir apibūdinti mikropluoštinį filtravimo substratą, tinkamą aerozolio dalelėms surinkti.
2. Ištirti nanopluoštinių mėginių ėmimo filtrų savybes įvairiais oro srauto režimais renkant įvairias daleles.
3. Validuoti sukurtus nanopluoštinius mėginių ėmimo filtrus kaip platformas surinktų dalelių citotoksiškumo analizei *in vitro*.

Ginamieji teiginiai

1. Elektrohidrodinaminis polimerų apdorojimo būdas – elektrinis verpimas – yra tinkamas metodas pluoštiniams filtrams iš įvairių polimerų gaminti ir tiksliai kontroliuoti pluoštinės matricos sudėtį ir dydį.
2. Naudojant tas pačias polimerines medžiagas nanopluošo ir mikropluošto sluoksnių gamybai, galima pagaminti tinkamų mechaninių savybių filtrą, kurio dalelių sulaikymo efektyvumas sudaro galimybes jį naudoti kaip aerozolio dalelių surinkimo filtrą.
3. Aerozolio dalelių surinkimo platformos, pagrįstos nanopluošine matrica, yra tinkamos dalelių citotoksiškumo tyrimams dėl savo suderinamumo ir ląstelių kiekybinio atsako į surinktas nanodaleles.

Mokslinis naujumas

Disertacijoje aprašomas naujo nanopluoštinio aerozolio dalelių ėminių ėmimo filtro gamybos būdas. Ėminių ėmimo filtrą sudaro sluoksniuotas kompozicinis

polimerinių pluoštų nuo nano- ir mikrometrinio dydžio išdėstymas, kuris užtikrina aukštą dalelių sulaikymo efektyvumą, gerą mechaninį stabilumą ir įvairias vėlesnio apdorojimo galimybes taikant įvairius fizikinius, cheminius ar toksikologinius analizės metodus. Šių ėminių ėmimo filtrų konstrukcija ir gamybos būdai pateikti 2022 m. balandžio 28 d. Europos patentų biurui pateiktoje Europos patento paraiškoje EP22170405.9.

Analizuojamas integruotas aerozolio dalelių citotoksiškumo tyrimo metodas, kurį taikant naudojamas nanopluoštinis aerozolio dalelių surinkimo filtras. Metodas pagrįstas viena integruota polimerinio pluošto platforma, skirta dalelių mėginiams imti ir (arba) rinkti, o vėliau ląstelėms kultivuoti.

Disertacijos struktūra ir planas

Šios daktaro disertacijos skyriai: įvadas, literatūros apžvalga, medžiaga ir metodai, rezultatai ir jų aptarimas, išvados, literatūros sąrašas ir su disertacijos tema susijusių publikacijų sąrašas. Disertacijos apimtis – 134 puslapiai, pateikta 30 paveikslų ir 8 lentelės.

Tyrimų rezultatų publikacijos

Šio tyrimo rezultatai paskelbti dviejuose recenzuojamuose straipsniuose žurnaluose, įtrauktuose į „CA Web of Science“ duomenų bazę. Eksperimentų rezultatai taip pat buvo pristatyti keturiose tarptautinėse konferencijose.

Praktinė reikšmė

Disertacijoje pristatomas aerozolio dalelių surinkimo ir citotoksiškumo tyrimo metodas gali būti taikomas oro užterštumo nustatymo tyrimuose patalpose, darbo ir aplinkos aplinkoje. Šie filtrai atlieka svarbų vaidmenį vyriausybinėse oro monitoringo kampanijose, kur jie plačiai naudojami. Tačiau jų reikšmė neapsiriboja vien tik mėginių ėmimu. Galimybė kontroliuoti dalelių surinkimo paviršiaus morfologiją ir pirmtakų polimerus atveria kelius moksliniams tyrimams, ypač kuriant naujus aerozolio dalelių analizės metodus.

Autoriaus indėlis

Autorius atliko didžiąją dalį tyrimų, aprašytų šiame doktorantūros baigiamajame darbe. Autorius visiškai pripažįsta eksperimentinių duomenų tikrumą.

Autorius atliko tyrimus ir aktyviai prisidėjo prie rezultatų rengimo publikuoti. Laboratoriniai tyrimai, duomenų analizė, interpretacija pristatomi skyriuje „Nanopluoštinių aerozolio mėginių ėmimo filtrų substratų projektavimas, gamyba ir charakterizavimas“.

Autorius atliko eksperimentinių duomenų analizę. Laboratoriniai eksperimentai, duomenų analizė, interpretacija pateikiami skyriuje „Kompozitinis nanopluoštas ant

3D spausdintuvu atspausdinto atraminio polikarbonato filtro, skirto aerozolio dalelėms filtruoti ir mėginiams imti“.

Laboratoriniai eksperimentai, duomenų apdorojimas, interpretavimas buvo vykdomi bendradarbiaujant su Vilniaus universitetu (IMC). Šios bendros pastangos pristatomos eksperimentų skyriuje „Vienos platformos, skirtos ir aerozolio dalelėms surinkti, ir citotoksiškumui vertinti *in vitro*, įvertinimas“.

5.2. Ankstesnių aerozolio mėginių ėmimo filtro ir citotoksiškumo tyrimų apžvalga

Vienas populiariausių aerozolių mėginių ėmimo metodų – aerozolio dalelių rinkimas ant filtravimo substrato. Filtravimo substratus sudaro įvairios membranų, putų ir pluoštinių matricų atmainos. Dažnai išskiriamos dvi membraninių filtrų grupės:

a) sudėtingos struktūros akytosios membranos, einančios vingiuotais keliais per filtravimo medžiagą. Šios membranos gaminamos iš politetrafluoretileno arba celiuliozės esterių;

b) kaip alternatyva – kapiliarinių porų filtrai, pagaminti iš polikarbonato, polietileno tereftalato ir kt., turi tiesias poras per visą membranos ilgį.

Membraniniai filtrai yra labai stabilūs ir veiksmingai sulaiko daleles. Tačiau jie pasižymi dideliu slėgio kritimu filtravimo membranos sluoksnio storyje. Putų filtrai gaminami palyginti didelio tūrio poromis, o tai leidžia sulaikyti stambias (įkvepiamas) daleles. Šie filtrai gaminami iš nerūdijančiojo plieno arba polimero (polipropileno). Pluoštinių matricų sudedamosios dalys yra tankios, netolygios orientacijos pluoštų akys. Filtravimo sluoksnio gylyje jie surenka aerozolio mėginius, užtikrindami didelį filtravimo efektyvumą, slėgiui palyginti mažai krintant. Paprastai pluoštinėms matricoms kurti naudojama celiuliozė arba natūralios medžiagos, pavyzdžiui, stiklas ar kvarcas.

Nors pluoštiniai filtrai yra vieni dažniausiai aerozolių mėginiams imti naudojamų substratų, jie turi nemažai trūkumų: a) kadangi filtrų paviršiaus plotas yra didelis, matuojamose dalelėse esančios didesnio lakumo medžiagos, pavyzdžiui, tam tikri policikliniai aromatiniai angliavandeniliai arba metaloorganiniai junginiai, laikui bėgant iš filtro išgaruoja; b) mineralinio pluošto natūralios priemaišos gali turėti įtakos tolesnėms cheminėms analizėms (tokių aerozolio dalelių, pvz., metalų); c) kai kurie gryno mineralinio pluošto preparatai (pavyzdžiui, kvarcas) yra mechaniškai trapūs ir tvarkant suyra. Pluoštinių aerozolio mėginių ėmimo filtrų galimybės yra ribotos dėl jų cheminės sudėties ir pluošto formos (akytumo, pluošto dydžio ir porų dydžio). Be to, taikant įvairius cheminės analizės metodus ir neseniai sukurtus surinktų dalelių cheminės analizės metodus, reikia sukurti unikalios cheminės sudėties filtrus. Kai reikia atlikti cheminį apibūdinimą, paprastai reikia imti mėginius iš įvairių substratų,

nes nė viena filtravimo terpė netinka visiems numatytiems cheminiams tyrimams atlikti.

Aerozolio dalelės – tai ore suspenduotos dalelės, kurios daro neigiamą poveikį žmonių sveikatai. Jos patenka į žmogaus kvėpavimo takus ir nusėda viršutiniuose kvėpavimo takuose, dar vadinamoje įkvepiamojoje aerozolio frakcijoje, viduriniuose kvėpavimo takuose, dar vadinamoje krūtinės ląstos frakcijoje, ir apatiniuose kvėpavimo takuose, dar vadinamoje kvėpuojamojoje frakcijoje. Pastaroji aerozolio dalelių dalis dėl savo mažo dydžio yra ypač svarbi, nes, patekusi į alveoles ir pasiekusi plaučius, gali patekti į kraują. Aerozolio dalelės didina kelių ligų, įskaitant vėžį, širdies ir kraujagyslių ligas bei astmą, paplitimą. Todėl šiuo metu atliekant poveikio žmonėms tyrimus, labai svarbu suprasti pagrindines neigiamo poveikio sveikatai priežastis.

Norint stebėti ir įvertinti toksiškumą ir jo poveikį ląstelėms, *in vitro* eksperimentai yra praktiškas, etiškai priimtinas ir mokomasis tyrimas.

Atliekant *in vitro* bandymus paprastai taikoma viena iš dviejų pagrindinių strategijų: tiesioginis (sąlytis su oru ir skysčiu) arba netiesioginis (poveikis panardinus) metodai. Tiesioginis metodas leidžia fiziologiškai imituoti įkvėpimo procesą per iš anksto nustatytą laiką, aerozolio daleles per specialiai sukurtą membraną (t. y. oro ir skysčio sąsają) užnešant tiesiai ant auginamų ląstelių. Šiuo požiūriu šis metodas yra pranašesnis už netiesioginį, nes leidžia tiksliau nustatyti dalelių dozę. Tačiau tiesioginiu oro ir skysčio sąsajos metodu dažniausiai vertinami įkvėpimo toksikologiniai rodikliai, o ne bendras citotoksiškumas. Šis metodas pagrįstas aerozolio srauto taikymu į tam tikroje poveikio kameroje esantį specialiai išaugintų ląstelių monosluoksnį. Naudojant šią technologiją realiuoju laiku gaunama nepakitusi toksikologinė reakcija į aerozolio daleles.

5.3. Tyrimų metodologija

5.3.1. Trisluoksnis aerozolio dalelių mėginių ėmimo filtras

Pluoštinei aerozolio dalelių mėginių ėmimo filtravimo medžiagai sukurti buvo naudojama elektrohidrodinaminio polimerų apdorojimo technologija, vadinamasis elektrinis verpimas. Galutinei filtro struktūrai sukurti buvo naudojami du šios technologijos variantai.

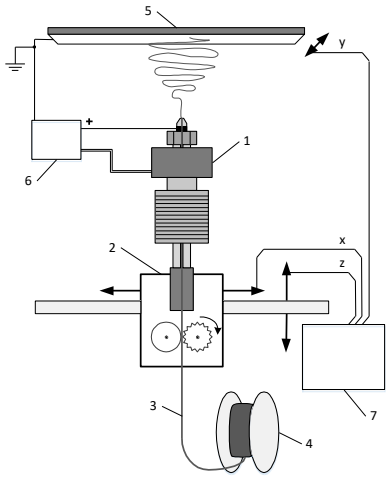

5.1 pav. 3D spausdinimo, naudojant pluoštus, sąranka: 1 – purkštuko kaitintuvas; 2 – pluošto ekstruderis; 3 – pluoštas; 4 – pluošto ritė; 5 – įžeminta surinkimo plokštelė; 6 – aukštosios įtampos šaltinis; 7 – ašies valdytuvas

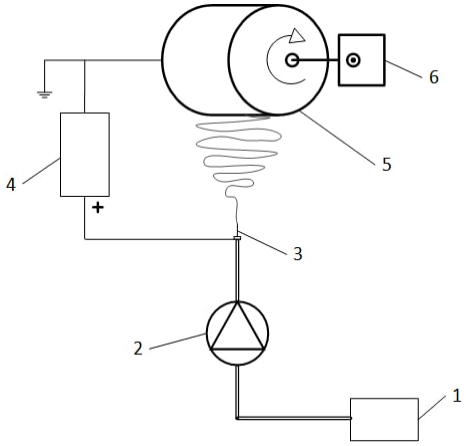

5.2 pav. Tirpalo elektrinio verpimo sąranka: 1 – tirpalo rezervuaras; 2 – švirkšto siurblys; 3 – metalinė adata; 4 –aukštosios įtampos šaltinis; 5 – įžemintas besisukantis kolektorius; 6 – sukimosi variklis

5.3.2. Modeliuojamų aerozolio dalelių filtravimo efektyvumas

Siekiant patikrinti filtrų gebėjimą filtruoti daleles, specialiai pagamintame įrenginyje buvo naudojamos aerozolinės NaCl ir DEHS dalelės. Naudojant elektrinį mažo slėgio impaktorių (ELPI +, Dekati Ltd., Suomija) buvo stebima dalelių koncentracija tiek prieš srovę, tiek už jos. Esant 5,3 cm/s srauto greičiui, slėgio jutikliu (modelis P300-5-in-D, Pace Scientific Inc., JAV) pirmiausia buvo stebimas slėgio kritimas prieš ir po mėginio terpės, o paskui 3–20 m/s intervalais.

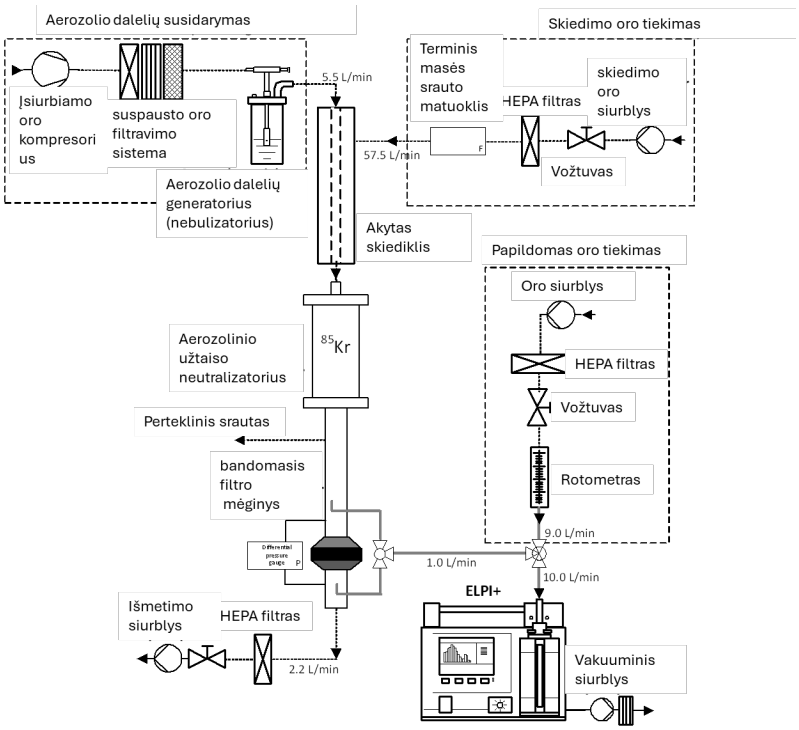

5.3 pav. Filtravimo medžiagos bandymų įranga dalelių surinkimo efektyvumui ir slėgio kritimui nustatyti

5.4. Nanopluoštinis polikarbonato sluoksnis ant 3D spausdintuvu atspausdinto substrato.

Polikarbonato nanopluošto formavimo elektrinio verpimo procesu parametrai pateikti 5.1 lentelėje. Elektrinio verpimas vyko organinio stiklo kameroje įprastomis aplinkos sąlygomis. Gautų pluoštų savybes galima keisti reguliuojant įvairius veiksnius, įskaitant polimero tirpalo savybes, taikomą įtampą (V), adatos gabaritą (n), srauto greitį (Q) ir atstumą (d). Siekiant sumažinti oro srovių įtaką polimero srovei, adata, elektrodas ir įžemintas taikinys yra kameroje.

5.1 lentelė. Slėgio kritimas polikarbonato filtruose esant skirtingiems oro srauto greičiams bei PC ir CTAB koncentracijoms

PC ir CTAB koncentracija (%)	**Slėgio kritimas (Pa)**	**Slėgio kritimas (Pa)**	**Slėgio kritimas (Pa)**	**Slėgio kritimas (Pa)**
Srauto greitis (l/min)	1,7	2,5	4,4	11,2
PC1	436,3	650,3	1212	2390,7
PC2	242,3	361,3	667,3	1877

PC3	119,3	158	292,3	808
PC4	87	126,7	234,7	652,3
PC5	222,7	415,7	593	1610,3
PC6	175,3	257,7	458,3	1208,7
PC7	225	332	602	1651

5.4.1. Viena aerozolio dalelių surinkimo ir citotoksiškumo *in vitro* platforma

5.4.2. Nanopluoštinės mėginių ėmimo platformos gamyba

Lydalo 3D spausdintuvu buvo sukurtas polikaprolaktono mikropluošto sluoksnis (substratas, apatinis sluoksnis, 5.1 pav.), ant kurio buvo sukurti mikropluošto ir nanopluošto sluoksniai. Gamybos proceso metu šie sluoksniai gaminami vienas ant kito.

Elektrohidrodinaminė procedūra (tirpalo elektrinis verpimas) buvo naudojama nano- ir mikropluoštiniams sluoksniams ant makropluoštinio pagrindo sukurti.

5.4.3. Aerozolinis nanodalelių nusodinimas

Nanodalelių suspensijai aerozolizuoti buvo naudojamas „Collison“ purkštuvas (modelis CN 6 J, BGI Inc., JAV), kuris aerozolį gamina 5,5 l/min srautu. Paskui ši suspensija buvo praskiesta sausu oru (57,5 l/min.) akytame vamzdeliniame skiediklyje, o krūvis išlygintas naudojant 85Kr dvipolį neutralizatorių (3054 A, TSI Inc., JAV). Laikiklyje buvo laikomi 37 mm skersmens platformos mėginiai, o oras su aerozolinėmis dalelėmis (2,2 l/min) buvo filtruojamas per platformos terpę. Kadangi kiekvieno tipo nanodalelių suspensija sukūrė pastovų aerozolio kiekį, nusodinimo trukmę buvo galima reguliuoti, siekiant kontroliuoti, kiek medžiagos susikaupia ant platformų. Dalelių nusėdimo aerozolio trukmė svyravo nuo 10 s iki 40 s.

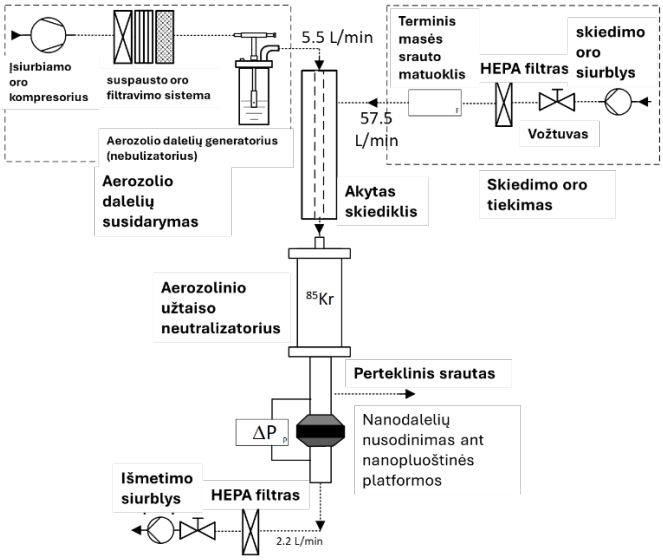

5.4 pav. Nanodalelių nusodinimo ant nanopluoštinių substratų metodo schema

5.5. Rezultatai ir diskusija

5.5.1. Pluoštinio trisluoksnio aerozolių mėginių ėmimo filtro konstrukcija, morfologija ir apibūdinimas

Galutinė dalelių mėginio terpė turėjo trisluoksnę struktūrą su pluošto ir porų skersmens gradientu (5.5 pav.). Trečias sluoksnis buvo bazinis sluoksnis trijų sluoksnių kompozito apačioje, užtikrinantis mechaninę atramą trapiems viršutiniams sluoksniams. Antrasis sluoksnis (vidurinis) buvo kaip rišamasis tarp pirmojo ir trečiojo makropluoštinio sluoksnio ir užtikrino geriausią sukibimą neleisdamas trečiajam nanopluoštiniam sluoksniui suirti imant mėginius mažu slėgiu. Trečiasis sluoksnis, t. y. viršutinis, buvo kaip nanopluoštinių aerozolio dalelių surinkimo paviršius.

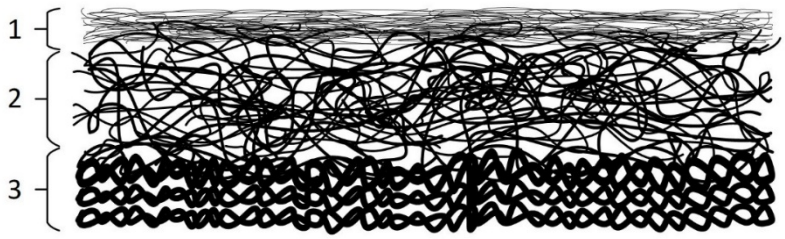

5.5 pav. Aerozolio ėminių ėmimo filtro trisluoksnio pagrindo skerspjūvio schema: trečias sluoksnis – makropluoštas, suteikiantis mechaninę atramą trapiems viršutiniams sluoksniams; antras sluoksnis – mikropluoštas, naudojamas kaip jungiamasis sluoksnis tarp pirmo ir trečio mikropluošto sluoksnių, o pirmas sluoksnis yra nanopluoštas, naudojamas kaip paviršius nanopluošto aerozolio dalelėms surinkti

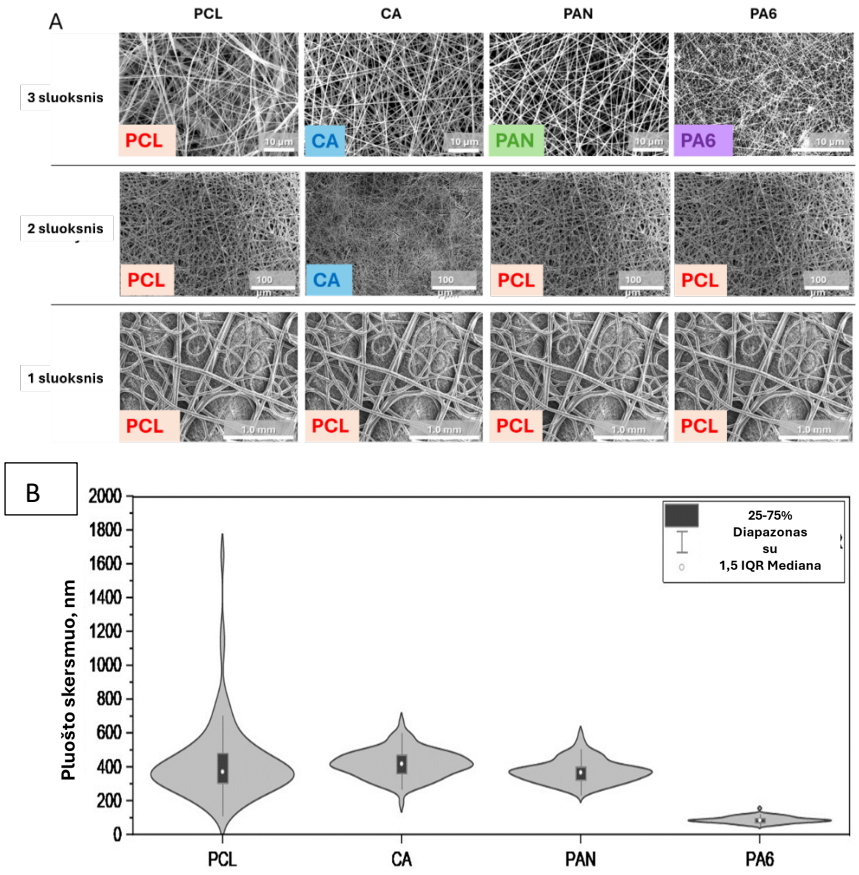

5.6 pav. A – aerozolio mėginių ėmimo filtro substrato sluoksnių SEM nuotraukos; B – viršutinio sluoksnio pluošto dydžio pasiskirstymas

Pirmas sluoksnis buvo naudojamas kaip tirpalo elektrinio verpimo substratas, o antras sluoksnis buvo gaminamas tiesiai ant pirmo sluoksnio. PCL tirpalas buvo pagrindas konstruojant antrą sluoksnį PCL, PAN ir PA6 atveju, todėl gaunamas vidutinis pluoštas skersmuo 2,80±1,31 µm (5.6 pav. 2 sluoksnis). Naudojant CA mėginį antras sluoksnis buvo pagamintas iš CA tirpalo, kurio polimero koncentracija buvo 20 %, todėl pluoštai buvo 0,71±0,22 µm skersmens, t. y. tris kartus mažesni nei PCL, bet didesni už viršutinį CA sluoksnį, pagamintą naudojant CA tirpalą, kurio polimero koncentracija buvo 17 %. Paaiškėjus, kad CA nanopluoštai efektyviai neprilimpa prie PCL vidurinio sluoksnio, CA buvo pasirinktas kaip vidurinis sluoksnis.

5.5.2. Filtravimo efektyvumas

Vidutinis sulaikymo efektyvumas sukurtuose substratuose buvo artimas numatytam 99,5 % efektyvumui naudojant NaCl aerozolį. PCL ir CA mėginiai artėjo prie kritinės vertės, kai dalelių dydis buvo didžiausias (apie 99,3–99,4 %). Šiuo atveju

morfologijos porėtumas ir pluošto dydis buvo glaudžiai susiję su efektyvumo vertėmis. Vidutinės poros celiuliozės acetate buvo didžiausios (1–5 mm), PCL – kiek mažesnės (0,7–3 mm). Šiek tiek sumažėjusį surinkimo efektyvumą, ypač CA ir PCL, lėmė suprojektuotų mėginių ėmimo filtrų sunkumai dirbti su skystu DEHS aerozoliu. Monodispersis DEHS aerozolio pasiskirstymas lemia didesnį skaitinės koncentracijos medianinį skersmenį (5.7 pav.), kuris yra artimesnis labiausiai prasiskverbiančios dalelės dydžiui ir turi įvairias dalelių krūvio savybes, galbūt net krūvį išlyginus.

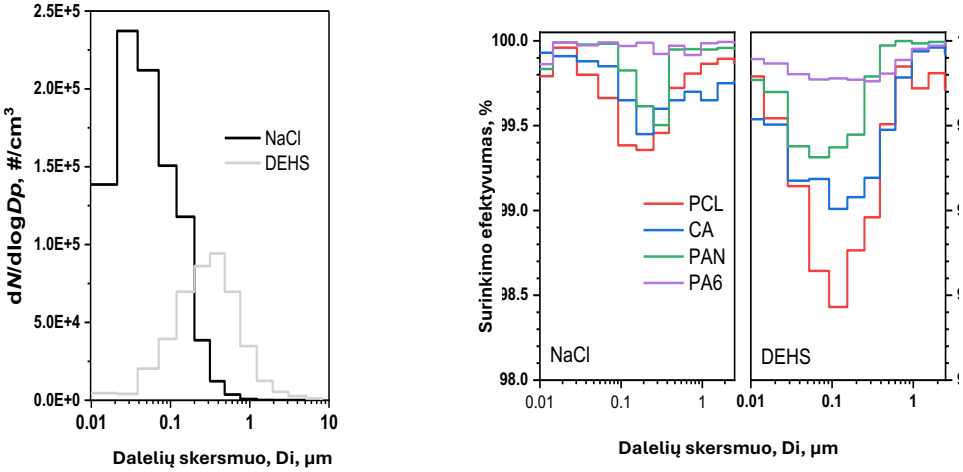

5.7 pav. NaCl ir DEHS aerozolio dalelių dydžio pasiskirstymas ant nanopluoštinių filtravimo substratų (kairėje) ir surinkimo efektyvumas (dešinėje)

5.5.3. Slėgio kritimas

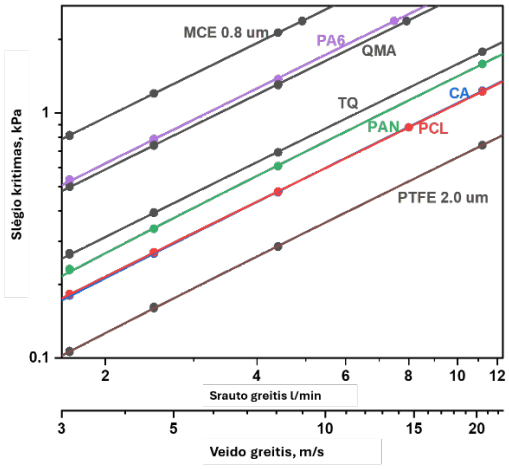

5.8 pav. Slėgio kritimo priklausomybė nuo filtro mėginio srauto: PTFE 2,0 m (SKC); QM-A – kvarciniai filtrai (Whatman Inc.); TQ – audinių kvarciniai filtrai (Pall Corp.) ir MCE 0,8

mm – mišrios celiuliozės esterio membranos, porų dydis – 0,8 mm (SKC Inc.), pateikiami kaip etaloniniai filtrai

Nors pagrindinis aerozolio dalelių mėginių filtrų tikslas – užtikrinti didelį surinkimo efektyvumą, slėgio kritimas, natūraliai atsirandantis per filtrą, taip pat kelia susirūpinimą, nes dėl jo padidėja mėginių ėmimo įrangos gedimų tikimybė ir reikia didesnių investicijų bei energijos sąnaudų. 5.8 pav. parodytas šio tyrimo metu sukurtų filtrų tyrimas. Nors PA6 membranos porų skersmuo yra apie 0,2 mm, ji gali veikti labai efektyviai ir palyginti siaurame slėgio kritimo diapazone, todėl ji yra vertinga platforma tais atvejais, kai reikia didelio našumo mėginių ėmimo.

5.6. Polikarbonato kompozitinis nanofiltras aerozolio dalelėms filtruoti

5.6.1. Morfologija

Visuose PC tirpaluose buvo gauti pluoštai, kurių vidutinis skersmuo buvo toks: 0,32 µm, 0,19 µm, 0,56 µm, 0,54 µm, 0,50 µm, 0,33 µm ir 0,37 µm. PC tirpumas labai padidėjo į tirpalą pridėjus CTAB. CTAB, katijoninė paviršinio aktyvumo medžiaga, didina jo laidumą, todėl pavyko pagaminti itin plonus PC pluoštus be jokių rutuliukų. Siekiant užtikrinti optimalų cheminį suderinamumą ir sukibimą, kiekviena iš 7 polikarbonato (PC) koncentracijų buvo elektriniu būdu verpiama ant pagrindo sluoksnio, kurį sudarė 3D spausdintuvu atspausdintas polikarbonato substratas. 5.9 pav. pavaizduoti aerozolio dalelių ėminiams imti naudojamo filtro polikarbonato nanopluošto sluoksnių SEM vaizdai.

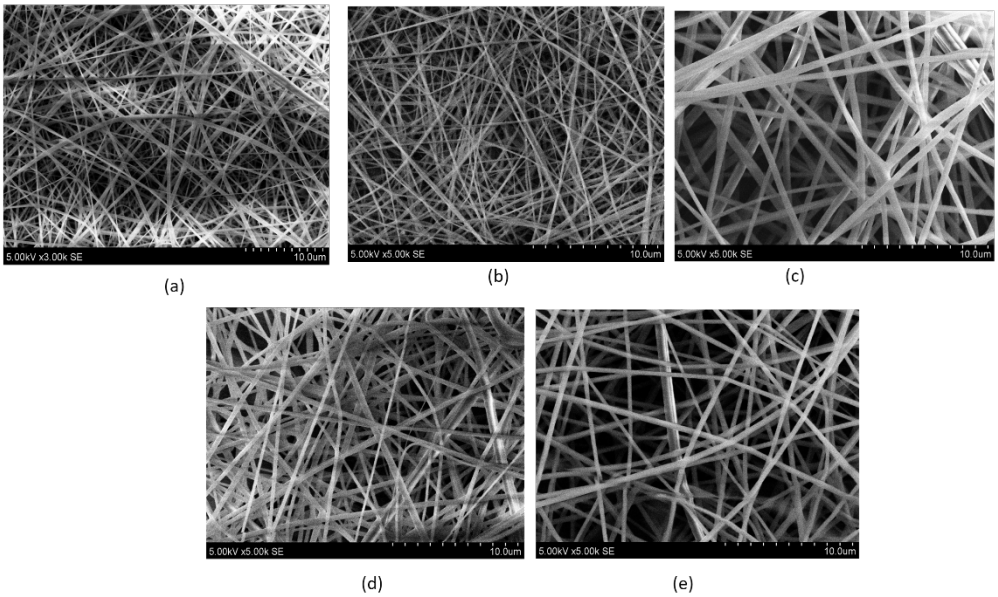

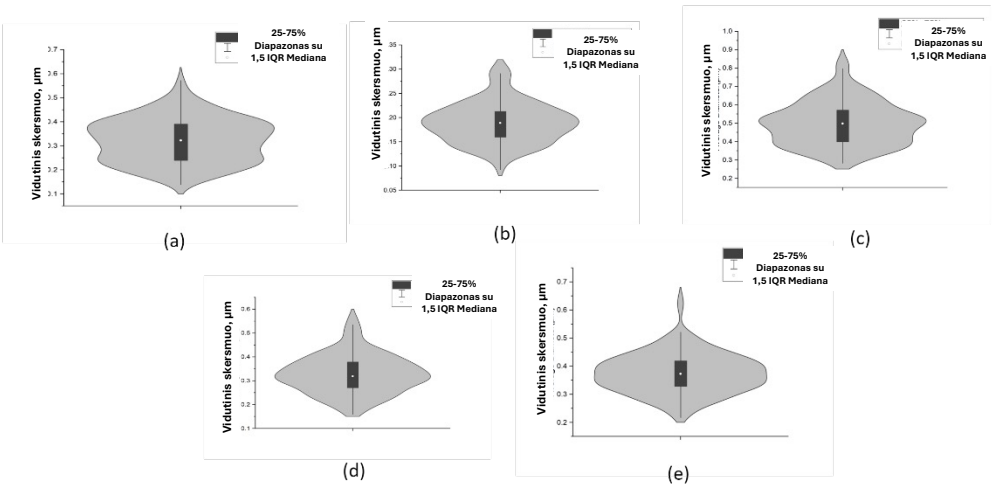

5.9 pav. SEM vaizduose matyti aerozolių ėminiams imti naudojamo filtro polikarbonato nanopluoštų sluoksniai: a – PC14 %, CTAB 0,2 %; b – PC14 %, CTAB 0,8 %; c – PC17 %, CTAB 0,5 %; d – PC17%, CTAB 0,5 %; e – PC17 %, CTAB 0,5 %; f – PC20 %, CTAB 0,2 %; g – PC20 %, CTAB 0,8 %. Nanopluošto dydžio pasiskirstymas parodytas toliau

5.6.2. Proceso parametrų modeliavimas

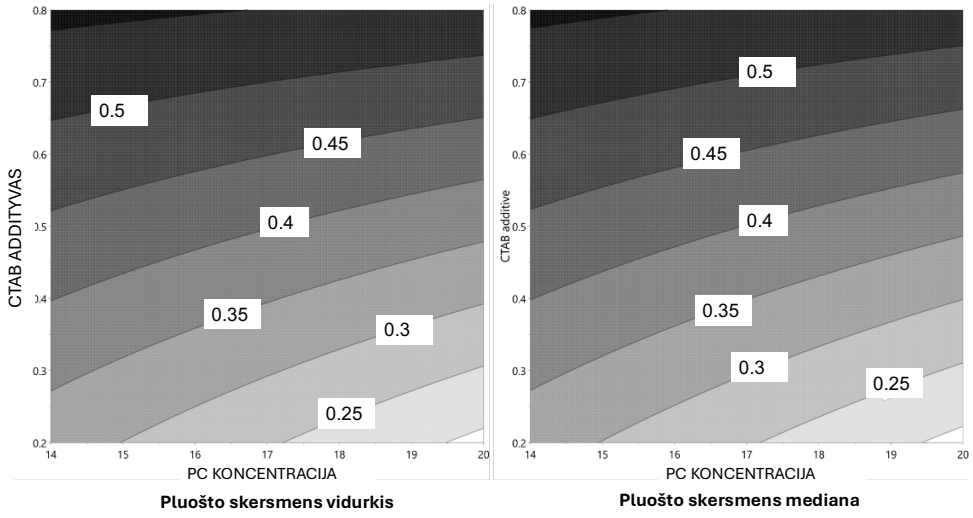

5.10 pav. PC koncentracijos su CTAB priedu ir pluošto skersmens vidurkio ir medianos paviršiaus diagramos

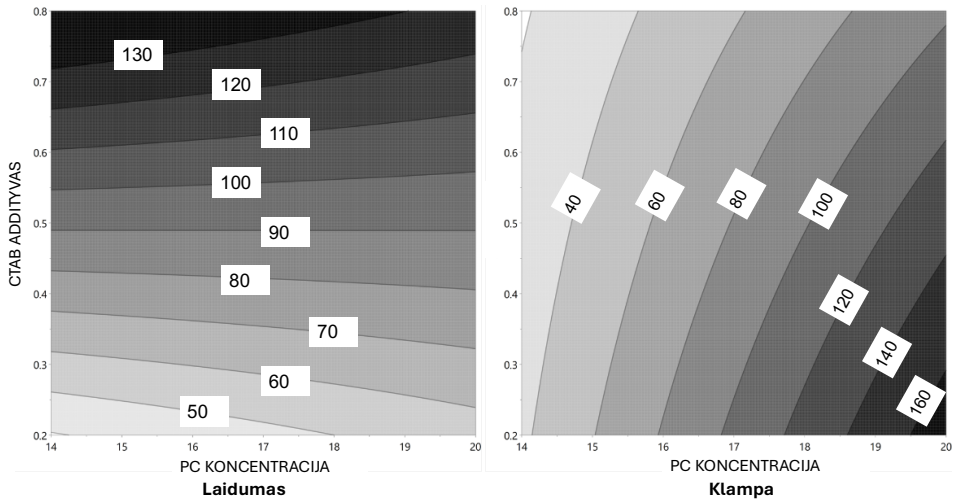

5.11 pav. PC koncentracijos su CTAB priedu priklausomybės nuo laidumo ir klampos paviršiaus grafikai

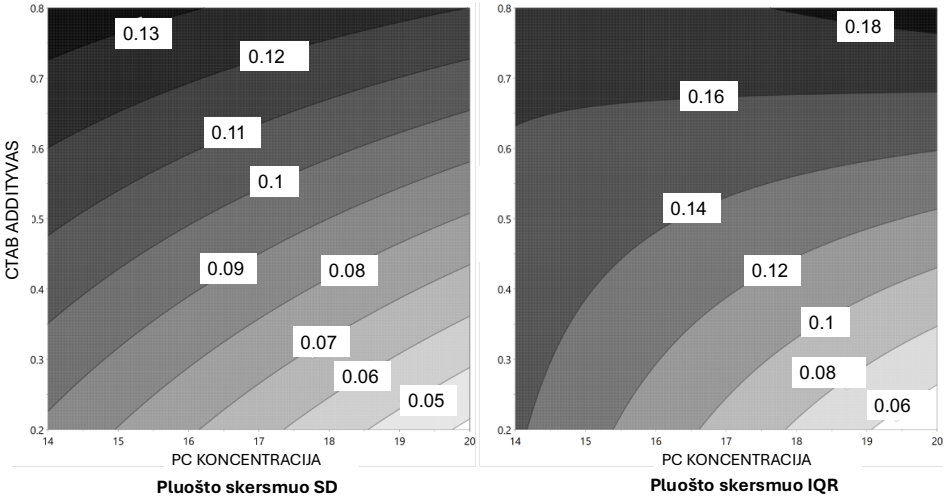

5.12 pav. PC koncentracijos su CTAB priedu poveikis pluošto skersmens vidurkiui, SD ir IQR, pavaizduoti atsako paviršiaus diagramomis

Šiais grafikais siekta nustatyti ryšį tarp veiksnių, tokių kaip CTAB ir PC polimero koncentracija, ir atitinkamų nanopluoštų reakcijų, įskaitant pluošto skersmens vidurkį, standartinį nuokrypį (SD) ir tarpkvartilinį intervalą (IQR). Eksperimentų planavimo metodika yra vertinga atrankos, optimizavimo ir

patikimumo tikrinimo tikslais. 5.12 pav. pavaizduoti atitinkamų parametrų atsako paviršiaus grafikai.

5.6.3. Filtravimo efektyvumas

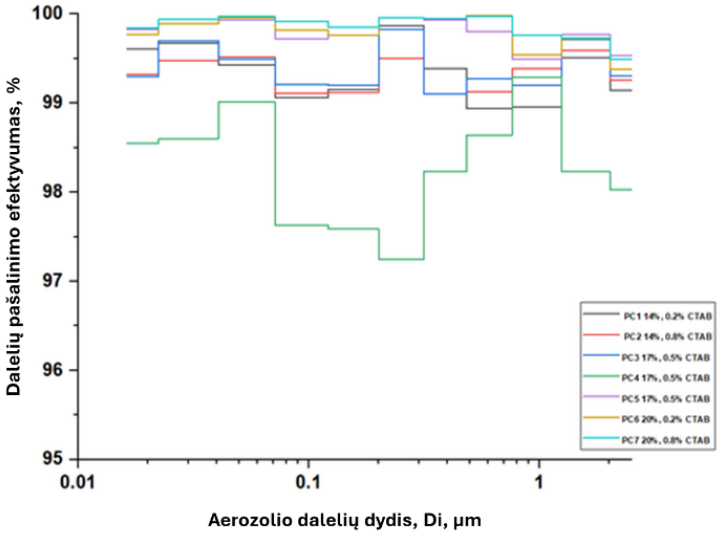

5.13 pav. NaCl aerozolio dalelių surinkimo efektyvumas iš 7 nanopluoštinių polikarbonato oro filtravimo substratų

Autoriai panaudojo optimizuotus rezultatus, kad sukurtų nanopluošto filtravimo laikmenas ant 3D spausdintų substratų pavyzdžių. Tada šie mėginiai buvo tiriami naudojant eksperimentinę filtravimo sistemą, aprašytą 2.3.2 skirsnyje ir pateiktą 5.13 pav. Išmatuotas septynių PC nanopluošto filtravimo terpės mėginių filtravimo efektyvumas ir slėgio kritimas. Filtravimo efektyvumas naudojant NaCl daleles labiausiai prasiskverbiančių dalelių dydžio diapazone buvo įvertintas naudojant elektrinį žemo slėgio imtuvą (ELPI+, Dekati Ltd., Suomija). Sukurti PC substratai pasiekė vidutinį sulaikymo efektyvumą, kuris priartėjo prie norimo 99,9 % kietųjų NaCl aerozolio dalelių. Didesnis filtravimo efektyvumas gali būti siejamas su didesniu pluoštų susikaupimu, nes tirpale yra didesnė polimero koncentracija. PC1–PC6 rodo puikų bendrą filtravimo efektyvumą, viršijantį 99 %. Tačiau PC 7 gali turėti nedidelį trūkumą dėl tam tikrų dydžių dalelių efektyvumo.

5.6.4. Slėgio kritimas

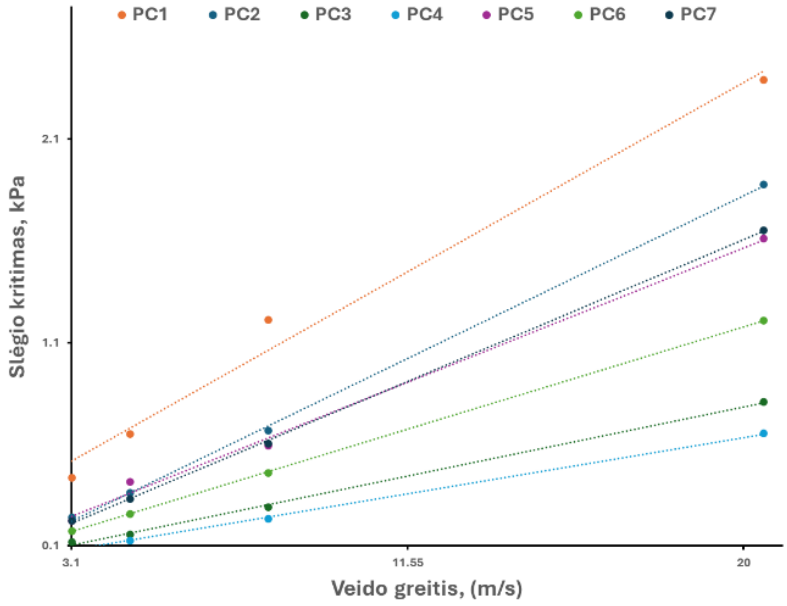

5.14 pav. Slėgio kritimas filtre kaip per filtrą tekančio srauto greičio funkcija

Esant 5,3 cm/s per filtrą tekančio srauto greičiui, slėgio kritimas per septynias nanodangas svyravo nuo 201,5 iki 721,5 Pa. Šis greitis laikomas standartiniu tiriant didelio efektyvumo filtrus. 5.14 pav. parodytas slėgio kritimas esant skirtingiems filtro paviršiaus greičiams Matuojant nanopluošto filtrų slėgio kritimą, buvo nustatytos palyginti didelės vertės. Tačiau tai pasiekiama dėl didesnio slėgio kritimo per filtravimo membranos sluoksnio storį. Gaminant PC kompozitinį filtrą atstumas tarp nanopluoštų išliko pastovus, todėl padidėjo filtravimo efektyvumas esant mažesniam slėgio kritimui. Tyrimai rodo, kad pluoštai turi tolygiai paskirstytą modelį, o poros yra mažesnės. Be to, dėl pluoštų artumo, atsirandančio sutrumpėjus porų atstumams, padidėjo slėgio kritimas. Todėl PC kompozitinis filtras parodė didesnį oro filtravimo efektyvumą, nepaisant didesnio slėgio kritimo.

5.7. „Ląstelių ant dalelių“ koncepcijos bandymas

5.7.1. Nanopluoštinių mėginių ėmimo platformos biologinio suderinamumo vertinimas

Žmogaus bronchų epitelio ląstelės iš BEAS-2B linijos galėjo prilipti ir vystytis ant įvairių nanopluoštinių bandymų ir mėginių ėmimo paviršių. Po 15 val. auginimo buvo pastebėtas žymus ląstelių proliferacijos ir (arba) gyvybingumo padidėjimas (5.15 pav., A.). Ant PA6 platformos išskleistos ląstelės pasižymėjo mažiausiu proliferacijos signalo padidėjimu.

Per 72 valandas auginant Beas-2B ląsteles ant įvairių membranų išsiskyrusio LDH kiekio skirtumo nepastebėta, palyginti su tuo pačiu ląstelių skaičiumi, auginamu

ant 24 duobučių plokštelės plastikinio paviršiaus (2D kontrolė) (5.15 pav., B.). Bendras LDH išsiskyrimo kiekis, rodantis ląstelių, išsivysčiusių ant substrato, skaičių, buvo nustatytas po 5 dienų ląstelių auginimo ant nanopluoštinių mėginių ėmimo ir testavimo platformų bei ant 2D plastikinių paviršių (5.15 pav., C.). Lyginant su tuo pačiu skaičiumi BEAS-2B ląstelių, auginamų ant tipinio plastikinio 2D paviršiaus, LDH išsiskyrimas iš ląstelių, augančių ant visų platformų, buvo daugiau nei du kartus didesnis. Ant PA6 membranos išaugintų ląstelių LDH išsiskyrimas buvo mažiausias, ir šie duomenys atitinka mažiausius tų pačių mėginių gyvybingumo ir (arba) proliferacijos signalus.

Remiantis citotoksiškumo (LDH išsiskyrimo ir BEAS-2B gyvybingumo) tyrimų su BEAS-2B ląstelėmis rezultatais, buvo nustatyta, kad CA ir PCL nanopluošto mėginių ėmimo ir bandymų platformos yra perspektyviausios. Tada šios platformos buvo išbandytos su suprojektuotomis sidabro, vario ir grafeno oksido nanodalelėmis.

A

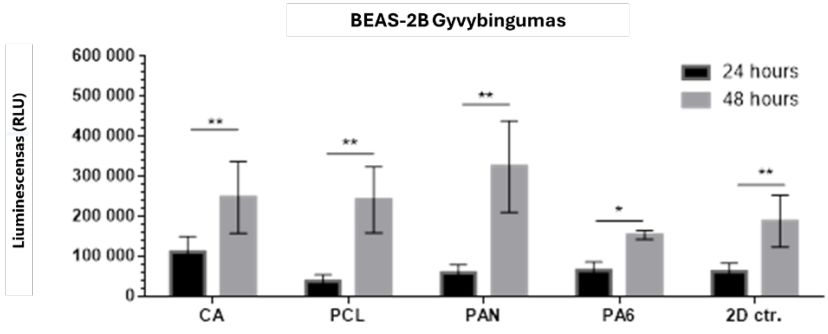

B

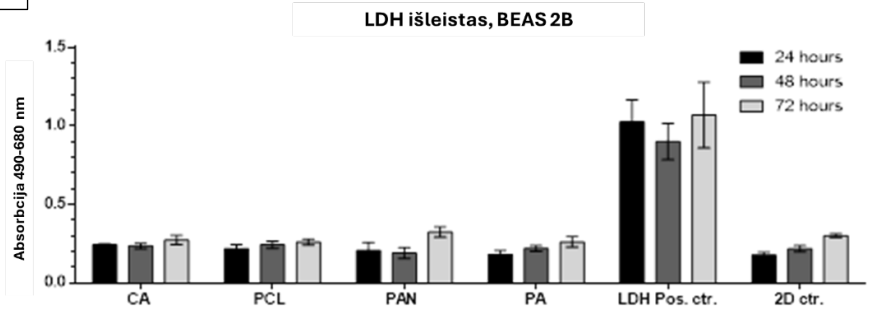

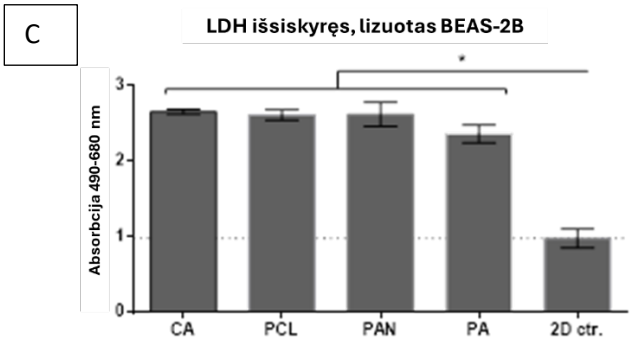

5.15 pav. A – BEAS-2B gyvybingumas ant skirtingų tipų platformų iki 48 valandų. *p < 0,05, **p < 0,01. 2D ctr. – BEAS-2B, auginamos ant standartinės (2D) 24 duobučių kultūros plokštelės dugno; B – BEAS-2B ląstelių citotoksiškumas, matuojamas kaip laktato dehidrogenazės (LDH) išsiskyrimas iš negyvų ląstelių auginant 72 val. ant skirtingo tipo platformų; C – LDH išsiskyrimas iš lizuotų BEAS-2B ląstelių, augintų ant skirtingų tipų platformų ir ant standartinio (2D) 24 duobučių auginimo plokštelės dugno. *p < 0,05, palyginti su 2D kontrole

5.7.2. Dalelių nusėdimo ant nanopluošto platformos apibūdinimas

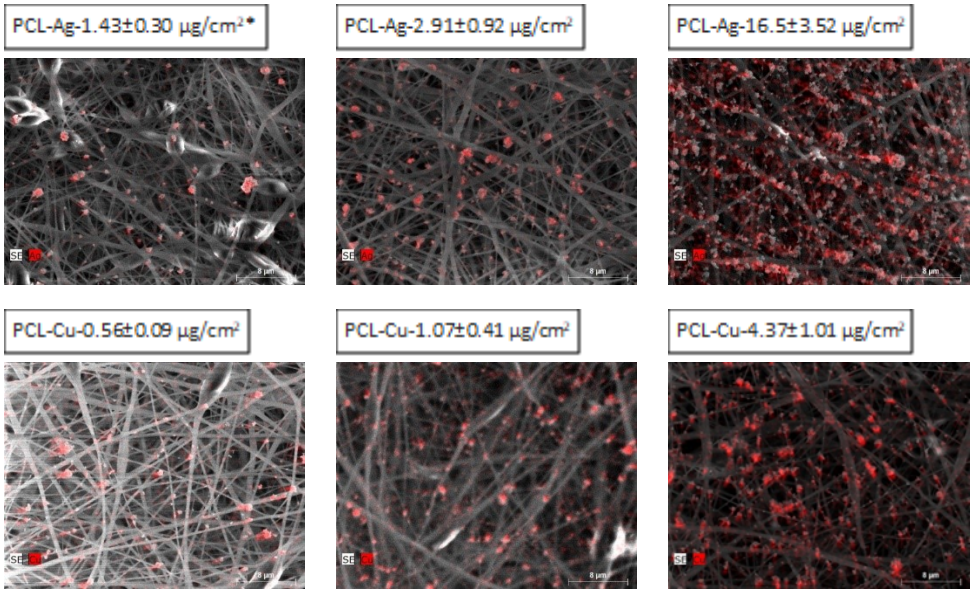

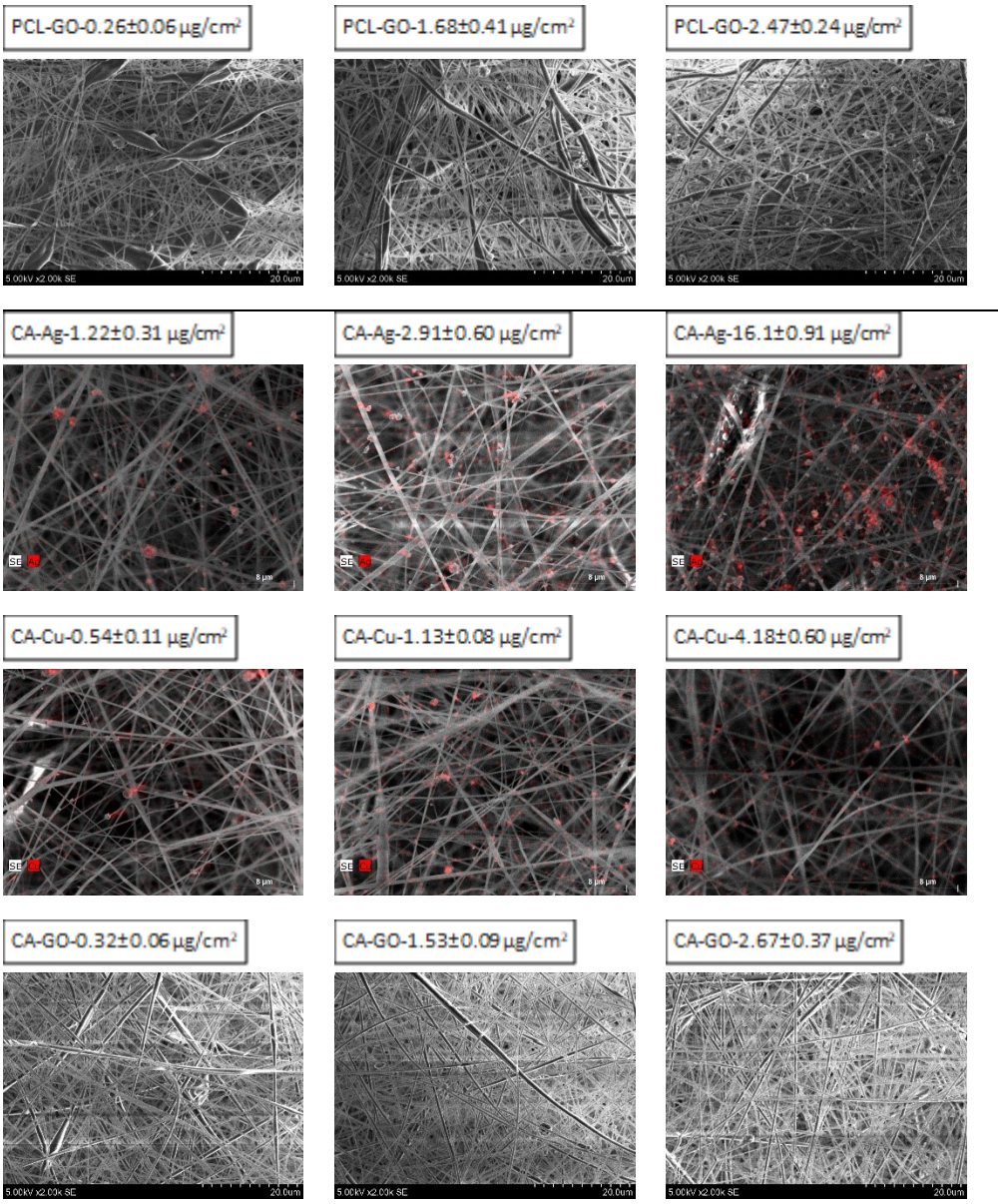

5.16 pav. Nanodalelių, nusodintų ant nanopluoštinės platformos, SEM vaizdai. PCL nanopluoštinė platforma: CA – celiuliozės acetato nanopluoštinė platforma, Ag – sidabro nanodalelės, Cu – vario nanodalelės ir GO – grafeno oksido nanodalelės. SEM (EDS analizė) vaizduose sidabro ir vario dalelės, nuspalvintos raudona spalva

Šiame tyrime buvo naudojamos sidabro, vario ir grafeno oksido nanodalelės. Trys skirtingi šių nanodalelių kiekiai buvo dedami ant nanopluoštinių mėginių ėmimo skruzdžių bandymo platformų paviršių. Remiantis pradinių ląstelių toksiškumo tyrimų išvadomis, buvo pasirinktos nanodalelių dozės. AgNP paviršiaus koncentracija svyravo nuo 4,99 iki 29,5 $\mu g/cm^2$. Vario nanodalelių paviršiaus lygis platformose svyravo nuo 0,54 iki 4,37 $\mu g/cm^2$. Grafeno oksido nanodalelių tankis paviršiuje svyravo nuo 0,26 iki 2,67 $\mu g/cm^2$.

5.16 pav. pateiktos paviršiuje įstrigusių nanodalelių SEM nuotraukos. Ant nanopluošto paviršiaus dalelės buvo vienodai išsklaidytos ir prilipusios prie nanosiūlų. Vidutinis sidabro ir vario dalelių dydis yra atitinkamai 84–1530 nm ir 110–3550 nm, o grafeno oksido vidutinis dydis – 3550 nm. Nanodalelių, pasklidusių distiliuotame vandenyje, dydžiai buvo šiek tiek didesni, nei teigė dalelių gamintojas. Ant mėginių ėmimo platformos nusėdusios ir aerozolinės dalelės buvo daug didesnės.

IŠVADOS

1. Disertacijoje aprašytas sėkmingas trisluoksnių kompozitinių aerozolio mėginių ėmimo filtrų, kurių darbinis paviršius sudarytas iš polimerinių nanopluoštų, sukūrimas. Taikydami elektrinio verpimo ir medžiagų inžinerijos metodus, sėkmingai sukūrėme substratus, turinčius gradientinį pluošto ir porų skersmenį, pasižyminčius geru filtravimo efektyvumu ir mechaninėmis savybėmis. Iš įvairių polimerų, įskaitant PCL, CA, PAN ir PA6, pagaminti substratai pasižymėjo konkurencingu slėgio kritimu (nuo 476 iki 2304 Pa esant 10 cm/s) ir puikiu sulaikymo efektyvumu (99,4 % su NaCl aerozoliu ties labiausiai prasiskverbiančiu dalelių dydžiu). Tiksliai kontroliuojant gamybos parametrus ir polimerų parinkimą, šie substratai yra individualiai pritaikomas sprendimas, atitinkantis unikalius aerozolio mėginių ėmimo reikalavimus visose mokslo ir pramonės srityse.

2. Disertacijoje pristatytas dvisluoksnių kompozitinių aerozolio mėginių ėmimo filtrų kūrimas, kuriuose nanopluoštinis sluoksnis formuojamas ant 3D atspausdintų polikarbonato (PC) substratų. Nanopluoštinio sluoksnio morfologija buvo optimizuota naudojant heksadeciltrimetilamoniobromido (CTAB) priedą PC tirpale. Tai leido sėkmingai pagaminti nanopluoštines matricas, kurios pasiekė aukštą kietųjų NaCl aerozolio dalelių sulaikymo lygį (iki 99,9 %). Nepaisant padidėjusio slėgio kritimo, filtrai išlaikė geresnį oro srautą, o tai rodo, kad jie gali būti naudojami didelio efektyvumo filtravimui.

3. Disertacijoje aprašytas nanopluoštinių aerozolio ėminių ėmimo filtrų taikymas surinktų dalelių citotoksiškumo tyrimams. Filtruose, pagamintuose iš biologiškai suderinamų polimerų celiuliozės acetato (CA), polikaprolaktono (PCL), poliamido 6 (PA6) ir poliakrilonitrilo (PAN), buvo geras ląstelių gyvybingumas ir mažiau išsiskyrė laktato dehidrogenazės (LDH). LDH išsiskyrimas iš ląstelių, kultivuotų ant PA6 platformos, buvo mažiausias iš visų tirtų paviršių. Tyrimas parodė aiškų dozės ir atsako ryšį tarp Cu, Ag ir grafeno oksido nanodalelių koncentracijos ir ląstelių gyvybingumo. Pavyzdžiui, esant 0,6 $\mu g/cm^2$ koncentracijai, vario nanodalelės sumažino ląstelių gyvybingumą iki mažiau nei 15 %, o esant 3,2 $\mu g/cm^2$ koncentracijai – iki mažiau nei 5 %. Taikant šį metodą supaprastinamos bandymų procedūros, gaunami reprezentatyvesni rezultatai ir paspartinamas bandymų atlikimo laikas.

REFERENCES

1. REQUIA, Weeberb J, ADAMS, Matthew D and KOUTRAKIS, Petros. Association of PM2.5 with diabetes, asthma, and high blood pressure incidence in Canada: A spatiotemporal analysis of the impacts of the energy generation and fuel sales. *Science of The Total Environment*. Online. April 2017. Vol. 584–585, p. 1077–1083. DOI 10.1016/j.scitotenv.2017.01.166.
2. GOSHUA, Anna, AKDIS, Cezmi A, NADEAU, Kari, AKDIS, Cezmi, NADEAU, Kari C, AUTHOR, Corresponding and PARKER, Sean N. World Health Organization global air quality guideline recommendations: Executive summary. *Wiley Online Library*. Online. 1 July 2022. Vol. 77, no. 7, p. 1955–1960. DOI 10.1111/all.15224.
3. KULKARNI, Pramod, BARON, Paul A., SORENSEN, Christopher M. and HARPER, Martin. Nonspherical Particle Measurement: Shape Factor, Fractals, and Fibers. *Aerosol Measurement: Principles, Techniques, and Applications: Third Edition*. 7 July 2011. P. 507–547. DOI 10.1002/9781118001684.CH23.
4. KAMPA, Marilena and CASTANAS, Elias. Human health effects of air pollution. *Environmental Pollution*. 1 January 2008. Vol. 151, no. 2, p. 362–367. DOI 10.1016/J.ENVPOL.2007.06.012.
5. 5. LEE, Byeong Jae, KIM, Bumseok and LEE, Kyuhong. Air pollution exposure and cardiovascular disease. *Toxicological Research*. Online. 30 December 2014. Vol. 30, no. 2, p. 71–75. DOI 10.5487/TR.2014.30.2.071/METRICS.
6. KRUGLY, Edvinas, RAVIKUMAR, Preethi, DABAŠINSKAITĖ, Lauryna, TICHONOVAS, Martynas, CIUZAS, Darius, PRASAUSKAS, Tadas, BANIUKAITIENĖ, Odeta, MASIONĖ, Goda, KAUNELIENĖ, Violeta and MARTUZEVIČIUS, Dainius. Nanofibrous aerosol sample filter substrates: Design, fabrication, and characterization. *Journal of Aerosol Science*. 1 March 2023. Vol. 169, p. 106118. DOI 10.1016/J.JAEROSCI.2022.106118.
7. HAYES, Richard B., LIM, Chris, ZHANG, Yilong, CROMAR, Kevin, SHAO, Yongzhao, REYNOLDS, Harmony R., SILVERMAN, Debra T., JONES, Rena R., PARK, Yikyung, JERRETT, Michael, AHN, Jiyoung and THURSTON, George D. PM2.5 air pollution and cause-specific cardiovascular disease mortality. *International Journal of Epidemiology*. Online. 1 February 2020. Vol. 49, no. 1, p. 25–35. DOI 10.1093/IJE/DYZ114.
8. SCAMPICCHIO, Matteo, BULBARELLO, Andrea, ARECCHI, Alessandra, COSIO, M. Stella, BENEDETTI, Simona and MANNINO, Saverio. Electrospun Nonwoven Nanofibrous Membranes for Sensors and Biosensors. *Electroanalysis*. Online. 1 April 2012. Vol. 24, no. 4, p. 719–725. DOI 10.1002/ELAN.201200005.
9. SELL, Scott A., MCCLURE, Michael J., GARG, Koyal, WOLFE, Patricia S. and BOWLIN, Gary L. Electrospinning of collagen/biopolymers for regenerative medicine and cardiovascular tissue engineering. *Advanced Drug Delivery Reviews*. 5 October 2009. Vol. 61, no. 12, p. 1007–1019. DOI 10.1016/J.ADDR.2009.07.012.
10. LI, Yuyao, YIN, Xia, YU, Jianyong and DING, Bin. Electrospun nanofibers for high-performance air filtration. *Composites Communications*. 1 October 2019. Vol. 15, p. 6–19. DOI 10.1016/J.COCO.2019.06.003.
11. SOO, Jhy-Charm, MONAGHAN, Keenan, LEE, Taekhee, KASHON, Mike and HARPER, Martin. Air sampling filtration media: Collection efficiency for respirable size-selective sampling. *Aerosol Science and Technology*. Online. 2 January 2016. Vol. 50, no. 1, p. 76–87. DOI 10.1080/02786826.2015.1128525.
12. MATULEVICIUS, Jonas, KLIUCININKAS, Linas, MARTUZEVICIUS, Dainius,

KRUGLY, Edvinas, TICHONOVAS, Martynas and BALTRUSAITIS, Jonas. Design and characterization of electrospun polyamide nanofiber media for air filtration applications. *Journal of Nanomaterials*. 2014. Vol. 2014. DOI 10.1155/2014/859656.

13. HE, Haijun, GAO, Min, ILLÉS, Balázs and MOLNAR, Kolos. 3D Printed and Electrospun, Transparent, Hierarchical Polylactic Acid Mask Nanoporous Filter. *International Journal of Bioprinting*. Online. 2020. Vol. 6, no. 4. DOI 10.18063/IJB.V6I4.278.

14. CAO, Mingyi, GU, Fu, RAO, Chengchen, FU, Jianzhong and ZHAO, Peng. Improving the electrospinning process of fabricating nanofibrous membranes to filter PM2.5. *Science of the Total Environment*. 20 May 2019. Vol. 666, p. 1011–1021. DOI 10.1016/J.SCITOTENV.2019.02.207.

15. GOSWAMI, Manoj, YADAV, Ashvini Kumar, CHAUHAN, Viplov, SINGH, Netrapal, KUMAR, Satendra, DAS, Abhradeep, YADAV, Vishal, MANDAL, Ajay, TIWARI, Jitendar Kumar, SIDDIQUI, Hafsa, ASHIQ, Mohammad, SATHISH, N., KUMAR, Surender, BISWAS, Debasis and SRIVASTAVA, A. K. Facile development of graphene-based air filters mounted on a 3D printed mask for COVID-19. *Journal of Science: Advanced Materials and Devices*. 1 September 2021. Vol. 6, no. 3, p. 407–414. DOI 10.1016/J.JSAMD.2021.05.003.

16. XU, Xi, XIAO, Shuning, WILLY, Habimana Jean, XIONG, Ting, BORAYEK, Ramadan, CHEN, Wei, ZHANG, Dieqing and DING, Jun. 3D-Printed Grids with Polymeric Photocatalytic System as Flexible Air Filter. *Applied Catalysis B: Environmental*. 1 March 2020. Vol. 262, p. 118307. DOI 10.1016/J.APCATB.2019.118307.

17. SZEWCZYK, Piotr K, URA, Daniel P, METWALLY, Sara, KNAPCZYK-KORCZAK, Joanna, GAJEK, Marcin, MARZEC, Mateusz M, BERNASIK, Andrzej and STACHEWICZ, Urszula. Roughness and fiber fraction dominated wetting of electrospun fiber-based porous meshes. *Polymers*. Online. 2018. DOI 10.3390/polym11010034.

18. BAKAR, S S S, FONG, K C, ELEYAS, A and NAZERI, M F M. Effect of Voltage and Flow Rate Electrospinning Parameters on Polyacrylonitrile Electrospun Fibers. *IOP Conference Series: Materials Science and Engineering*. Online. 1 March 2018. Vol. 318, no. 1, p. 012076. DOI 10.1088/1757-899X/318/1/012076.

19. AL-ATTABI, Riyadh, DUMÉE, Ludovic F., KONG, Lingxue, SCHÜTZ, Jürg A. and MORSI, Yosry. High Efficiency Poly(acrylonitrile) Electrospun Nanofiber Membranes for Airborne Nanomaterials Filtration. *Advanced Engineering Materials*. 1 January 2018. Vol. 20, no. 1. DOI 10.1002/ADEM.201700572.

20. KAO, Tzu-Hao, SU, Shuenn-Kung, SU, Ching-Iuan, LEE, Ai-Wei and CHEN, Jem-Kun. Polyacrylonitrile microscaffolds assembled from mesh structures of aligned electrospun nanofibers as high-efficiency particulate air filters. *Aerosol Science and Technology*. Online. 2 June 2016. Vol. 50, no. 6, p. 615–625. DOI 10.1080/02786826.2016.1171822.

21. MA, Yanan, ZHOU, Tao, SU, Gehong, LI, Yan and ZHANG, Aiming. Understanding the crystallization behavior of polyamide 6/polyamide 66 alloys from the perspective of hydrogen bonds: projection moving-window 2D correlation FTIR spectroscopy and the enthalpy. *RSC Advances*. Online. 13 September 2016. Vol. 6, no. 90, p. 87405–87415. DOI 10.1039/C6RA09611E.

22. HUGGINS, Maurice L. Principles of Polymer Chemistry. *Journal of the American Chemical Society*. May 1954. Vol. 76, no. 10, p. 2854–2854.

DOI 10.1021/JA01639A090.
23. BAUR, Erwin, OSSWALD, Tim A. and RUDOLPH, Natalie. Plastics Handbook. In : *Plastics Handbook*. Online. München : Carl Hanser Verlag GmbH & Co. KG, 2019. p. I–XXI.
24. HANFORD, W. E. and JOYCE, R. M. Polymeric amides from epsilon-caprolactam. *Journal of Polymer Science*. Online. 1 April 1948. Vol. 3, no. 2, p. 167–172. DOI 10.1002/POL.1948.120030203.
25. CSIHONY, Szilárd, BEAUDETTE, Tristan T., SENTMAN, Alan C., NYCE, Gregory W., WAYMOUTH, Robert M. and HEDRICK, James L. Bredereck's reagent revisited: Latent anionic ring-opening polymerization and transesterification reactions. *Advanced Synthesis and Catalysis*. Online. August 2004. Vol. 346, no. 9–10, p. 1081–1086. DOI 10.1002/ADSC.200404097.
26. DUBOIS, Philippe, COULEMBIER, Olivier and RAQUEZ, Jean Marie. Handbook of Ring-Opening Polymerization. *Handbook of Ring-Opening Polymerization*. Online. 6 August 2009. P. 1–408. DOI 10.1002/9783527628407.
27. BUIVYDIENE, Dalia, KRUGLY, Edvinas, CIUZAS, Darius, TICHONOVAS, Martynas, KLIUCININKAS, Linas, MARTUZEVICIUS, Dainius, D., Buivydiene, E., Krugly, D., Ciuzas, M., Tichonovas, L., Kliucininkas and D., Martuzevicius. Formation and characterisation of air filter material printed by melt electrospinning. *Journal of Aerosol Science*. 1 May 2019. Vol. 131, p. 48–63. DOI 10.1016/J.JAEROSCI.2019.03.003.
28. FISCHER, Steffen, THÜMMLER, Katrin, VOLKERT, Bert, HETTRICH, Kay, SCHMIDT, Ingeborg and FISCHER, Klaus. Properties and Applications of Cellulose Acetate. *Macromolecular Symposia*. Online. 18 January 2008. Vol. 262, no. 1, p. 89–96. DOI 10.1002/masy.200850210.
29. HUANG, Zheng Ming, ZHANG, Y. Z., KOTAKI, M. and RAMAKRISHNA, S. A review on polymer nanofibers by electrospinning and their applications in nanocomposites. *Composites Science and Technology*. 1 November 2003. Vol. 63, no. 15, p. 2223–2253. DOI 10.1016/S0266-3538(03)00178-7.
30. SHIBATA, Tohru. 5.6 Cellulose acetate in separation technology. *Macromolecular Symposia*. Online. 1 March 2004. Vol. 208, no. 1, p. 353–370. DOI 10.1002/MASY.200450415.
31. EDGAR, Kevin J., BUCHANAN, Charles M., DEBENHAM, John S., RUNDQUIST, Paul A., SEILER, Brian D., SHELTON, Michael C. and TINDALL, Debra. Advances in cellulose ester performance and application. *Progress in Polymer Science*. 1 November 2001. Vol. 26, no. 9, p. 1605–1688. DOI 10.1016/S0079-6700(01)00027-2.
32. LIU, Haiqing and HSIEH, You-Lo. Ultrafine fibrous cellulose membranes from electrospinning of cellulose acetate. *Journal of Polymer Science Part B: Polymer Physics*. Online. 15 September 2002. Vol. 40, no. 18, p. 2119–2129. DOI 10.1002/polb.10261.
33. TUNGPRAPA, Santi, PUANGPARN, Tanarinthorn, WEERASOMBUT, Monchawan, JANGCHUD, Ittipol, FAKUM, Porntiva, SEMONGKHOL, Somsak, MEECHAISUE, Chidchanok and SUPAPHOL, Pitt. Electrospun cellulose acetate fibers: Effect of solvent system on morphology and fiber diameter. *Cellulose*. Online. 14 December 2007. Vol. 14, no. 6, p. 563–575. DOI 10.1007/S10570-007-9113-4/TABLES/4.
34. CELEBIOGLU, Asli and UYAR, Tamer. Electrospun porous cellulose acetate fibers from volatile solvent mixture. *Materials Letters*. 31 July 2011. Vol. 65, no. 14, p. 2291–2294. DOI 10.1016/J.MATLET.2011.04.039.
35. WOODRUFF, Maria Ann and HUTMACHER, Dietmar Werner. The return of a

forgotten polymer—Polycaprolactone in the 21st century. *Progress in Polymer Science*. 1 October 2010. Vol. 35, no. 10, p. 1217–1256. DOI 10.1016/J.PROGPOLYMSCI.2010.04.002.

36. SALERNO, Aurelio, ZEPPETELLI, Stefania, MAIO, Ernesto Di, IANNACE, Salvatore and NETTI, Paolo A. Novel 3D porous multi-phase composite scaffolds based on PCL, thermoplastic zein and ha prepared via supercritical CO2 foaming for bone regeneration. *Composites Science and Technology*. 15 November 2010. Vol. 70, no. 13, p. 1838–1846. DOI 10.1016/J.COMPSCITECH.2010.06.014.

37. ZHANG, Y. Z., VENUGOPAL, J., HUANG, Z. M., LIM, C. T. and RAMAKRISHNA, S. Characterization of the surface biocompatibility of the electrospun PCL-Collagen nanofibers using fibroblasts. *Biomacromolecules*. September 2005. Vol. 6, no. 5, p. 2583–2589. DOI 10.1021/BM050314K.

38. FERESHTEH, Zeinab, NOOEAID, Patcharakamon, FATHI, Mohammadhossein, BAGRI, Akbar and BOCCACCINI, Aldo R. Mechanical properties and drug release behavior of PCL/zein coated 45S5 bioactive glass scaffolds for bone tissue engineering application. *Data in Brief*. 1 September 2015. Vol. 4, p. 524–528. DOI 10.1016/J.DIB.2015.07.013.

39. SCHUURMAN, W., KHRISTOV, V., POT, M. W., VAN WEEREN, P. R., DHERT, W. J.A. and MALDA, J. Bioprinting of hybrid tissue constructs with tailorable mechanical properties. *Biofabrication*. Online. 20 May 2011. Vol. 3, no. 2, p. 021001. DOI 10.1088/1758-5082/3/2/021001.

40. REPANAS, Alexandros and GLASMACHER, Birgit. Dipyridamole embedded in Polycaprolactone fibers prepared by coaxial electrospinning as a novel drug delivery system. *Journal of Drug Delivery Science and Technology*. 1 October 2015. Vol. 29, p. 132–142. DOI 10.1016/J.JDDST.2015.07.001.

41. SURUCU, Seda and TURKOGLU SASMAZEL, Hilal. Development of core-shell coaxially electrospun composite PCL/chitosan scaffolds. *International Journal of Biological Macromolecules*. 1 November 2016. Vol. 92, p. 321–328. DOI 10.1016/J.IJBIOMAC.2016.07.013.

42. PERSENAIRE, O., ALEXANDRE, M., DEGÉE, P. and DUBOIS, P. Mechanisms and kinetics of thermal degradation of poly(ε-caprolactone). *Biomacromolecules*. 1 January 2001. Vol. 2, no. 1, p. 288–294. DOI 10.1021/bm0056310.

43. KHATIWALA, Vinay K., SHEKHAR, Nilanshu, AGGARWAL, Saroj and MANDAL, U. K. Biodegradation of Poly(ε-caprolactone) (PCL) Film by Alcaligenes faecalis. *Journal of Polymers and the Environment*. Online. 23 January 2008. Vol. 16, no. 1, p. 61–67. DOI 10.1007/S10924-008-0104-9/TABLES/4.

44. JAMEELA, S. R., SUMA, N. and JAYAKRISHNAN, A. Protein release from poly(ε-caprolactone) microspheres prepared by melt encapsulation and solvent evaporation techniques: A comparative study. *Journal of Biomaterials Science, Polymer Edition*. Online. 1 January 1997. Vol. 8, no. 6, p. 457–466. DOI 10.1163/156856297X00380.

45. BABY, Thomas, JOSE E, Tomlal, GEORGE, Gejo, VARKEY, Vinitha and CHERIAN, Shijo K. A new approach for the shaping up of very fine and beadless UV light absorbing polycarbonate fibers by electrospinning. *Polymer Testing*. 1 December 2019. Vol. 80, p. 106103. DOI 10.1016/J.POLYMERTESTING.2019.106103.

46. YUAN, Shangqin, SHEN, Fei, CHUA, Chee Kai and ZHOU, Kun. Polymeric composites for powder-based additive manufacturing: Materials and applications. *Progress in Polymer Science*. 1 April 2019. Vol. 91, p. 141–168. DOI 10.1016/J.PROGPOLYMSCI.2018.11.001.

47. GREINER, Andreas and WENDORFF, Joachim H. Electrospinning: A Fascinating Method for the Preparation of Ultrathin Fibers. *Angewandte Chemie International Edition*. Online. 23 July 2007. Vol. 46, no. 30, p. 5670–5703. DOI 10.1002/ANIE.200604646.
48. LI, Qian, XU, Yiyang, WEI, Hanghang and WANG, Xiaofeng. An electrospun polycarbonate nanofibrous membrane for high efficiency particulate matter filtration †. Online. 2016. DOI 10.1039/c6ra12320a.
49. LIU, Qin, ZHU, Jinghui, ZHANG, Liwen and QIU, Yejun. Recent advances in energy materials by electrospinning. *Renewable and Sustainable Energy Reviews*. 1 January 2018. Vol. 81, p. 1825–1858. DOI 10.1016/J.RSER.2017.05.281.
50. ZHANG, Lu, LI, Lingfeng, WANG, Lincai, NIE, Jun and MA, Guiping. Multilayer electrospun nanofibrous membranes with antibacterial property for air filtration. *Applied Surface Science*. 15 June 2020. Vol. 515. DOI 10.1016/J.APSUSC.2020.145962.
51. KULKARNI, Aditya, BAMBOLE, V A and MAHANWAR, P A. Electrospinning of polymers, their modeling and applications. *Taylor & Francis*. Online. March 2010. Vol. 49, no. 5, p. 427–441. DOI 10.1080/03602550903414019.
52. NOTTER, Robert H. Lung surfactants: Basic science and clinical applications. *Lung Surfactants: Basic Science and Clinical Applications*. 1 January 2000. Vol. 149, p. 1–444. DOI 10.1201/9781482270426.
53. GHIO, Andrew J., CARRAWAY, Martha Sue and MADDEN, Michael C. Composition of Air Pollution Particles and Oxidative Stress in Cells, Tissues, and Living Systems. *Journal of Toxicology and Environmental Health, Part B*. Online. 1 January 2012. Vol. 15, no. 1, p. 1–21. DOI 10.1080/10937404.2012.632359.
54. FEENEY, Patrick, CAHILL, Thomas, OLIVERA, John and GUIDARA, Rick. Gravimetric Determination of Mass on Lightly Loaded Membrane Filters. *Journal of the Air Pollution Control Association*. Online. April 1984. Vol. 34, no. 4, p. 376–378. DOI 10.1080/00022470.1984.10465760.
55. DUNMORE, Joan H, HAMILTON, R J and SMITH, D S G. An instrument for the sampling of respirable dust for subsequent gravimetric assessment. *Journal of Scientific Instruments*. Online. November 1964. Vol. 41, no. 11, p. 669–672. DOI 10.1088/0950-7671/41/11/304.
56. BEAMISH, F. E. Inorganic gravimetric analysis. *Analytical Chemistry*. 1 January 1949. Vol. 21, no. 1, p. 144–160. DOI 10.1021/AC60025A027.
57. KULKARNI, Pramod, BARON, Paul A. and WILLEKE, Klaus. Aerosol Measurement: Principles, Techniques, and Applications: Third Edition. *Aerosol Measurement: Principles, Techniques, and Applications: Third Edition*. Online. 7 July 2011. DOI 10.1002/9781118001684.
58. CHOW, Judith C. Measurement methods to determine compliance with ambient air quality standards for suspended particles. *Journal of the Air and Waste Management Association*. 1995. Vol. 45, no. 5, p. 320–382. DOI 10.1080/10473289.1995.10467369.
59. WATSON, John G. and CHOW, Judith C. Ambient Aerosol Sampling. *Aerosol Measurement: Principles, Techniques, and Applications: Third Edition*. 7 July 2011. P. 591–613. DOI 10.1002/9781118001684.CH26.
60. WATSON, John G., CHOW, Judith C., CHEN, L.-W. Antony and FRANK, Neil H. Methods to Assess Carbonaceous Aerosol Sampling Artifacts for IMPROVE and Other Long-Term Networks. *Journal of the Air & Waste Management Association*. Online. 22 August 2009. Vol. 59, no. 8, p. 898–911. DOI 10.3155/1047-3289.59.8.898.

61. CHOW, J C, WATSON, J G, CHEN, L.-W A, RICE, J and FRANK, N H. Quantification of PM2.5 organic carbon sampling artifacts in US networks. *acp.copernicus.org*. Online. 2010. Vol. 10, p. 5223–5239. DOI 10.5194/acp-10-5223-2010.
62. CORRÊA, Sérgio Machado and ARBILLA, Graciela. Aromatic hydrocarbons emissions in diesel and biodiesel exhaust. *Atmospheric Environment*. 1 November 2006. Vol. 40, no. 35, p. 6821–6826. DOI 10.1016/J.ATMOSENV.2006.05.068.
63. JAWOREK, A. Electrospray droplet sources for thin film deposition. *Journal of materials science*. Online. January 2007. Vol. 42, no. 1, p. 266–297. DOI 10.1007/s10853-006-0842-9.
64. CHANDRU, RA, CHAPPA, S, BHARATH, R.S., OOMMEN, C. and RAGHUNANDAN, B.N. Micro-fibre based Porous Composite Propellants with High Regression Rates. *Defence Science Journal*. Online. 25 April 2017. Vol. 67, no. 3, p. 240. DOI 10.14429/dsj.67.10279.
65. ZHENG, G, LI, W, WANG, X, WU, D and SUN, D. Precision deposition of a nanofibre by near-field electrospinning. *Journal of Physics D*. Online. 2010. Available from: https://iopscience.iop.org/article/10.1088/0022-3727/43/41/415501/meta
66. CHANG, Chieh, LIMKRAILASSIRI, Kevin and LIN, Liwei. Continuous near-field electrospinning for large area deposition of orderly nanofiber patterns. *Applied Physics Letters*. Online. 22 September 2008. Vol. 93, no. 12. DOI 10.1063/1.2975834.
67. Nanofibers are the future of your products | Elmarco. Online. Available from: https://www.elmarco.com/
68. LITANI-BARZILAI, Iris, FISHER, Michal, GRIDIN, Vladimir V. and SCHECHTER, Israel. Fast filter-sampling and analysis of PAH aerosols by laser multiphoton ionization. *Analytica Chimica Acta*. 17 July 2001. Vol. 439, no. 1, p. 1–8. DOI 10.1016/S0003-2670(01)01026-1.
69. WADSWORTH, Larry C. Book Review: "Handbook of Nonwoven Filter Media." *Journal of Engineered Fibers and Fabrics*. March 2007. Vol. 2, no. 1, p. 155892500700200. DOI 10.1177/155892500700200106.
70. JONES, TC, DUNGWORTH, DL and MOHR, U. Respiratory system. Online. 2012. Available from: https://books.google.com/books?hl=lt&lr=&id=NfDuCAAAQBAJ&oi=fnd&pg=PA3&dq=related:SKLk6Aj42hIJ:scholar.google.com/&ots=5xE0iboUQH&sig=a6ha8TWF0CWTYDGOChkkZRwQzgQ
71. WEIBEL, Ewald R. It takes more than cells to make a good lung. *American Journal of Respiratory and Critical Care Medicine*. 15 February 2013. Vol. 187, no. 4, p. 342–346. DOI 10.1164/RCCM.201212-2260OE.
72. MÜLLER, Loretta, LEHMANN, Andrea D., JOHNSTON, Blair D., BLANK, Fabian, WICK, Peter, FINK, Alke and ROTHEN-RUTISHAUSER, Barbara. Inhalation Pathway as a Promising Portal of Entry: What Has to Be Considered in Designing New Nanomaterials for Biomedical Application? *Handbook of Nanotoxicology, Nanomedicine and Stem Cell Use in Toxicology*. 3 June 2014. P. 205–222. DOI 10.1002/9781118856017.CH12.
73. NICOD, L. P. Lung defences: an overview. *European Respiratory Review*. Online. 1 December 2005. Vol. 14, no. 95, p. 45–50. DOI 10.1183/09059180.05.00009501.
74. HSIA, Connie C.W., HYDE, Dallas M. and WEIBEL, Ewald R. Lung Structure and the Intrinsic Challenges of Gas Exchange. *Comprehensive Physiology*. Online. 1 April 2016. Vol. 6, no. 2, p. 827. DOI 10.1002/CPHY.C150028.

75. PHALEN, R. F., YEH, H. C., SCHUM, G. M. and RAABE, O. G. Application of an idealized model to morphometry of the mammalian tracheobronchial tree. *The Anatomical Record*. Online. 26 February 1978. Vol. 190, no. 2, p. 167–176. DOI 10.1002/ar.1091900202.

76. CAO, Junyue, O'DAY, Diana R., PLINER, Hannah A., KINGSLEY, Paul D., DENG, Mei, DAZA, Riza M., ZAGER, Michael A., ALDINGER, Kimberly A., BLECHER-GONEN, Ronnie, ZHANG, Fan, SPIELMANN, Malte, PALIS, James, DOHERTY, Dan, STEEMERS, Frank J., GLASS, Ian A., TRAPNELL, Cole and SHENDURE, Jay. A human cell atlas of fetal gene expression. *Science*. 13 November 2020. Vol. 370, no. 6518. DOI 10.1126/SCIENCE.ABA7721.

77. SCHILLER, Herbert B., MONTORO, Daniel T., SIMON, Lukas M., RAWLINS, Emma L., MEYER, Kerstin B., STRUNZ, Maximilian, VIEIRA BRAGA, Felipe A., TIMENS, Wim, KOPPELMAN, Gerard H., BUDINGER, G. R.Scott, BURGESS, Janette K., WAGHRAY, Avinash, VAN DEN BERGE, Maarten, THEIS, Fabian J., REGEV, Aviv, KAMINSKI, Naftali, RAJAGOPAL, Jayaraj, TEICHMANN, Sarah A., MISHARIN, Alexander V. and NAWIJN, Martijn C. The human lung cell atlas: A high-resolution reference map of the human lung in health and disease. *American Journal of Respiratory Cell and Molecular Biology*. 2019. Vol. 61, no. 1, p. 31–41. DOI 10.1165/RCMB.2018-0416TR.

78. POLK, William W., SHARMA, Monita, SAYES, Christie M., HOTCHKISS, Jon A. and CLIPPINGER, Amy J. Aerosol generation and characterization of multi-walled carbon nanotubes exposed to cells cultured at the air-liquid interface. *Particle and Fibre Toxicology*. 23 April 2016. Vol. 13, no. 1. DOI 10.1186/S12989-016-0131-Y.

79. SCHMID, Otmar, JUD, Corinne, UMEHARA, Yuki, MUELLER, Dominik, BUCHOLSKI, Albert, GRUBER, Friedrich, DENK, Oliver, EGLE, Roman, PETRI-FINK, Alke and ROTHEN-RUTISHAUSER, Barbara. Biokinetics of Aerosolized Liposomal Ciclosporin A in Human Lung Cells in Vitro Using an Air-Liquid Cell Interface Exposure System. *Journal of Aerosol Medicine and Pulmonary Drug Delivery*. 1 December 2017. Vol. 30, no. 6, p. 411–424. DOI 10.1089/JAMP.2016.1361.

80. PATTON, John S. and BYRON, Peter R. Inhaling medicines: delivering drugs to the body through the lungs. *Nature Reviews Drug Discovery*. Online. January 2007. Vol. 6, no. 1, p. 67–74. DOI 10.1038/nrd2153.

81. STUART, B. O. Deposition and clearance of inhaled particles. *Environmental Health Perspectives*. 1984. Vol. VOL. 55, p. 369–390. DOI 10.1289/EHP.8455369.

82. STUMBLES, Philip A., UPHAM, John W. and HOLT, Patrick G. Airway dendritic cells: Co-ordinators of immunological homeostasis and immunity in the respiratory tract. *APMIS*. July 2003. Vol. 111, no. 7–8, p. 741–755. DOI 10.1034/J.1600-0463.2003.11107806.X.

83. CHENG, Ru, FENG, Fang, MENG, Fenghua, DENG, Chao, FEIJEN, Jan and ZHONG, Zhiyuan. Glutathione-responsive nano-vehicles as a promising platform for targeted intracellular drug and gene delivery. *Journal of Controlled Release*. 30 May 2011. Vol. 152, no. 1, p. 2–12. DOI 10.1016/J.JCONREL.2011.01.030.

84. ORIVE, G., ALI, O. A., ANITUA, E., PEDRAZ, J. L. and EMERICH, D. F. Biomaterial-based technologies for brain anti-cancer therapeutics and imaging. *Biochimica et Biophysica Acta (BBA) - Reviews on Cancer*. 1 August 2010. Vol. 1806, no. 1, p. 96–107. DOI 10.1016/J.BBCAN.2010.04.001.

85. CONNOR, Ellen E, MWAMUKA, Judith, GOLE, Anand, MURPHY, Catherine J, WYATT, Michael D, CONNOR, E E, WYATT, M D, MWAMUKA, J, GOLE, A and

MURPHY, C J. Gold Nanoparticles Are Taken Up by Human Cells but Do Not Cause Acute Cytotoxicity. *Small*. Online. 1 March 2005. Vol. 1, no. 3, p. 325–327. DOI 10.1002/SMLL.200400093.

86. ITO, Akira, SHINKAI, Masashige, HONDA, Hiroyuki and KOBAYASHI, Takeshi. Medical application of functionalized magnetic nanoparticles. *Journal of Bioscience and Bioengineering*. Online. July 2005. Vol. 100, no. 1, p. 1–11. DOI 10.1263/jbb.100.1.

87. GUPTA, Ajay Kumar and GUPTA, Mona. Synthesis and surface engineering of iron oxide nanoparticles for biomedical applications. *Biomaterials*. 1 June 2005. Vol. 26, no. 18, p. 3995–4021. DOI 10.1016/J.BIOMATERIALS.2004.10.012.

88. VEISEH, Omid, GUNN, Jonathan W, KIEVIT, Forrest M, SUN, Conroy, FANG, Chen, LEE, Jerry S H and ZHANG, Miqin. Inhibition of tumor cell invasion with chlorotoxin-bound superparamagnetic nanoparticles. *Small*. Online. 19 January 2009. Vol. 5, no. 2, p. 256–264. DOI 10.1002/smll.200800646.

89. WILKINSON, LJ, WHITE, RJ and CHIPMAN, J.K. Silver and nanoparticles of silver in wound dressings: a review of efficacy and safety. *Journal of Wound Care*. Online. November 2011. Vol. 20, no. 11, p. 543–549. DOI 10.12968/jowc.2011.20.11.543.

90. YANG, Wei, PETERS, Jay I. and WILLIAMS, Robert O. Inhaled nanoparticles—A current review. *International Journal of Pharmaceutics*. 22 May 2008. Vol. 356, no. 1–2, p. 239–247. DOI 10.1016/J.IJPHARM.2008.02.011.

91. PATTON, JS John Stuart JS and BYRON, PR Peter. Inhaling medicines: delivering drugs to the body through the lungs. *Nature reviews Drug discovery*. Online. 2007. DOI 10.1038/nrd2153.

92. AKHTAR, Mohd Javed, AHAMED, Maqusood, KUMAR, Sudhir, SIDDIQUI, Huma, PATIL, Govil, ASHQUIN, Mohd and AHMAD, Iqbal. Nanotoxicity of pure silica mediated through oxidant generation rather than glutathione depletion in human lung epithelial cells. Online. 9 October 2010. Vol. 276, no. 2, p. 95–102. DOI 10.1016/J.TOX.2010.07.010.

93. LIN, Weisheng, HUANG, Yue-wern, ZHOU, Xiao-Dong and MA, Yinfa. In vitro toxicity of silica nanoparticles in human lung cancer cells. *Toxicology and Applied Pharmacology*. Online. December 2006. Vol. 217, no. 3, p. 252–259. DOI 10.1016/j.taap.2006.10.004.

94. SCIENCE ; CHAN, P, NIE, W C W, TAYLOR, S, FANG, J R, NIE, M M, SHENTON, S M, DAVIS, W, MANN, S A, ELGHANIAN, S, STORHOFF, R, MUCIC, J J, LETSINGER, R C, MIRKIN, R L, MUCIC, C A, STORHOFF, R C, MIRKIN, J J, LETSINGER, C A, MITCHELL, R L, MIRKIN, G P, HARMA, R L, LEHTINEN, H, TAKALO, P, LOVGREN, H, GIUNCHEDI, T, CONTE, P, CHETONI, U, SAETTONE, P, ADLER, M F, JAYAN, J, MELIA, A, BOUREL, C D, ROLLAND, D, LEVERGE, A, GENETET, R, SHIBATA, B, YANO, S, YAMANE, T, SHIBATA, M, TANIGUCHI, S and YANO, T. Conjugation of biomolecules with luminophore-doped silica nanoparticles for photostable biomarkers. *Analytical chemistry*. Online. 2001. Vol. 281, no. 2, p. 4988. DOI 10.1021/ac010406.

95. HIRSCH, L. R., STAFFORD, R. J., BANKSON, J. A., SERSHEN, S. R., RIVERA, B., PRICE, R. E., HAZLE, J. D., HALAS, N. J. and WEST, J. L. Nanoshell-mediated near-infrared thermal therapy of tumors under magnetic resonance guidance. *Proceedings of the National Academy of Sciences*. Online. 11 November 2003. Vol. 100, no. 23, p. 13549–13554. DOI 10.1073/PNAS.2232479100.

96. VENKATESAN, Natarajan, YOSHIMITSU, Junichiro, ITO, Yukako, SHIBATA,

Nobuhito and TAKADA, Kanji. Liquid filled nanoparticles as a drug delivery tool for protein therapeutics. *Biomaterials*. 1 December 2005. Vol. 26, no. 34, p. 7154–7163. DOI 10.1016/J.BIOMATERIALS.2005.05.012.

97. VON MIKECZ, Anna, CHEN, Min, ROCKEL, Thomas and SCHARF, Andrea. The nuclear ubiquitin-proteasome system: Visualization of proteasomes, protein aggregates, and proteolysis in the cell nucleus. *Methods in Molecular Biology*. 2008. Vol. 463, p. 191–202. DOI 10.1007/978-1-59745-406-3_14.

98. RABOLLI, Virginie, THOMASSEN, Leen C.J., PRINCEN, Catherine, NAPIERSKA, Dorota, GONZALEZ, Laetitia, KIRSCH-VOLDERS, Micheline, HOET, Peter H., HUAUX, François, KIRSCHHOCK, Christine E.A., MARTENS, Johan A. and LISON, Dominique. Influence of size, surface area and microporosity on the in vitro cytotoxic activity of amorphous silica nanoparticles in different cell types. *Nanotoxicology*. September 2010. Vol. 4, no. 3, p. 307–318. DOI 10.3109/17435390.2010.482749.

99. NAPIERSKA, Dorota, THOMASSEN, Leen C J, RABOLLI, Virginie, LISON, Dominique, GONZALEZ, Laetitia, KIRSCH-VOLDERS, Micheline, MARTENS, Johan A and HOET, Peter H. Size-dependent cytotoxicity of monodisperse silica nanoparticles in human endothelial cells. Wiley Online Library. Online. 6 April 2009. Vol. 5, no. 7, p. 846–853. DOI 10.1002/smll.200800461.

100. CHOI, Mina, CHO, Wan Seob, HAN, Beom Seok, CHO, Minjung, KIM, Seung Yeul, YI, Jung Yeon, AHN, Byeongwoo, KIM, Seung Hee and JEONG, Jayoung. Transient pulmonary fibrogenic effect induced by intratracheal instillation of ultrafine amorphous silica in A/J mice. Toxicology Letters. 10 November 2008. Vol. 182, no. 1–3, p. 97–101. DOI 10.1016/J.TOXLET.2008.08.019.

101. BARBARIN, Virginie, XING, Zhou, DELOS, Monique, LISON, Dominique and HUAUX, Francois. Pulmonary overexpression of IL-10 augments lung fibrosis and Th2 responses induced by silica particles. American Journal of Physiology - Lung Cellular and Molecular Physiology. Online. May 2005. Vol. 288, no. 5 32-5, p. 841–848.
DOI 10.1152/AJPLUNG.00329.2004/ASSET/IMAGES/LARGE/ZH5005052160000 7.JPEG.

102. OBERDÖRSTER, Günter, SHARP, Zachary, ATUDOREI, Viorel, ELDER, Alison, GELEIN, Robert, LUNTS, Alex, KREYLING, Wolfgang and COX, Christopher. Extrapulmonary translocation of ultrafine carbon particles following whole-body inhalation exposure of rats. *Environmental Health …*. Online. 25 October 2002. Vol. 65, no. 20, p. 1531–1543. DOI 10.1080/00984100290071658.

103. SEMMLER, Manuela, SEITZ, J., ERBE, F., MAYER, P., HEYDER, J., OBERDÖRSTER, G. and KREYLING, W. G. Long-term clearance kinetics of inhaled ultrafine insoluble iridium particles from the rat lung, including transient translocation into secondary organs. *Inhalation Toxicology*. June 2004. Vol. 16, no. 6–7, p. 453–459. DOI 10.1080/08958370490439650.

104. 106. CHEN, Ying, CHEN, Jie, DONG, Jing and JIN, Yihe. Comparing study of the effect of nanosized silicon dioxide and microsized silicon dioxide on fibrogenesis in rats. *Toxicology and Industrial Health*. Online. February 2004. Vol. 20, no. 1–5, p. 21–27. DOI 10.1191/0748233704th190oa.

105. DABROWSKI, Bartlomiej, ZUCHOWSKA, Agnieszka, KASPRZAK, Artur, ZUKOWSKA, Grażyna Zofia and BRZOZKA, Zbigniew. Cellular uptake of biotransformed graphene oxide into lung cells. *Chemico-Biological Interactions*. 1 May 2023. Vol. 376, p. 110444. DOI 10.1016/J.CBI.2023.110444.

106. 108. MATSUO, Yukiko, ISHIHARA, Tsutomu, ISHIZAKI, Junko, MIYAMOTO, Ken ichi, HIGAKI, Megumu and YAMASHITA, Naomi. Effect of betamethasone phosphate loaded polymeric nanoparticles on a murine asthma model. *Cellular Immunology*. 1 January 2009. Vol. 260, no. 1, p. 33–38. DOI 10.1016/J.CELLIMM.2009.07.004.

107. 109. SARFATI, Gadi, DVIR, Tal, ELKABETS, Moshe, APTE, Ron N. and COHEN, Smadar. Targeting of polymeric nanoparticles to lung metastases by surface-attachment of YIGSR peptide from laminin. *Biomaterials*. 1 January 2011. Vol. 32, no. 1, p. 152–161. DOI 10.1016/J.BIOMATERIALS.2010.09.014.

108. 110. WAGNER, Ulrich, STAATS, Petra, FEHMANN, Hans Christoph, FISCHER, Axel, WELTE, Tobias and GRONEBERG, David A. Analysis of airway secretions in a model of sulfur dioxide induced chronic obstructive pulmonary disease (COPD). *Journal of Occupational Medicine and Toxicology*. 2006. Vol. 1, no. 1. DOI 10.1186/1745-6673-1-12.

109. 111. RINK, Jonathan S., MCMAHON, Kaylin M., CHEN, Xiaojuan, MIRKIN, Chad A., THAXTON, C. Shad and KAUFMAN, Dixon B. Transfection of pancreatic islets using polyvalent DNA-functionalized gold nanoparticles. *Surgery*. 1 August 2010. Vol. 148, no. 2, p. 335–345. DOI 10.1016/J.SURG.2010.05.013.

110. 112. MANSOUR, Heidi, HAEMOSU and WU, Xiao. Nanomedicine in pulmonary delivery. *International Journal of Nanomedicine*. Online. December 2009. Vol. 4, p. 299. DOI 10.2147/IJN.S4937.

111. 113. PISON, Ulrich, WELTE, Tobias, GIERSIG, Michael and GRONEBERG, David A. Nanomedicine for respiratory diseases. *European Journal of Pharmacology*. 8 March 2006. Vol. 533, no. 1–3, p. 341–350. DOI 10.1016/J.EJPHAR.2005.12.068.

112. SOSNIK, Alejandro, CARCABOSO, Ángel M., GLISONI, Romina J., MORETTON, Marcela A. and CHIAPPETTA, Diego A. New old challenges in tuberculosis: Potentially effective nanotechnologies in drug delivery. *Advanced Drug Delivery Reviews*. 18 March 2010. Vol. 62, no. 4–5, p. 547–559. DOI 10.1016/J.ADDR.2009.11.023.

113. YILDIRIMER, Lara, THANH, Nguyen T.K., LOIZIDOU, Marilena and SEIFALIAN, Alexander M. Toxicology and clinical potential of nanoparticles. *Nano Today*. 1 December 2011. Vol. 6, no. 6, p. 585–607. DOI 10.1016/J.NANTOD.2011.10.001.

114. YANG, Rui, YANG, Su-Geun, SHIM, Won-Sik, CUI, Fude, CHENG, Gang, KIM, In-Wha, KIM, Dae-Duk, CHUNG, Suk-Jae and SHIM, Chang-Koo. Lung-specific delivery of paclitaxel by chitosan-modified PLGA nanoparticles via transient formation of microaggregates. *Elsevier*. Online. 2009. Vol. 98, no. 3, p. 970–984. DOI 10.1002/jps.21487.

115. ROMERO, Gabriela, ESTRELA-LOPIS, Irina, ZHOU, Jie, ROJAS, Elena, FRANCO, Ana, ESPINEL, Christian Sanchez, FERNÁNDEZ, Africa González, GAO, Changyou, DONATH, Edwin and MOYA, Sergio E. Surface engineered poly(lactide-co-glycolide) nanoparticles for intracellular delivery: Uptake and cytotoxicity - A confocal Raman microscopic study. *Biomacromolecules*. 8 November 2010. Vol. 11, no. 11, p. 2993–2999. DOI 10.1021/BM1007822.

116. TAHARA, Kohei, SAKAI, Takeshi, YAMAMOTO, Hiromitsu, TAKEUCHI, Hirofumi, HIRASHIMA, Naohide and KAWASHIMA, Yoshiaki. Improved cellular uptake of chitosan-modified PLGA nanospheres by A549 cells. *International Journal of Pharmaceutics*. 1 December 2009. Vol. 382, no. 1–2, p. 198–204. DOI 10.1016/J.IJPHARM.2009.07.023.

117. MAYNARD, Andrew D., BARON, Paul A., FOLEY, Michael, SHVEDOVA, Anna A., KISIN, Elena R. and CASTRANOVA, Vincent. Exposure to carbon nanotube material: Aerosol release during the handling of unrefined single-walled carbon nanotube material. *Journal of Toxicology and Environmental Health - Part A*. 2004. Vol. 67, no. 1, p. 87–107. DOI 10.1080/15287390490253688.

118. JI, Jun Ho, JUNG, Jae Hee, KIM, Sang Soo, YOON, Jin Uk, PARK, Jung Duck, CHOI, Byung Sun, CHUNG, Yong Hyun, KWON, Il Hoon, JEONG, Jayoung, HAN, Beom Seok, SHIN, Jae Hyeg, SUNG, Jae Hyuck, SONG, Kyung Seuk and YU, Il Je. Twenty-eight-day inhalation toxicity study of silver nanoparticles in Sprague-Dawley rats. *Inhalation Toxicology*. January 2007. Vol. 19, no. 10, p. 857–871. DOI 10.1080/08958370701432108.

119. KIM, JS, SUNG, JH, CHOI, BG, RYU, HY and SONG, KS. In vivo genotoxicity evaluation of lung cells from Fischer 344 rats following 28 days of inhalation exposure to MWCNTs, plus 28 days and 90 days post-exposure. *Toxicology*. Online. March 2014. Vol. 26, no. 4, p. 222–234. DOI 10.3109/08958378.2013.878006.

120. PARK, Kwangsik, PARK, Eun-Jung, CHUN, In Koo, CHOI, Kyunghee, LEE, Sang Hee, YOON, Junheon and LEE, Byung Chun. Bioavailability and toxicokinetics of citrate-coated silver nanoparticles in rats. *Archives of pharmaceutical ...* Online. January 2011. Vol. 34, no. 1, p. 153–158. DOI 10.1007/s12272-011-0118-z.

121. KWON, Jung-Taek, MINAI-TEHRANI, Arash, HWANG, Soon-Kyung, KIM, Ji-Eun, SHIN, Ji-Young, YU, Kyeong-Nam, CHANG, Seung-Hee, KIM, Dae-Seong, KWON, Yong-Taek, CHOI, In-Ja, CHEONG, Yun-Hee, KIM, Jun Sung and CHO, Myung-Haing. Acute pulmonary toxicity and body distribution of inhaled metallic silver nanoparticles. *Toxicological*. Online. March 2012. Vol. 28, no. 1, p. 25–31. DOI 10.5487/TR.2012.28.1.025.

122. TIAN, Furong, RAZANSKY, Daniel, ESTRADA, Giovani Gomez, SEMMLER-BEHNKE, Manuela, BEYERLE, Andrea, KREYLING, Wolfgang, NTZIACHRISTOS, Vasilis and STOEGER, Tobias. Surface modification and size dependence in particle translocation during early embryonic development. *Inhalation Toxicology*. 2009. Vol. 21, no. SUPPL. 1, p. 92–96. DOI 10.1080/08958370902942624.

123. TAGHDISI, Seyed Mohammad, DANESH, Noor Mohammad, LAVAEE, Parirokh, SARRESHTEHDAR EMRANI, Ahmad, RAMEZANI, Mohammad and ABNOUS, Khalil. Aptamer Biosensor for Selective and Rapid Determination of Insulin. *Analytical Letters*. 4 March 2015. Vol. 48, no. 4, p. 672–681. DOI 10.1080/00032719.2014.956216.

124. ZHU, Zhi, TANG, Zhiwen, PHILLIPS, Joseph A., YANG, Ronghua, WANG, Hui and TAN, Weihong. Regulation of singlet oxygen generation using single-walled carbon nanotubes. *Journal of the American Chemical Society*. 20 August 2008. Vol. 130, no. 33, p. 10856–10857. DOI 10.1021/JA802913F.

125. VENKATESAN, Jayachandran and KIM, Se-Kwon. Chitosan Composites for Bone Tissue Engineering—An Overview. *Marine Drugs*. Online. 2 August 2010. Vol. 8, no. 8, p. 2252–2266. DOI 10.3390/md8082252.

126. TAKAGI, Atsuya, HIROSE, Akihiko, FUTAKUCHI, Mitsuru, TSUDA, Hiroyuki and KANNO, Jun. Dose-dependent mesothelioma induction by intraperitoneal administration of multi-wall carbon nanotubes in p53 heterozygous mice. *Cancer Science*. Online. 1 August 2012. Vol. 103, no. 8, p. 1440–1444. DOI 10.1111/J.1349-7006.2012.02318.X.

127. WARHEIT, David B., LAURENCE, B. R., REED, K. L., ROACH, D. H.,

REYNOLDS, G. A.M. and WEBB, T. R. Comparative Pulmonary Toxicity Assessment of Single-wall Carbon Nanotubes in Rats. *Toxicological Sciences*. Online. 1 January 2004. Vol. 77, no. 1, p. 117–125. DOI 10.1093/TOXSCI/KFG228.

128. MULLER, Julie, HUAUX, François, MOREAU, Nicolas, MISSON, Pierre, HEILIER, Jean François, DELOS, Monique, ARRAS, Mohammed, FONSECA, Antonio, NAGY, Janos B. and LISON, Dominique. Respiratory toxicity of multi-wall carbon nanotubes. *Toxicology and Applied Pharmacology*. 15 September 2005. Vol. 207, no. 3, p. 221–231. DOI 10.1016/J.TAAP.2005.01.008.

129. LIU, Zhuang, TABAKMAN, Scott, WELSHER, Kevin and DAI, Hongjie. Carbon nanotubes in biology and medicine: In vitro and in vivo detection, imaging and drug delivery. *Nano Research*. 2009. Vol. 2, no. 2, p. 85–120. DOI 10.1007/S12274-009-9009-8.

130. BONNER, James C., SILVA, Rona M., TAYLOR, Alexia J., BROWN, Jared M., HILDERBRAND, Susana C., CASTRANOVA, Vincent, PORTER, Dale, ELDER, Alison, OBERDÖRSTER, Günter, HARKEMA, Jack R., BRAMBLE, Lori A., KAVANAGH, Terrance J., BOTTA, Dianne, NEL, Andre and PINKERTON, Kent E. Interlaboratory Evaluation of Rodent Pulmonary Responses to Engineered Nanomaterials: The NIEHS Nano GO Consortium. *Environmental Health Perspectives*. Online. June 2013. Vol. 121, no. 6, p. 676–682. DOI 10.1289/EHP.1205693.

131. LIN, Weisheng, HUANG, Yue-wern, ZHOU, Xiao-Dong and MA, Yinfa. In vitro toxicity of silica nanoparticles in human lung cancer cells. *Toxicology and Applied Pharmacology*. Online. 15 December 2006. Vol. 217, no. 3, p. 252–259. DOI 10.1016/j.taap.2006.10.004.

132. CHEN, Min and VON MIKECZ, Anna. Formation of nucleoplasmic protein aggregates impairs nuclear function in response to SiO2 nanoparticles. *Experimental Cell Research*. 15 April 2005. Vol. 305, no. 1, p. 51–62. DOI 10.1016/J.YEXCR.2004.12.021.

133. NAPIERSKA, Dorota, THOMASSEN, Leen C J, RABOLLI, Virginie, LISON, Dominique, GONZALEZ, Laetitia, KIRSCH-VOLDERS, Micheline, MARTENS, Johan A and HOET, Peter H. Size-dependent cytotoxicity of monodisperse silica nanoparticles in human endothelial cells. *Small*. Online. 6 April 2009. Vol. 5, no. 7, p. 846–853. DOI 10.1002/smll.200800461.

134. SCHMIDT, Susanne, ALTENBURGER, Rolf and KÜHNEL, Dana. From the air to the water phase: implication for toxicity testing of combustion-derived particles. *Biomass Conversion and Biorefinery 2017 9:1*. Online. 11 December 2017. Vol. 9, no. 1, p. 213–225. DOI 10.1007/S13399-017-0295-1.

135. SENGUPTA, Arunima, ROLDAN, Nuria, KIENER, Mirjam, FROMENT, Laurène, RAGGI, Giulia, IMLER, Theo, DE MADDALENA, Lea, RAPET, Aude, MAY, Tobias, CARIUS, Patrick, SCHNEIDER-DAUM, Nicole, LEHR, Claus Michael, KRUITHOF-DE JULIO, Marianna, GEISER, Thomas, MARTI, Thomas Michael, STUCKI, Janick D., HOBI, Nina and GUENAT, Olivier T. A New Immortalized Human Alveolar Epithelial Cell Model to Study Lung Injury and Toxicity on a Breathing Lung-On-Chip System. *Frontiers in Toxicology*. 2022. Vol. 4. DOI 10.3389/FTOX.2022.840606/FULL.

136. MÜLHOPT, Sonja, DILGER, Marco, DIABATÉ, Silvia, SCHLAGER, Christoph, KREBS, Tobias, ZIMMERMANN, Ralf, BUTERS, Jeroen, OEDER, Sebastian, WÄSCHER, Thomas, WEISS, Carsten and PAUR, Hanns-Rudolf. Toxicity testing of

combustion aerosols at the air–liquid interface with a self-contained and easy-to-use exposure system. *Journal of Aerosol Science*. Online. 1 June 2016. Vol. 96, p. 38–55. DOI 10.1016/j.jaerosci.2016.02.005.

137. KIM, Jong Sung, PETERS, Thomas M., O'SHAUGHNESSY, Patrick T., ADAMCAKOVA-DODD, Andrea and THORNE, Peter S. Validation of an in vitro exposure system for toxicity assessment of air-delivered nanomaterials. *Toxicology in Vitro*. 1 February 2013. Vol. 27, no. 1, p. 164–173. DOI 10.1016/J.TIV.2012.08.030.

138. LIU, Ling, ZHOU, Qiuhua, YANG, Xuezhi, LI, Gang, ZHANG, Jingzhu, ZHOU, Xuehua and JIANG, Wei. Cytotoxicity of the soluble and insoluble fractions of atmospheric fine particulate matter. *Journal of Environmental Sciences*. 1 May 2020. Vol. 91, p. 105–116. DOI 10.1016/J.JES.2020.01.012.

139. KROLL, Alexandra, PILLUKAT, Mike H., HAHN, Daniela and SCHNEKENBURGER, Jürgen. Current in vitro methods in nanoparticle risk assessment: Limitations and challenges. *European Journal of Pharmaceutics and Biopharmaceutics*. 1 June 2009. Vol. 72, no. 2, p. 370–377. DOI 10.1016/J.EJPB.2008.08.009.

140. BUS, James S. and BECKER, Richard A. Toxicity Testing in the 21st Century: A View from the Chemical Industry. *Toxicological Sciences*. Online. 1 December 2009. Vol. 112, no. 2, p. 297–302. DOI 10.1093/TOXSCI/KFP234.

141. PAUR, Hanns.-R., MÜLHOPT, S, WEISS, C and DIABATÉ, S. In Vitro Exposure Systems and Bioassays for the Assessment of Toxicity of Nanoparticles to the Human Lung. *Journal für Verbraucherschutz und Lebensmittelsicherheit*. Online. 5 August 2008. Vol. 3, no. 3, p. 319–329. DOI 10.1007/s00003-008-0356-2.

142. OBERDÖRSTER, Günter, OBERDÖRSTER, Eva and OBERDÖRSTER, Jan. Nanotoxicology: An emerging discipline evolving from studies of ultrafine particles. *Environmental Health Perspectives*. July 2005. Vol. 113, no. 7, p. 823–839. DOI 10.1289/EHP.7339.

143. ELDER, Alison, VIDYASAGAR, Sadasivan and DELOUISE, Lisa. Physicochemical factors that affect metal and metal oxide nanoparticle passage across epithelial barriers. *Wiley Interdisciplinary Reviews: Nanomedicine and Nanobiotechnology*. 2009. Vol. 1, no. 4, p. 434–450. DOI 10.1002/WNAN.44.

144. ELSAESSER, Andreas and HOWARD, C. Vyvyan. Toxicology of nanoparticles. *Advanced Drug Delivery Reviews*. 1 February 2012. Vol. 64, no. 2, p. 129–137. DOI 10.1016/J.ADDR.2011.09.001.

145. MONTEIRO-RIVIERE, N. A., INMAN, A. O. and ZHANG, L. W. Limitations and relative utility of screening assays to assess engineered nanoparticle toxicity in a human cell line. *Toxicology and Applied Pharmacology*. 15 January 2009. Vol. 234, no. 2, p. 222–235. DOI 10.1016/J.TAAP.2008.09.030.

146. YACOBI, Nazanin R., PHULERIA, Harish C., DEMAIO, Lucas, LIANG, Chi H., PENG, Ching An, SIOUTAS, Constantinos, BOROK, Zea, KIM, Kwang Jin and CRANDALL, Edward D. Nanoparticle effects on rat alveolar epithelial cell monolayer barrier properties. *Toxicology in Vitro*. 1 December 2007. Vol. 21, no. 8, p. 1373–1381. DOI 10.1016/J.TIV.2007.04.003.

147. ROBERTS, Joan E., WIELGUS, Albert R., BOYES, William K., ANDLEY, Usha and CHIGNELL, Colin F. Phototoxicity and cytotoxicity of fullerol in human lens epithelial cells. *Toxicology and Applied Pharmacology*. 1 April 2008. Vol. 228, no. 1, p. 49–58. DOI 10.1016/J.TAAP.2007.12.010.

148. LISON, Dominique, THOMASSEN, Leen C.J., RABOLLI, Virginie, GONZALEZ, Laetitia, NAPIERSKA, Dorota, SEO, Jin Won, KIRSCH-VOLDERS, Micheline,

HOET, Peter, KIRSCHHOCK, Christine E.A. and MARTENS, Johan A. Nominal and Effective Dosimetry of Silica Nanoparticles in Cytotoxicity Assays. *Toxicological Sciences*. Online. 1 July 2008. Vol. 104, no. 1, p. 155–162. DOI 10.1093/TOXSCI/KFN072.

149. SAYES, Christie M., REED, Kenneth L. and WARHEIT, David B. Assessing Toxicity of Fine and Nanoparticles: Comparing In Vitro Measurements to In Vivo Pulmonary Toxicity Profiles. *Toxicological Sciences*. Online. 1 May 2007. Vol. 97, no. 1, p. 163–180. DOI 10.1093/TOXSCI/KFM018.

150. NACHLAS, Marvin M., MARGULIES, Stanley I., GOLDBERG, Jerome D. and SELIGMAN, Arnold M. The determination of lactic dehydrogenase with a tetrazolium salt. *Analytical Biochemistry*. Online. December 1960. Vol. 1, no. 4–5, p. 317–326. DOI 10.1016/0003-2697(60)90029-4.

151. PRAT, Denis, HAYLER, John and WELLS, Andy. A survey of solvent selection guides. *Green Chemistry*. Online. 23 September 2014. Vol. 16, no. 10, p. 4546–4551. DOI 10.1039/C4GC01149J.

152. ČIUŽAS, Darius, KRUGLY, Edvinas and PETRIKAITĖ, Vilma. Fibrous 3D printed poly(ε)caprolactone tissue engineering scaffold for in vitro cell models. *Biochemical Engineering Journal*. 1 July 2022. Vol. 185. DOI 10.1016/J.BEJ.2022.108531.

153. MATULEVICIUS, Jonas, KLIUCININKAS, Linas, PRASAUSKAS, Tadas, BUIVYDIENE, Dalia and MARTUZEVICIUS, Dainius. The comparative study of aerosol filtration by electrospun polyamide, polyvinyl acetate, polyacrylonitrile and cellulose acetate nanofiber media. *Journal of Aerosol Science*. 1 February 2016. Vol. 92, p. 27–37. DOI 10.1016/J.JAEROSCI.2015.10.006.

154. BIFARI, EN, KHAN, S Bahadar and ALAMRY, KA. Cellulose acetate based nanocomposites for biomedical applications: A review. *Current*. Online. 2016. DOI 10.2174/1381612822666160316160016.

155. HOMAEIGOHAR, Shahin and BOCCACCINI, Aldo R. Nature-Derived and Synthetic Additives to poly(ε-Caprolactone) Nanofibrous Systems for Biomedicine; an Updated Overview. *Frontiers in Chemistry*. 19 January 2022. Vol. 9. DOI 10.3389/FCHEM.2021.809676/FULL.

156. SHAKIBA, Mohamadreza, REZVANI GHOMI, Erfan, KHOSRAVI, Fatemeh, JOUYBAR, Shirzad, BIGHAM, Ashkan, ZARE, Mina, ABDOUSS, Majid, MOAREF, Roxana and RAMAKRISHNA, Seeram. Nylon—A material introduction and overview for biomedical applications. *Polymers for Advanced Technologies*. 1 September 2021. Vol. 32, no. 9, p. 3368–3383. DOI 10.1002/PAT.5372.

157. HAIDER, Md Kaiser, SUN, Lei, ULLAH, Azeem, ULLAH, Sana, SUZUKI, Yuji, PARK, Soyoung, KATO, Yo, TAMADA, Yasushi and KIM, Ick Soo. Polyacrylonitrile/Carbon Black nanoparticle/Nano-Hydroxyapatite (PAN/nCB/HA) composite nanofibrous matrix as a potential biomaterial scaffold for bone regenerative applications. *Materials Today Communications*. 1 June 2021. Vol. 27, p. 102259. DOI 10.1016/J.MTCOMM.2021.102259.

158. LI, Dapeng, FREY, Margaret W. and JOO, Yong L. Characterization of nanofibrous membranes with capillary flow porometry. *Journal of Membrane Science*. 15 December 2006. Vol. 286, no. 1–2, p. 104–114. DOI 10.1016/J.MEMSCI.2006.09.020.

159. BOSKOVIC, Lucija, AGRANOVSKI, Igor E., ALTMAN, Igor S. and BRADDOCK, Roger D. Filter efficiency as a function of nanoparticle velocity and shape. *Journal of Aerosol Science*. 1 July 2008. Vol. 39, no. 7, p. 635–644.

DOI 10.1016/J.JAEROSCI.2008.03.003.
160. Whatman Qm-A quartz filters Circles, 47 mm, pack of 100 glass fiber filters. Online. Available from: https://www.sigmaaldrich.com/LT/en/product/aldrich/wha1851047
161. Pallflex® Tissuquartz™ Filters | VWR. Online. Available from: https://us.vwr.com/store/product/4831719/pallflex-tissuquartztm-filters
162. 164. MCE Filter, Preloaded in Cassette, 0.8 µm, 37 mm, pk/50 | Order High-Quality MCE Filter, Preloaded in Cassette, 0.8 µm, 37 mm, pk/50 Products at SKC, Inc. Online. Available from: https://www.skcinc.com/products/mce-filters-preloaded-in-cassettes-08-m-37-mm-1
163. PATEL, Priya, YADAV, Bindu Kumari and PATEL, Gayatri. State-of-the-Art and Projected Developments of Nanofiber Filter Material for Face Mask Against COVID-19. *Recent Patents on Nanotechnology*. 10 June 2021. Vol. 16, no. 4, p. 262–270. DOI 10.2174/1872210515666210604110946.
164. HABIBI MOHRAZ, Majid, JE YU, Il, BEITOLLAHI, Ali, FARHANG DEHGHAN, Somayeh, HOON SHIN, Jae and GOLBABAEI, Farideh. Assessment of the potential release of nanomaterials from electrospun nanofiber filter media. *NanoImpact*. 1 July 2020. Vol. 19, p. 100223. DOI 10.1016/J.IMPACT.2020.100223.
165. HAAS, Daniel, HEINRICH, Stefan and GREIL, Peter. Solvent control of cellulose acetate nanofibre felt structure produced by electrospinning. *Journal of Materials Science*. March 2010. Vol. 45, no. 5, p. 1299–1306. DOI 10.1007/S10853-009-4082-7.
166. NAM, Jin, HUANG, Yan, AGARWAL, Sudha and LANNUTTI, John. Materials selection and residual solvent retention in biodegradable electrospun fibers. *Journal of Applied Polymer Science*. 5 February 2008. Vol. 107, no. 3, p. 1547–1554. DOI 10.1002/APP.27063.
167. PAN, N and ZHONG, W. Fluid Transport Phenomena in Fibrous Materials. *Textile Progress*. Online. January 2006. Vol. 38, no. 2, p. 1–93. DOI 10.1533/tepr.2006.0002.
168. MACGREGOR-RAMIASA, Melanie N, VASILEV, Krasimir, MACGREGOR-RAMIASA, Dr M N and VASILEV, K. Questions and answers on the wettability of nano-engineered surfaces. *Advanced Materials*. Online. 21 August 2017. Vol. 4, no. 16. DOI 10.1002/admi.201700381.
169. WOOLFENDEN, Elizabeth. Sorbent-based sampling methods for volatile and semi-volatile organic compounds in air. Part 2. Sorbent selection and other aspects of optimizing air monitoring methods. *Journal of Chromatography A*. 16 April 2010. Vol. 1217, no. 16, p. 2685–2694. DOI 10.1016/J.CHROMA.2010.01.015.
170. SOO, Jhy-Charm, MONAGHAN, Keenan, LEE, Taekhee, KASHON, Mike and HARPER, Martin. Air sampling filtration media: Collection efficiency for respirable size-selective sampling. *Aerosol Science and Technology*. Online. 2 January 2016. Vol. 50, no. 1, p. 76–87. DOI 10.1080/02786826.2015.1128525.
171. WANG, Jing and TRONVILLE, Paolo. Toward standardized test methods to determine the effectiveness of filtration media against airborne nanoparticles. *Journal of Nanoparticle Research*. 2014. Vol. 16, no. 6. DOI 10.1007/S11051-014-2417-Z.
172. SAMBAER, Wannes, ZATLOUKAL, Martin and KIMMER, Dusan. 3D air filtration modeling for nanofiber based filters in the ultrafine particle size range. *Chemical Engineering Science*. 12 September 2012. Vol. 82, p. 299–311. DOI 10.1016/J.CES.2012.07.031.
173. CHEN, Hui, ZHANG, Zhenyi, ZHANG, Zhenzhong, JIANG, Feng and DU, Ruiming. Enhancement of filtration efficiency by electrical charges on nebulized particles. *Particuology*. 1 April 2018. Vol. 37, p. 81–90. DOI 10.1016/J.PARTIC.2017.07.008.
174. RENGASAMY, Samy, ZHUANG, Ziqing, NIEZGODA, George, WALBERT, Gary,

LAWRENCE, Robert, BOUTIN, Brenda, HUDNALL, Judith, MONAGHAN, William P., BERGMAN, Michael, MILLER, Colleen, HARRIS, James and COFFEY, Christopher. A comparison of total inward leakage measured using sodium chloride (NaCl) and corn oil aerosol methods for air-purifying respirators. *Journal of Occupational and Environmental Hygiene*. 3 August 2018. Vol. 15, no. 8, p. 616–627. DOI 10.1080/15459624.2018.1479064.

175. SOO, Jhy-Charm, MONAGHAN, Keenan, LEE, Taekhee, KASHON, Mike and HARPER, Martin. Air sampling filtration media: Collection efficiency for respirable size-selective sampling. *Aerosol Science and*. Online. 2 January 2016. Vol. 50, no. 1, p. 76–87. DOI 10.1080/02786826.2015.1128525.

176. UYAR, Tamer and BESENBACHER, Flemming. Electrospinning of uniform polystyrene fibers: The effect of solvent conductivity. *Polymer*. 10 November 2008. Vol. 49, no. 24, p. 5336–5343. DOI 10.1016/J.POLYMER.2008.09.025.

177. YANG, Da Yong, WANG, Yang, ZHANG, Dong Zhou, LIU, Ying Yi and JIANG, Xing Yu. Control of the morphology of micro/nano-structures of polycarbonate via electrospinning. *Chinese Science Bulletin*. Online. 30 September 2009. Vol. 54, no. 17, p. 2911–2917. DOI 10.1007/S11434-009-0241-0/METRICS.

178. ZHENG, Gaofeng, SHAO, Zungui, CHEN, Junyu, JIANG, Jiaxin, ZHU, Ping, WANG, Xiang, LI, Wenwang and LIU, Yifang. Self-Supporting Three-Dimensional Electrospun Nanofibrous Membrane for Highly Efficient Air Filtration. *Nanomaterials 2021, Vol. 11, Page 2567*. Online. 29 September 2021. Vol. 11, no. 10, p. 2567. DOI 10.3390/NANO11102567.

179. AHNE, Joerg, LI, Qinghai, CROISET, Eric and TAN, Zhongchao. Electrospun cellulose acetate nanofibers for airborne nanoparticle filtration. *Textile Research Journal*. Online. 1 August 2019. Vol. 89, no. 15, p. 3137–3149. https://journals.sagepub.com/doi/10.1177/0040517518807440

180. LI, Qian, XU, Yiyang, WEI, Hanghang and WANG, Xiaofeng. An electrospun polycarbonate nanofibrous membrane for high efficiency particulate matter filtration. *RSC Advances*. Online. 11 July 2016. Vol. 6, no. 69, p. 65275–65281. DOI 10.1039/C6RA12320A.

181. WANG, Jingwei, CAHYADI, Andy, WU, Bing, PEE, Wenxi, FANE, Anthony G. and CHEW, Jia Wei. The roles of particles in enhancing membrane filtration: A review. *Journal of Membrane Science*. 1 February 2020. Vol. 595. DOI 10.1016/J.MEMSCI.2019.117570.

182. WANG, Zhe and PAN, Zhijuan. Preparation of hierarchical structured nano-sized/porous poly(lactic acid) composite fibrous membranes for air filtration. *Applied Surface Science*. 30 November 2015. Vol. 356, p. 1168–1179. DOI 10.1016/J.APSUSC.2015.08.211.

183. YUN, Ki Myoung, HOGAN, Christopher J., MATSUBAYASHI, Yasuko, KAWABE, Masaaki, ISKANDAR, Ferry and OKUYAMA, Kikuo. Nanoparticle filtration by electrospun polymer fibers. *Chemical Engineering Science*. 1 September 2007. Vol. 62, no. 17, p. 4751–4759. DOI 10.1016/J.CES.2007.06.007.

184. BESSA, Maria João, BRANDÃO, Fátima, ROSÁRIO, Fernanda, MOREIRA, Luciana, REIS, Ana Teresa, VALDIGLESIAS, Vanessa, LAFFON, Blanca, FRAGA, Sónia and TEIXEIRA, João Paulo. Assessing the in vitro toxicity of airborne (nano)particles to the human respiratory system: from basic to advanced models. *Journal of Toxicology and Environmental Health - Part B: Critical Reviews*. 2023. Vol. 26, no. 2, p. 67–96. DOI 10.1080/10937404.2023.2166638.

185. CAO, Xuefei, COYLE, Jayme P., XIONG, Rui, WANG, Yiying, HEFLICH, Robert H., REN, Baiping, GWINN, William M., HAYDEN, Patrick and ROJANASAKUL, Liying. Invited review: human air-liquid-interface organotypic airway tissue models derived from primary tracheobronchial epithelial cells—overview and perspectives. *In Vitro Cellular and Developmental Biology - Animal*. 1 February 2021. Vol. 57, no. 2, p. 104–132. DOI 10.1007/S11626-020-00517-7.

186. CLARK, A. R. Medical Aerosol Inhalers: Past, Present, and Future. *Aerosol Science and Technology*. Online. 1 January 1995. Vol. 22, no. 4, p. 374–391. DOI 10.1080/02786829408959755.

187. DREWNICK, Frank, PIKMANN, Julia, FACHINGER, Friederike, MOORMANN, Lasse, SPRANG, Fiona and BORRMANN, Stephan. Aerosol filtration efficiency of household materials for homemade face masks: Influence of material properties, particle size, particle electrical charge, face velocity, and leaks. *Aerosol Science and Technology*. Online. 2021. Vol. 55, no. 1, p. 63–79. DOI 10.1080/02786826.2020.1817846.

188. LENZ, Anke Gabriele, KARG, Erwin, BRENDEL, Ellen, HINZE-HEYN, Helga, MAIER, Konrad L., EICKELBERG, Oliver, STOEGER, Tobias and SCHMID, Otmar. Inflammatory and oxidative stress responses of an alveolar epithelial cell line to airborne zinc oxide nanoparticles at the air-liquid interface: A comparison with conventional, submerged cell-culture conditions. *BioMed Research International*. 2013. Vol. 2013. DOI 10.1155/2013/652632.

189. ROPER, Courtney, DELGADO, Lisandra Santiago, BARRETT, Damien, MASSEY SIMONICH, Staci L. and TANGUAY, Robert L. PM 2.5 Filter Extraction Methods: Implications for Chemical and Toxicological Analyses. *Environmental Science and Technology*. 2 January 2019. Vol. 53, no. 1, p. 434–442. DOI 10.1021/ACS.EST.8B04308.

190. AZARI, Arezo, GOLCHIN, Ali, MAYMAND, Maryam Mahmoodinia, MANSOURI, Fatemeh and ARDESHIRYLAJIMI, Abdolreza. Electrospun Polycaprolactone Nanofibers: Current Research and Applications in Biomedical Application. *Advanced Pharmaceutical Bulletin*. Online. 2022. Vol. 12, no. 4, p. 658. DOI 10.34172/APB.2022.070.

191. OU, Lingling, SONG, Bin, LIANG, Huimin, LIU, Jia, FENG, Xiaoli, DENG, Bin, SUN, Ting and SHAO, Longquan. Toxicity of graphene-family nanoparticles: a general review of the origins and mechanisms. *Particle and Fibre Toxicology*. Online. 31 December 2016. Vol. 13, no. 1, p. 57. DOI 10.1186/s12989-016-0168-y.

192. INGLE, Avinash P., DURAN, Nelson and RAI, Mahendra. Bioactivity, mechanism of action, and cytotoxicity of copper-based nanoparticles: A review. *Applied Microbiology and Biotechnology*. Online. 5 February 2014. Vol. 98, no. 3, p. 1001–1009. DOI 10.1007/s00253-013-5422-8.

193. HUFNAGEL, Matthias, SCHOCH, Sarah, WALL, Johanna, STRAUCH, Bettina Maria and HARTWIG, Andrea. Toxicity and gene expression profiling of copper- And titanium-based nanoparticles using air-liquid interface exposure. *Chemical Research in Toxicology*. 18 May 2020. Vol. 33, no. 5, p. 1237–1249. DOI 10.1021/ACS.CHEMRESTOX.9B00489.

194. GURUNATHAN, Sangiliyandi, IQBAL, Muhammad Arsalan, QASIM, Muhammad, PARK, Chan Hyeok, YOO, Hyunjin, HWANG, Ho, UHM, Sang Jun, SONG, Hyuk, PARK, Chankyu, DO, Jeong Tae, CHOI, Youngsok, KIM, Jin-Hoi and HONG, Kwonho. Evaluation of graphene oxide induced cellular toxicity and transcriptome analysis in human embryonic kidney cells. *Nanomaterials*. Online. 2019.

DOI 10.3390/nano9070969.

195. TANAKA, Yujiro, NAKAMURA, Aya, MORIOKA, Masaki Suimye, INOUE, Shoko, TAMAMORI-ADACHI, Mimi, YAMADA, Kazuhiko, TAKETANI, Kenji, KAWAUCHI, Junya, TANAKA-OKAMOTO, Miki, MIYOSHI, Jun, TANAKA, Hiroshi and KITAJIMA, Shigetaka. Systems analysis of ATF3 in stress response and cancer reveals opposing effects on pro-apoptotic genes in p53 pathway. *PLoS ONE*. 2011. Vol. 6, no. 10. DOI 10.1371/JOURNAL.PONE.0026848.

196. BUHA, Aleksandra, BARALI´CBARALI´C, Katarina, DJUKIC-COSIC, Danijela, BULAT, Zorica, TINKOV, Alexey, PANIERI, Emiliano and SASO, Luciano. The role of toxic metals and metalloids in Nrf2 signaling. *Antioxidants*. Online. 1 May 2021. Vol. 10, no. 5. DOI 10.3390/antiox10050630.

197. MUHAMAD, Musthahimah, AB.RAHIM, Nurhidayah, WAN OMAR, Wan Adnan and NIK MOHAMED KAMAL, Nik Nur Syazni. Cytotoxicity and Genotoxicity of Biogenic Silver Nanoparticles in A549 and BEAS-2B Cell Lines. *Bioinorganic Chemistry and Applications*. 2022. Vol. 2022. DOI 10.1155/2022/8546079.

198. WANG, Zhenyu, LI, Na, ZHAO, Jian, WHITE, Jason C., QU, Pei and XING, Baoshan. CuO nanoparticle interaction with human epithelial cells: Cellular uptake, location, export, and genotoxicity. *Chemical Research in Toxicology*. 16 July 2012. Vol. 25, no. 7, p. 1512–1521. DOI 10.1021/TX3002093.

199. XIAO, Xinzhe, ZHANG, Yumin, ZHOU, Lei, LI, Bin and GU, Lin. Photoluminescence and Fluorescence Quenching of Graphene Oxide: A Review. *Nanomaterials*. Online. 17 July 2022. Vol. 12, no. 14, p. 2444. DOI 10.3390/nano12142444.

200. WU, Xu, XING, Yuqian, ZENG, Kevin, HUBER, Kirby and ZHAO, Julia Xiaojun. Study of Fluorescence Quenching Ability of Graphene Oxide with a Layer of Rigid and Tunable Silica Spacer. *Langmuir*. 16 January 2018. Vol. 34, no. 2, p. 603–611. DOI 10.1021/ACS.LANGMUIR.7B03465.

201. FU, Pengfei, GUO, Xinbiao, CHEUNG, Felix Man Ho and YUNG, Ken Kin Lam. The association between PM2.5 exposure and neurological disorders: A systematic review and meta-analysis. *Science of The Total Environment*. Online. March 2019. Vol. 655, p. 1240–1248. DOI 10.1016/j.scitotenv.2018.11.218.

CURRICULUM VITAE

Name, Surname: Preethi Ravikumar

E-mail: preethi.ravikumar@ktu.edu

Education

2012–2016	Bachelor's degree in Biotechnology
2016–2018	Master's degree in Molecular Biology and Biotechnology
2019–2023	PhD in Environmental Engineering

Professional experience:

2020 12–2022 01 Junior Researcher in Aerocelltox project

2023 04–05	Guest Researcher in Paul Scherrer Institute, Villigen, Switzerland Involved in the study of aging of pollutants from biomass burning to better understand the atmospheric chemistry involved and develop effective strategies for mitigating the negative impacts of this source of pollution using Aerosol Mass Spectrometry (AMS)
2022 04–07	Research Intern in Alchemia Nova, Vienna, Austria Assistance in different tasks related to EU/national projects, potential assistance in the writing of EU/international proposal, daily assistance in the laboratory

Areas of research interest:

Research and development of electrospun air filtration substrates using solution and melt electrospinning, cytotoxicity testing of the developed substrates.

Scientific papers related to the topic of dissertation

Articles in peer-reviewed scientific publications

In publications indexed in the Web of Science with Impact Factor (JCR SCIE)

International (foreign) publishers

1. [S1; GB] Krugly, Edvinas; Ravikumar, Preethi; Dabašinskaitė, Lauryna; Tichonovas, Martynas; Ciuzas, Darius; Prasauskas, Tadas; Baniukaitienė, Odeta; Masionė, Goda; Kaunelienė, Violeta; Martuzevičius, Dainius. Nanofibrous aerosol sample filter substrates: design, fabrication, and characterization // Journal of aerosol science. Oxford: Elsevier. ISSN 0021-8502. eISSN 1879-1964. 2023, vol. 169, art. no. 106118, p. 1-12. DOI: 10.1016/j.jaerosci.2022.106118. [Science Citation Index Expanded (Web of Science); Scopus] [IF: 4,500; AIF: 5,475; IF/AIF: 0,821; Q1 (2022, InCites JCR SCIE)] [FOR: T 004] [Input: 0,100].

2. [S1; IE] Krugly, Edvinas; Bagdonas, Edvardas; Raudoniute, Jovile; Ravikumar, Preethi; Bagdoniene, Lauryna; Ciuzas, Darius; Prasauskas, Tadas; Aldonyte, Ruta; Gutleb, Arno C.; Martuzevicius, Dainius. A novel "cells-onparticles" cytotoxicity testing platform in vitro: design, characterization, and validation against engineered nanoparticle aerosol // Toxicology. East Park Shannom: Elsevier. ISSN 0300-483X. eISSN 1879-3185. 2024, vol. 508 In progress (November 2024), iss. 00, art. no. 153936, p. 1-10. DOI: 10.1016/j.tox.2024.153936. [Science Citation Index Expanded (Web of Science); Scopus] [IF: 4,800; AIF: 3,900; IF/AIF: 1,230; Q1 (2023, InCites JCR SCIE)] [CiteScore: 7,80; SNIP: 0,996; SJR: 1,014; Q1 (2023, Scopus Sources)] [FoR: T 004] [Input: 0,100].

Book Chapter in Springer Nature without impact factor

3. Ravikumar, Preethi "Composite nanofibrous on 3D printed support polycarbonate filter for aerosol particle filtration and sampling" has been peer reviewed and accepted to be included in the book "Sustainable Environmental Remediation: Avenues in Nano and Biotechnology" to be published in September/October 2024 by Springer Nature.

Patents and patent applications

Patent applications registered in EPO, USPTO, JPO patent offices 1. [N2a; DE; OA] Ravikumar, Preethi (author of the invention); Tichonovas, Martynas (author of the invention); Kauneliene, Violeta (author of the invention); Dabasinskaite, Lauryna (author of the invention); Krugly, Edvinas (author of the invention); Martuzevicius, Dainius (author of the invention); Prasauskas, Tadas (author of the invention). Nano/micro composite fibrous filter for sampling aerosol particles and production method thereof: European patent application / inventors: P. Ravikumar, M. Tichonovas, V. Kauneliene, L. Dabasinskaite, E. Krugly, D. Martuzevicius, T. Prasauskas; applicant: Kaunas university of technology. EP 4194596 A1. 2023-06-14. [Espacenet] [FOR: T 004] [Input: 0,148].

Presentation of the research results at conferences

Other conference presentation abstracts and non-peer reviewed conference papers

1. [T3; ES; OA] Ravikumar, Preethi; Čiužas, Darius; Krugly, Edvinas; Martuzevičius, Dainius. Electrospun polycarbonate nanocoating on 3D printed support for air filtration application // EAC 2023: European Aerosol Conference, 3-8 September 2023, Malaga, Spain. Malaga: European Aerosol Assembly. 2023, art. no. 1.07-8. p. 1. [FoR: T 004]
2. [T3; GR] Martuzevicius, D.; Krugly, E.; Ravikumar, P.; Dabasinskaite, L.; Tichonovas, M.; Prasauskas, T.; Ciuzas, D.; Kaunelienė, V. Design and validation of nanofibrous filters for aerosol particle sampling // 11th international aerosol conference, IAC 2022: 4-9 September 2022, Athens, Greece: abstract book. Athens: IARA. 2022, AT-P2_006, p. 1138. [FoR: T 004]

3. [T3; LT] Ravikumar, Preethi; Prasauskas, Tadas; Krugly, Edvinas; Čiužas, Darius; Martuzevičius, Dainius. Nanofibrous airborne particle sampling membrane // Technorama 2020: from vision to innovation. Kaunas: KTU. 2020, p. 52-53. [FoR: T 004]
4. [T3; KR] Prasauskas, Tadas; Krugly, Edvinas; Ravikumar, Preethi; Ciuzas, Darius; Dabašinskaitė, Lauryna; McDonald, Ryan; Martuzevicius, Dainius. Electrospun nanofibrous membranes for sampling of fine fraction of particulate matter // Indoor Air 2020: Creative & smart solutions for better built environments: 16th conference of the International Society of Indoor Air Quality & Climate, Seoul, Korea, November 1 - 5, 2020: proceeding book: extended abstracts & full papers. Seoul: Korean Society for Indoor Environment. 2020, ABS-0618, p. 2334-2335. [FoR: T 004]

Courses attended by the author of the thesis:
1. Nanotechnologies and Environmental Protection (T270D102), 6 credits,
2. Theory and Technologies of Air Pollution Abatement (T270D104),
3. Sustainable Industrial Development (T270D106), 9 credits,
4. Advanced Polymer Chemistry and Technology (T390D249), 9 credits,
5. The Sustainable City: An Integrated Perspective Summer School (XXXXD065), 2 credits.

ACKNOWLEDGEMENTS

As I complete this significant milestone in my academic journey, I want to take a moment to express my deepest gratitude for the invaluable support and contributions. The unwavering guidance and collaboration have played a pivotal role in the successful completion of my PhD research.

First and foremost, I extend my heartfelt thanks to my esteemed PhD supervisor, Professor Dr. Dainius Martuzevičius. His mentorship, dedication and wealth of knowledge have not only shaped my research but fostered my growth as a scholar as well. His insightful guidance and encouragement have been the cornerstone of my academic progress.

I am indebted to the entire group at the Department of Environmental Technologies for their camaraderie and collaborative spirit. A special mention goes to Dr. Edvinas Krugly, whose support has added depth to my research experience. I must acknowledge the technical expertise and guidance provided by Dr. Darius Ciuzas and Dr. Martynas Tichonovas, whose insights from a technical perspective have been indispensable in navigating the complexities of my research.

Furthermore, I express my gratitude to Dr. Edvardas Bagdonas and the dedicated scientists from the Innovative Medicine Centre who have made significant contributions to my work. Their interdisciplinary collaboration has broadened the scope and impact of my research.

Beyond the academic sphere, I am deeply thankful to my family, especially my father Ravikumar, mother Janaki, sister Gayathiri and husband Prasad Shimpi. Their unwavering support, patience and understanding have been my pillars of strength throughout this journey.

With sincere appreciation,
Preethi Ravikumar

UDK 628.5+544.772+620.168.3] (043.3)

SL 344. 2024-09-13, 16,75 leidyb. apsk. l. Tiražas 14 egz. Užsakymas 162.
Išleido Kauno technologijos universitetas, K. Donelaičio g. 73, 44249 Kaunas
Spausdino leidyklos „Technologija“ spaustuvė, Studentų g. 54, 51424 Kaunas